

A diagrammatic approach towards the thermodynamics of integrable systems

Dinh-Long Vu

Université Paris-Saclay, CNRS, CEA, Institut de physique théorique, 91191, Gif-sur-Yvette, France.

We propose an exact summation method to compute thermodynamic observables in integrable quantum field theories. The key idea is to use the matrix-tree theorem to write the Gaudin determinants that appear in the cluster expansion as a sum over graphs. For theories with a diagonal S-matrix, this method is more powerful than the standard Thermodynamic Bethe Ansatz (TBA) technique as it is exact to all orders of powers in inverse volume. We have obtained using this method the TBA equation, the excited state energies in finite volume, the Leclair-Mussardo formula for one point functions, the finite-temperature boundary entropy and cumulants of conserved charges in Generalized Gibbs Ensembles. Moreover, the graph expansion can also be regarded as an alternative to algebraic manipulations involving Gaudin determinants. We have applied this idea to derive the equations of state and other transport properties in Generalized Hydrodynamics. For theories with a non-diagonal S-matrix, the description of a complete set of states is more involved and it is not known how a cluster expansion can be implemented. It is nevertheless possible to apply the direct summation method in reverse and interpret known TBA equations with complex strings in terms of diagrams.

Contents

1	Preliminary	13
1.1	Basics of integrable quantum field theories	13
1.1.1	Some examples	13
1.1.2	Consequences of higher conserved charges on the S matrix	14
1.1.3	The two particle S-matrix	16
1.1.4	Finding the two-particle S-matrix: an example	19
1.1.5	The Bethe equation of SU(2) chiral Gross-Neveu model	20
1.1.6	Integrability in open systems	21
1.2	Thermodynamic Bethe Ansatz	23
1.2.1	The traditional derivation	23
1.2.2	UV limit of the ground-state energy	27
1.2.3	Non-diagonal scattering and string hypothesis	28
1.2.4	TBA equations and Y-system for SU(2) chiral Gross-Neveu model	30
1.2.5	Excited state energies from analytic continuation	34
1.3	Application of form factors in finite volume	37
1.3.1	Motivation and axioms	37
1.3.2	Connected and symmetric evaluation of diagonal form factors	39
1.3.3	Finite volume matrix elements	41
1.3.4	Leclair-Mussardo formula	42
1.4	Generalized hydrodynamics	44
1.4.1	Maximal entropy states	44
1.4.2	Equations of state and hydrodynamic matrices	46
1.4.3	Local entropy maximisation and Euler hydrodynamics	48
1.4.4	The partitioning protocol	50
2	Closed systems	53
2.1	The TBA equation	53
2.1.1	The sum over mode numbers	53
2.1.2	From mode numbers to rapidities	55
2.1.3	The Gaudin determinant and its diagrammatic expansion	56
2.1.4	Summing over the trees	58
2.1.5	A comment on theories with non-diagonal S-matrix	59
2.2	The charge statistics in GGE	61
2.2.1	Charge average	61
2.2.2	Charge covariance	62
2.2.3	Higher cumulants	63
2.3	The Leclair-Mussardo formula	67
2.4	Excited state energies	70

3	Open systems with diagonal scattering	72
3.1	Finite temperature g-function: definition	72
3.2	Known results	73
3.3	New derivation	75
3.3.1	The sum over mode number	75
3.3.2	From mode numbers to rapidities	77
3.3.3	Matrix-tree theorem	78
3.3.4	Graph expansion of the partition function	79
3.3.5	Summing over trees: saddle point TBA approximation	80
3.3.6	Summing over loops: Fredholm determinants	81
3.4	Summary and outlook	82
4	Open systems with non-diagonal scattering	84
4.1	The current perturbed $SU(2)_k$ WZNW theories	86
4.1.1	Off-critical g-function	88
4.2	The TBA equations and Y system	89
4.3	The reflection factors	92
4.4	The divergence and the normalized g-function	94
4.4.1	Level 1- Gross Neveu model	94
4.4.2	Higher levels	95
4.5	Conclusion	97
5	Applications in Generalized Hydrodynamics	98
5.1	Equations of state from form factors	98
5.1.1	The connected and the symmetric form factors	99
5.1.2	Establishing the equations of state	101
5.1.3	Conclusion	104
5.2	Full counting statistics	104
5.2.1	Hydrodynamics approximation	104
5.2.2	Comparison with diagrams	106
5.2.3	Comments on the conjecture	108
5.2.4	Summary and outlook	109
	Appendices	113
A	TBA and Y system	114
A.1	Chiral $SU(2)$ Gross-Neveu model	114
A.2	Higher levels	116
A.2.1	The scattering and the kernels	116
A.2.2	Maximal string reduction and reduced TBA	117
A.2.3	Y system	118
B	Determinants	120
B.0.1	The IR determinant	120
B.0.2	The UV determinant	121

C Normal modes of hydrodynamics	122
Bibliography	124

Introduction

Quantum integrable systems are important for at least two reasons

- They can be realized in experiments. Here are some examples. The Heisenberg spin $1/2$ chain [1, 2] is expected to describe magnetic properties of crystals in which magnetic ions are arranged in one dimensional rays and interaction between rays is screened by large non-magnetic ions [3]. The dynamical structure factors (Fourier transform of the spin-spin correlation function) of KCuF_3 measured by inelastic neutron scattering experiments [4] have been shown to be in astounding agreement with theoretical computation [5] using Bethe ansatz (see below). The Lieb-Liniger gas in repulsive regime [6, 7] was replicated in laboratory [8] by ^{87}Rb atoms trapped in an optical lattice. The probability of observing two particles at the same position measured by photoassociation conforms with the prediction [9] that the overlap of bosonic wave functions decreases as interaction strength increases, a phenomenon known as the fermionization of bosons. Moreover, the same authors prepared in their famous *quantum Newton cradle* experiment [10] an out-of-equilibrium initial state using the same atoms. They observed that even after thousands of collisions, the gas does not equilibrate, thus experimentally verified of the lack of thermalization in integrable systems.
- Exact theoretical computations are available. In 1931, Hans Bethe [11] solved the Heisenberg spin $1/2$ chain by writing its eigenvectors as superpositions of plane waves that properly take into account the exchange of particles. The proposed form of the eigenvectors and the equations that govern the momenta of these plane waves are known respectively as *Bethe's ansatz* and *Bethe's equations*. Although Bethe's idea was later extended to other models [12–14], it was not known at that time why such a simple ansatz works for these precise models? The answer to this question was found in a coherent framework that can explain the origin of quantum integrability: an algebraic formulation of Bethe's ansatz discovered in the late 70's by Faddeev, Sklyanin and Taktadjan [15, 16]. The central object in their construction is a transfer matrix that encodes within itself an infinite number of commuting observables the Hamiltonian is one of which. Bethe's ansatz and Bethe's equations can both be written in terms of the elements of this matrix. It should be noted however that the notion of transfer matrix appeared in fact earlier in the work of Baxter [17] on two dimensional statistical models. This algebraic formalism works for a wide class of models with higher-rank symmetry groups [18, 19], in that case Bethe's ansatz is particularly known as *nested Bethe ansatz*.

When applied in the thermodynamic setting of an integrable gas, Bethe's ansatz provides information about the distribution of particle momenta at thermal equilibrium. This was first illustrated for the Lieb-Liniger model in the seminal work of Yang and Yang [7]. Forgetting technical details, their idea consists of solving Bethe equations for the thermodynamic state that minimizes the free energy of the system, hence the name *thermodynamic Bethe ansatz* (TBA). Accordingly, the functional equation that governs the momenta distribution is called the TBA equation. The validity of this equation has recently been confirmed in an experiment of ultracold atoms [20]. Soon after the work of Yang and Yang, the TBA has been extended

to the XXZ spin chain [21] and critical exponents of its susceptibility and specific heat were subsequently obtained [22, 23]. Compared to the Lieb-Linger model, the TBA of XXZ spin chain is considerably more complicated as it involves an infinite number of bound states with complex momenta that arrange themselves in string patterns, a feature that became known as *the string hypothesis*. The TBA of other lattice models such as the Hubbard model was also obtained quickly [24]. On the other hand, it took almost twenty years for TBA to find its applications in integrable quantum field theories. With his revolutionary idea of a double Wick rotation [25], Zamolodchikov pointed out that the ground state energy of the *physical theory* at volume R is nothing but the TBA free energy density of the *mirror theory* at temperature $1/R$. The twenty-year gap between the work of Yang and Yang and that of Zamolodchikov is partly due to the fact that the first result on factorized quantum S-matrix appeared as late as in 1978 [26]. In the context of the AdS/CFT correspondence, Zamolodchikov's idea allows the spectrum of classical strings on $\text{AdS}_5 \times S^5$ and the scaling dimensions in planar $\mathcal{N} = 4$ SYM to both be computed by TBA [27–37]. On the other hand, the relevance of TBA in higher-point correlation functions in planar $\mathcal{N} = 4$ SYM is much less known. Embracing Zamolodchikov's idea, Basso, Komatsu and Vieira proposed a two-step program [38] to compute three point functions of this theory. The first step consists of cutting them into two hexagon form factors and the second step is to glue them back by inserting a complete basis of mirror states on each one of the three mirror sides. Although there is not much trouble in bootstrapping these form factors, their expression is sufficiently involved. Combined with the not so simple bound state structure of the theory, this makes the summation over mirror particles extremely challenging. The strategy often adopted in the literature is to either compute the leading-order terms or to consider particular limits in which the contribution from mirror particles can be neglected. Given the tremendous success of TBA in the spectral problem of planar $\mathcal{N} = 4$ SYM, one can nevertheless expect some TBA-like structures in the wrapping correction to the structure constants or to other observables of the theory.

Originally motivated by this problem, the purpose of this thesis is to investigate, to what extent a direct thermal summation could reproduce TBA-like quantities. Before working with planar $\mathcal{N} = 4$ SYM, we must implement this approach in the simpler case of 1+1 dimensional integrable quantum field theories. We first have to make sure that it can recover the well-known TBA equation. Then, we probe its limit by testing it on observables that the original TBA method has shown considerable difficulty to derive. Here are some candidates

- For the one point function of a local observable, a formula involving the TBA density function and the connected evaluation of diagonal form factors (connected form factors for short) was conjectured by Leclair and Mussardo in [39]. Saleur provided some supporting arguments [40] for this conjecture and although he could not prove it, he proposed a relation between connected form factors and diagonal matrix elements in finite volume that could potentially justify the formula. Even with this hint, a proof was not ready until Pozsgay [41] understood how to apply Saleur proposal in the thermodynamic setting. On a side note, the relation proposed by Saleur has only been recently proved by Bajnok and Wu [42]. The similarity between the problem of one point functions and the wrapping correction to three point functions in the hexagon approach is that both cases involve a summation over a complete set of states along with some form factors. There is an

important difference however, here there is only one theory, the *mirror theory* in the sense that it is of large volume. For one point functions in finite volume, see [43].

- Excited state energies. The double Wick rotation singles out the ground state and the ground state only. To get access to higher energy levels, Dorey and Tateo [44] proposed an analytic continuation in some parameter of the theory (temperature, mass scale). If one starts with a real value of this parameter and one moves in the complex plane in such a way that the singularity in the TBA equation crosses the real axis then upon coming back one ends up in a different sheet of energy. Here, both the physical and the mirror theory are at play.
- In situations where $O(1)$ corrections to extensive quantities are needed, the original derivation of TBA shows weaknesses. This is due to its inherent approximations: the length of the interval over which the momentum density is defined can vary between inverse volume and unity, the Stirling formula used to compute the entropy is also insensitive to $O(1)$ correction. An example is the boundary correction to the free energy, also known as the finite-temperature g-function. It was partially obtained by Leclair *et al.* in [45] using TBA saddle point approximation. Fluctuations around the saddle point coming from correction to the Stirling formula was then added by Woynarovich [46]. A paradox arose from the work of Woynarovich however as it predicts a similar contribution for periodic systems. Meanwhile, the authors of [47] took a different route towards this problem. By means of a cluster expansion, a considerable amount of guess work, and possibly some hints from the result of Woynarovich they obtained a formula for the g-function with similar appearance to a Leclair-Mussardo series. Various UV limit tests suggest that their result is correct, and yet the mismatch with the result of Woynarovich stayed unexplained. This discrepancy was finally understood by Pozsgay as a nontrivial measure that must be taken into account when the discrete quantum number description is replaced by a continuous distribution of momenta. For a periodic system, this measure precisely cancels the fluctuations around the saddle point, the paradox is resolved. The lesson we can draw from this rather long history is that there could be serious flaw in our understanding of TBA.

As we will show throughout this thesis, these quantities can all be obtained by the direct summation method in a uniform fashion. We also obtain with this method an observable that is inaccessible by the original approach: the cumulants of the conserved charges in a generalized Gibbs ensemble (see below).

Let us explain how the method works. The first step is to choose a complete basis of states each one of which is labeled by a set of Bethe quantum numbers. The thermal observable that we seek to compute is then written as a double sum: over the number of particles and over the quantum numbers. The second step is to remove the constraint (if any) between mode numbers. This constraint is model dependent, for instance if Bethe's wave functions are of *fermionic* type, then mode numbers are pairwise different and this constraint can be eliminated by insertion of $1 - \delta$ symbol. The next step is to approximate the sums over mode numbers by integrals over the corresponding rapidities. This approximation is exact up to exponential correction in volume. The Jacobians of this change of variables are Gaudin determinants, which

are known in the literature for describing the norm of Bethe's wave functions. Such determinant also appeared in Pozsgay derivation of g-function. We note however that Pozsgay performed a change of variables for the thermodynamic state, thus leading to a thermodynamic version of the Gaudin determinant that we consider here. Before describing the next steps, let us take a moment to make some comments regarding the nature of this approach

- Compared to the traditional derivation, the direct summation method is certainly more involved. There is only one state in the original approach: the thermodynamic state. Moreover, the determination of this state can be relied on a powerful physics principle in addition to Bethe's ansatz, namely the minimization of the free energy. There is nothing similar to that in our approach as we just write down the thermal trace and perform the infinite sum. The partial absence of physical laws means more freedom however and can sometimes be in favor of our method, attributing to its versatility. For instance, it can derive the three above mentioned observables without the need for fundamental modifications.
- The steps described above are "textbook" manipulations of low-temperature expansion and are very common in the literature. Usually the series is truncated and explicit analytic expressions of the first few terms are obtained. With enough supporting evidences one can even guess the entire series based on these terms. In fact this is exactly how the Leclair-Mussardo series was conjectured and also how Dorey *et al.* obtained their formula of the finite-temperature g-function. The peculiarity in our approach is that we treat the entire series, no truncation is needed.

So, how can we perform an exact summation of such infinite series? The trick is not to compute the Gaudin determinants analytically but to consider their diagrammatic expansion. As a direct consequence of Bethe's equations, the Gaudin matrix is the sum of a diagonal matrix and a Laplacian matrix i.e. a matrix in which the elements in each row sum up to zero. The matrix-tree theorem and its variants from graph theory allow its determinant to be written as a sum over combinatorial objects. The equation satisfied by the generating function of these objects can be read off from their combinatorial structure prescribed by the theorem. In the simplest case of the free energy of a periodic system the graphs are trees and this equation is nothing but the well-known TBA equation. For more involved observables, there are additional types of graphs and/or extra structures imposed on them.

Now that we have described the method of direct summation and some of its applications, let us discuss the limitations.

- In the first step we made two assumptions: first, there is no constraint between the numbers of different types of Bethe roots and second, all rapidities are real. These assumptions hold only for theories with a non-degenerate mass spectrum and the S-matrix is thus purely elastic. In other models at least one of them is violated.
- In the second step, unphysical states appear when we remove the constraint between mode numbers. For instance, if we expand the product of Kronecker symbols then some rapidities are forced to take coinciding values. To perform the sum over these states, we

must know how the observable in question acts on them. For the observables that we have considered, such action is a straightforward generalization of the action on physical states. However, there could be cases where this generalization is no longer trivial.

- Finally, what is the extend of the matrix tree theorem? Can it describe the Gaudin determinant corresponding to more exotic Bethe equations? Up to this point the various forms and corollaries of this theorem provided in the work of Chaiken [48] suffice our needs. On the other hand, it would be interesting to find a physically meaningful Bethe equation that leads to a variant of the matrix-tree theorem that has never appeared in the mathematical literature before.

The issue with the first step is serious and at this point we do not have a satisfying solution. However, we can have a diagrammatic interpretation of the known TBA equations of models with non-diagonal S-matrix. Let us illustrate this idea for the $SU(2)$ chiral Gross-Neveu model. The Bethe equations of this theory involve physical roots and auxiliary roots, the number of latter should not exceed half the number of the former, as dictated by their algebraic construction. To derive the TBA of this model by the direct summation method, we must perform the sum over the number of particles while respecting this constraint, which is an impossible task. The traditional approach however, succeeded in obtaining the correct TBA using the string hypothesis. The resulting TBA system involves the physical Bethe root and an infinite number of strings of auxiliary roots. Now if we apply the steps described above in the reverse order, we could say that had we started with not two, but an infinite number of Bethe roots without any algebraic constraint between their numbers, then we would end up with the correct TBA equations. Needless to say, both assumptions are incorrect: strings of auxiliary roots only exist in the thermodynamic limit and the inequality between their number and the number of physical root must always be respected. The point is however, that if we incorporate these assumptions into the summation method, then the final result is a correct system of TBA equations. In other words, the original honest sum over physical roots and auxiliary roots with constraint can be mimicked by a sum over physical roots and strings of auxiliary roots without constraint.

This replacement of the honest summation could either be seen as a mundane manipulation of the known TBA equations or it could be taken more seriously, namely it could work for other observables as well. Both points of view are justified and in this thesis we decide to experiment with the second: suppose the equivalence between the two summations described above, what is the implication on other observables of the theory, such as its g-function? Applying this idea for the $SU(2)$ chiral Gross-Neveu model and more generally for the current-perturbed $SU(2)_k$ WZNW model, we find that the resulting g-function is divergent, at least in the IR and UV limit. This means that we cannot simply replace the honest summation by an unrestricted sum involving magnon strings in the case of theories with boundary. However we find that the two divergences are of the same order and if we normalize the g-function by its IR value then the result is finite and can even match a CFT g-function for even values of k . This normalization amounts to removing graphs made entirely of auxiliary Bethe roots.

Our conclusion regarding the efficiency of the method of direct summation in $1+1$ dimensional integrable quantum field theories is the following. For theories with diagonal S-matrix, it can derive any known observable that can be obtained within the original TBA approach. It is

in fact more robust than the latter, as the derivation of these observables does not require any significant modification of the method. On the other hand, the original approach appears to be more suitable for theories with non-diagonal S-matrix, with the string hypothesis as an advantage. Nonetheless, our partial result shows that the method of direct summation is not completely impotent in this case and further study is needed for a definitive settlement.

Before I could investigate the applications of this method in the wrapping problem of $\mathcal{N} = 4$ SYM, I stumbled upon some unexpected connections with *Generalized Hydrodynamics* (GHD), a recently proposed framework to describe transport properties of integrable systems out-of-equilibrium. Quantum transport has attracted much attention lately in view of the groundbreaking advances in experiments that can now probe the dynamics of one-dimensional many-body systems in a controlled manner [10, 49, 50]. From a theoretical point of view, transports in one dimension is somewhat special in that most of them are expected to be anomalous (non-diffusive) [51–53]. An exception being integrable systems where not only ballistic transport [54–56], but also other type of transports such as diffusive and super-diffusive transports can in fact occur [57–60]. In order to provide a coherent understanding in the transport phenomena in integrable systems, a hydrodynamic approach was proposed [61, 62] and coined Generalized Hydrodynamics. It was originally capable of describing only the dynamics at the Euler scale (leading contribution of the derivative expansion with respect to the space coordinates), but was later extended to capture the sub-leading i.e. diffusive effect [63]. Moreover, it can take into account the presence of an external potential [64], which is necessary to simulate ultracold atom gases. To this end, there have been experimental supports [65] for the validity of GHD.

Being a hydrodynamic theory, the main assumption of GHD is that, inside an appropriate time window (the hydrodynamic time scale), the average of local operators can be evaluated in a local state with maximum local entropy. In integrable systems, maximal entropy states are described by *generalized Gibbs ensembles* (GGE): an extension of Gibbs ensembles with an infinite number of inverse temperatures β^i coupled to the conserved charges. The assumption of local maximal entropy hence reads explicitly

$$\langle \mathcal{O}(x, t) \rangle \approx \langle \mathcal{O}(0, 0) \rangle_{\tilde{\beta}(x, t)}. \quad (1)$$

This equation is the main source of criticism towards GHD: what is its order of exactitude, what is its precise domain of validity, how can it be rigorously proven?... On the other hand, if we ignore these questions then equation (1) allows GHD to exploit the power of exact solubility. If the inverse temperatures (GGE profile) are known at every point in space-time then the average of local operators can be computed using TBA¹. The main problem in GHD is therefore to determine the space-time dependence of the GGE profile. At Euler scale this problem can be solved, provided that we know the average currents carried by the local state. The form of the average currents is a cornerstone of GHD, as all transport properties of the theory are derived from it.

¹The TBA of GGE was first derived in [66], there is not much difference compared to the TBA of a Gibbs ensemble, one simply includes in the TBA source term an infinite number of chemical potentials.

The currents are related to the corresponding conserved charge densities through a continuity equation. Although this equation is simple and the average of the conserved charge densities is well-known in TBA, the task of finding the average currents is not so trivial. For integrable quantum field theories, the first derivation was presented in [61, 62] using a double Wick rotation. The main idea is to regard the currents as the conserved charge densities of the mirror theory (as a result of the continuity equation) and to use the mirror TBA to recover their average. There are however two issues with this derivation. First, the assumed analyticity of the TBA source term does not necessarily hold for all GGEs. Second, the trick of using a double Wick rotation works solely for quantum field theories and this derivation cannot be extended to spin chains or integrable gases, which constitute a large part of GHD applications. We find a new derivation of the average currents using the Leclair-Mussardo formula and a diagrammatic representation of the relation between connected and symmetric form factors. Our derivation has recently been extended to integrable spin chains by Pozsgay *et al.* [67].

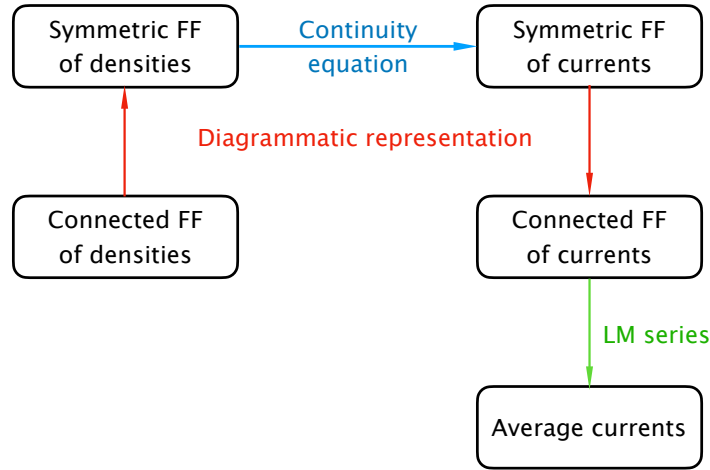


Figure 1: The schema of our derivation of the average currents in GHD.

Going beyond the average currents, one can study transport fluctuation, manifested by rare events with large deflection from their expected values. The probabilities of these events are encoded in the cumulants of the time-integrated currents carried by the local state. Although these cumulants were predicted by linear fluctuating hydrodynamics [68, 69], their complicated expressions obscure their physical virtues. We conjecture that they are in fact very similar to the cumulants of the corresponding conserved charges. The latter can be obtained by the direct summation method and are represented by a sum over trees with TBA quantities on their vertices and propagators. With only minor modifications, the same diagrams can be used to express the cumulants of the time-integrated currents. We confirm this proposal by a non-trivial matching with the analytic results of [68, 69] up to the fourth cumulant. Our conjecture highlights a remarkably simple duality between time-integrated currents and conserved charges.

It should be stressed that neither the average currents nor higher cumulants were obtained by the direct summation method. They are simply related to quantities which can be derived by this method. Given their diagrammatic representations however, one can apply the method in reverse to find the corresponding matrix element. This has been done in [67] for the current.

The thesis is organized as follows. In chapter 1 we summarize basic features of integrable quantum field theories. Chapter 2-4 present the applications of the direct summation method: the TBA equation, the Leclair-Mussardo series, the excited state energies and the cumulants of conserved charges in chapter 2, the g-function for theories with diagonal S-matrix in chapter 3 and the g-function for integrable perturbed $SU(2)_k$ WZNW models in chapter 4. Finally, connections with GHD are presented in chapter 5. Except for the derivation of the TBA equation, which has previously appeared in the literature [70–72] in an almost identical form, all results from chapter 2 to 5 are original.

The thesis is based on the following papers

- I. Kostov, D. Serban, D-L. Vu, "*TBA and tree expansion*", Springer Proc.Math.Stat. 255 (2017) 77-98. (chapter 2)
- I. Kostov, D. Serban, D-L. Vu, "*Boundary TBA, trees and loops*", Nucl.Phys.B 949 (2019) 114817. (chapter 3)
- I. Kostov, D. Serban, D-L. Vu, "*Boundary entropy of integrable perturbed $SU(2)_k$ WZNW*", JHEP 08 (2019) 154. (chapter 4)
- D-L. Vu, T. Yoshimura, "*Equations of state in generalized hydrodynamics*", SciPost Phys. 6 (2019) 2, 023. (chapter 5)
- D-L. Vu, "*Cumulants of conserved charges in GGE and cumulants of total transport in GHD: exact summation of matrix elements?*", J.Stat.Mech. 2002 (2020) 2, 023103. (chapter 2 and 5)

Chapter 1

Preliminary

1.1 Basics of integrable quantum field theories

1.1.1 Some examples

We present in this subsection a list of integrable quantum field theories that will later appear at some point in this thesis. One of the most famous iQFT's is the sine-Gordon model, the Lagrangian density of which is given by

$$L_{\text{SG}} = \frac{1}{2}(\partial_\mu \phi)^2 + \frac{m_0^2}{\beta^2} \cos(\beta \phi). \quad (1.1)$$

The existence of classically conserved currents in this theory was established by the inverse scattering method [73–75]. These conservation laws were then shown to survive after quantization by the perturbation theory approach [76]. The particle content of the theory includes a soliton, an anti-soliton and their bound states (breathers) with masses $m_k = 2m \sin(k\gamma/16)$ for $k = 1, 2, \dots < 8\pi/\gamma$, where m is the mass of the soliton and $\gamma = \beta^2/[1 - \beta^2/(8\pi)]$ [77, 78]. It was argued in the seminal work [79] that this theory is actually equivalent to the massive Thirring model with Lagrangian density

$$L_{\text{Thirring}} = i\bar{\psi}\gamma_\mu \partial^\mu \psi - m\bar{\psi}\psi - \frac{g}{2}(\bar{\psi}\gamma_\mu \psi)^2, \quad (1.2)$$

where $\psi, \bar{\psi}$ is the Dirac field and the four-fermion coupling constant g is related to β in (1.1) as $g/\pi = 4\pi/\beta^2 - 1$. When the Dirac field belongs to the fundamental representation of the $SU(N)$ group, the massive Thirring model is also known as the chiral Gross-Neveu model

$$L_{\text{GN}} = \bar{\psi}_a(i\not{\partial} - m)\psi_a + g[(\bar{\psi}_a\psi_a)^2 - (\bar{\psi}_a\gamma^5\psi_a)^2], \quad a = \overline{1, N}. \quad (1.3)$$

The theory was shown to be integrable at classical level in [80] and at quantum level in [26]. Each particle of the theory is in one-to-one correspondence with fundamental representations of the $SU(N)$ group [81]. The particle corresponding to the Young tableau of one column and a rows is a bound state of a vector particles and has mass $m_a = m \sin(\pi a/N)/\sin(a/N)$, $a = \overline{1, N-1}$. In particular the $SU(2)$ chiral Gross-Neveu model is equivalent to the sine-Gordon theory at $\beta^2 = 8\pi$.

A cousin of the sine-Gordon theory is the sinh-Gordon theory

$$L_{\text{SnhG}} = \frac{1}{2}(\partial_\mu \phi)^2 - \frac{m_0^2}{\beta^2} \cosh(\beta \phi). \quad (1.4)$$

Compared to the sine-Gordon theory, the particle content of the sinh-Gordon theory is much simpler as there is only one particle. The sinh-Gordon theory is an example of affine Toda field

theories [82], which form a large family of integrable models. The Lagrangian density of the Toda field theory corresponding to a Lie algebra \mathfrak{g} of rank r is defined as

$$L_{\text{Toda}} = \frac{1}{2} \partial_\mu \phi^a \partial^\mu \phi^a - \frac{m_0^2}{\beta^2} \sum_{i=0}^r e^{\beta \alpha_i \cdot \vec{\phi}}, \quad (1.5)$$

where $\phi^a, a = 1, \dots, r$ are r real scalar fields and $\alpha_i, i = 1, \dots, r$ are positive simple roots of \mathfrak{g} while α_0 is the negative of its maximal root. Without the α_0 term, the theory is conformal [83–85], and is referred to as conformal Toda field theories. With the α_0 term, conformal invariance is broken but integrability is preserved, one talks about an *integrable perturbation of CFT*. The classical and quantum integrability of affine Toda field theories was shown in [86–88] and [89] respectively.

The systematic study of integrable perturbations of CFTs was initiated by Zamolodchikov in [25]. The author explicitly constructed the integrals of motion of the three-state Potts model in terms of the operator algebra of the conformal field theory describing its critical point. This CFT is the minimal model $\mathcal{M}_{5,6}$ and the perturbing operator is $\Phi_{1,2}$ of dimension $(2/5, 2/5)$. It is the intersection of two families of integrable perturbed CFTs: the first is $\mathcal{M}_{p,p+1}$ perturbed by $\Phi_{1,2}$ operator [90] and the second is \mathbb{Z}_n parafermion perturbed by operator of dimension $(2/(n+2), 2/(n+2))$ [91, 92]. The case of perturbed \mathbb{Z}_4 parafermion is equivalent to the sine Gordon model at the coupling $\beta^2 = 6\pi$. Another example of integrable perturbed CFTs is the scaling Lee Yang model. It is obtained by deforming the minimal model $\mathcal{M}_{2,5}$ in the direction of its only relevant operator namely the $\Phi_{1,3}$ operator. Moreover it was shown that the $\mathcal{M}_{2,2n+3}$ minimal models perturbed by their $\Phi_{1,3}$ operator [93, 94] are also integrable. The general procedure to construct integrals of motion in perturbed CFTs is described in [95].

The $SU(N)$ chiral Gross-Neveu can itself be regarded as a perturbed CFT. Indeed, using the technique of nonabelian bosonization [96], the Lagrangian (1.3) can be written as the current-perturbed $U(N)_1$ WZNW theory [97], [98]. The $U(1)$ center is identified with a massless boson that decouples from the rest of the spectrum.

Another source of iQFT comes from sigma models. A sigma model is a field theory where the field takes values in a manifold \mathcal{M} with a metric g_{ij}

$$L_\Sigma = g_{ij}(X) \partial_\mu X^i \partial^\mu X^j.$$

The theory is classically integrable for a large family of manifolds called a symmetric spaces [99]. A symmetric space is a manifold G/H where G and H are Lie groups, and H is a maximal subgroup of G i.e. no normal sub group other than G itself contains H . On the other hand, quantum integrability is more restricted. Two well known examples are *principal chiral model*, where $G = H \times H$ and H is a simple Lie group [100] and the $O(n)$ model [101, 102], where $G = O(n)$ and $H = O(n-1)$.

1.1.2 Consequences of higher conserved charges on the S matrix

The existence of infinitely many conserved charges in a theory impose the following constraints on its scattering processes

- There is no particle production,

- the sets of initial and final momenta are identical,
- *factorization*: the n -to- n S-matrix is a product of $n(n-1)/2$ two-to-two S-matrices

The validity of these properties was first backed up by an heuristic argument of Zamolodchikov and Zamolodchikov [26]. More arguments were given in [103,104] and a relatively rigorous proof was presented in [105]. We sketch here the essential ideas of this proof.

In the far past (future) the *in* (*out*) state can be regarded as a collection of non-interacting particles, if we assume that all interactions are short-ranged. In an *in* state, the fastest moving particle is found on the furthest left while the slowest one on the furthest right. In an *out* state, the inversed order applies. The existence of a higher conserved charge Q implies that

$$\langle \text{out} | \mathcal{S} | \text{in} \rangle = \langle \text{out} | e^{i\alpha Q} \mathcal{S} e^{-i\alpha Q} | \text{in} \rangle \quad (1.6)$$

As the asymptotic states are tensor products of one-particle wavefunction, the charge Q acts on these states component-wise. Due to its higher Lorenz spin, the effect of Q on an one-particle wavefunction is to shift it in space-time by an amount that depends on the particle momentum. The precise amount of this shift can be obtained by saddle point approximation on a Gaussian wave function peaked around the particle momentum, we refer to the original paper for more details.

With this in mind, consider now a $2 \rightarrow n$ scattering process, with the particles labelled as in figure 1.1. Let us denote by t_{12} and t_{23} the collision time between the particle 1 and 2 and particle 2 and 3 respectively. According to the principle of macrocausality, the following inequality must be respected

$$t_{12} \leq t_{23} \quad (1.7)$$

Assume for a moment that the momentum of the particle 3 is not the same as that of the particle 1. According to the above statement, one can choose the parameter α in (1.6) in such a way that the charge Q shifts the collision time t_{12} arbitrarily high and t_{23} arbitrarily low. This violation of macrocausality leads to the conclusion that the momentum of the fastest out-going particle must coincide with that of the fastest incoming particle. Similary, one can match the momentum of the slowest out-going particle with that of the slowest incoming one. Energy-momentum conservation then dictates the absence of particle production. To summarize, the only possible outcome of a two particle scattering process is two particles with the same momenta as the incoming ones.

For an n -particle scattering process, we can once again act with Q on a certain incoming particle, moving it away from the scattering region of the other $n-1$ particles. Once all the

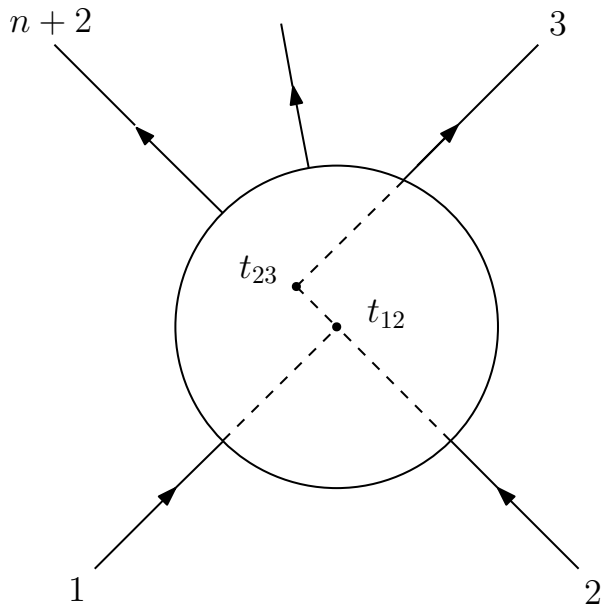
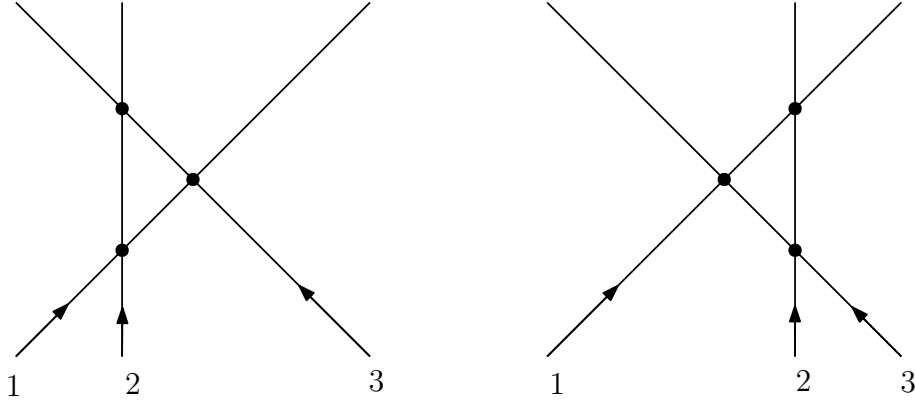


Figure 1.1: Space-time diagram of a two-to- n scattering process

interactions among these particles have occurred, one can consider the scattering of the outgoing particles with that particular particle. By induction, we see that there is no particle production, and the final set of momenta must be identical to the initial set of momenta. Furthermore, the n -to- n S-matrix is a product of $n(n-1)/2$ two-to-two S-matrices. \square

The factorization property gives rise to important characteristics of the two-to-two S-matrix. Indeed, we have found that all the possible ways of factorizing an n -to- n S-matrix into two-to-two S-matrices must lead to the same result. In particular, let us consider a three-to-three scattering process. We can use the charge Q to separate either the first or the third particle. This leads to two different scenarios



The equivalence between the two processes leads to the Yang-Baxter equation

$$\mathcal{S}_{23}\mathcal{S}_{13}\mathcal{S}_{12} = \mathcal{S}_{12}\mathcal{S}_{13}\mathcal{S}_{23}. \quad (1.8)$$

We note that the Yang-Baxter equation is a consequence of the existence of higher conserved charges, it is by no mean a sufficient condition for integrability.

1.1.3 The two particle S-matrix

The previous section has shown the importance of the two particle S-matrix. In this section we study its physical properties and analytic structure.

Let us denote by θ_1 and θ_2 the rapidities of the incoming particle, with $\theta_1 > \theta_2$ and by θ_3 and θ_4 the rapidities of out-going particles, with $\theta_3 < \theta_4$. As established above, we only have non-trivial scattering for $\theta_4 = \theta_1, \theta_3 = \theta_2$. A two-particle elastic relativistic S-matrix is then given by

$$|\theta_1, \theta_2\rangle_{i,j}^{\text{in}} = S_{ij}^{kl}(\theta_{12})|\theta_1, \theta_2\rangle_{k,l}^{\text{out}} \quad (1.9)$$

and represented graphically in figure 1.2, the indices i, j, k, l denote particle type and $\theta_{12} \equiv \theta_1 - \theta_2$. When $S_{ij}^{kl} \propto \delta_i^k \delta_j^l$ we say that the S-matrix is *diagonal*, otherwise we say that it is *non-diagonal*. One can also work in Mandelstam variables

$$\begin{aligned} s &= (p_1 + p_2)^2 = m_i^2 + m_j^2 + 2m_i m_j \cosh(\theta_{12}) \\ t &= (p_1 - p_3)^2 = m_i^2 + m_l^2 - 2m_i m_l \cosh(\theta_{13}) \\ u &= (p_1 - p_4)^2 = m_i^2 + m_k^2 - 2m_i m_k \cosh(\theta_{14}) \end{aligned} \quad (1.10)$$

which are the square of the center-of-mass energies in the channels defined by the process $i + j \rightarrow k + l$ (s -channel), $i + \bar{l} \rightarrow k + \bar{j}$ (t -channel) and $i + \bar{k} \rightarrow l + \bar{j}$ (u -channel) respectively. One finds that $u = 0$ and $t(\theta_{12}) = s(i\pi - \theta_{12})$, meaning the S-matrix depends only on one variable, say $S = S(s)$.

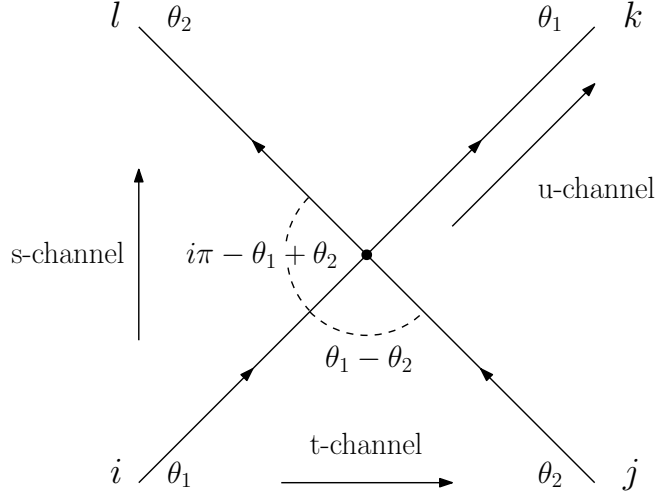


Figure 1.2: The two particle scattering

The C, P, T invariance dictates the symmetry of S as a matrix

$$S_{\bar{i}\bar{j}}^{\bar{k}\bar{l}}(s) = S_{ij}^{kl}(s), \quad S_{ij}^{kl}(s) = S_{ji}^{lk}(s), \quad S_{ij}^{kl}(s) = S_{lk}^{ji}(s). \quad (1.11)$$

Let us now discuss analytic properties of S . One important property is crossing symmetry. It means the freedom to choose between the s - and t -channels without affecting the scattering amplitude

$$S_{ij}^{kl}(s) = S_{\bar{i}\bar{l}}^{\bar{j}\bar{k}}(t). \quad (1.12)$$

As in a generic QFT [106], the S-matrix has a branch cut running from the two-particle threshold $s = (m_i + m_j)^2$ to infinity. Due to crossing symmetry (1.12), another cut runs from $(m_i - m_j)^2$ towards minus infinity. However, S has a distinctive feature owed to the lack of particle production namely it does not have further cuts coming from multi-particle thresholds. With these two cuts, S is a single-valued, meromorphic function on the complex s -plane. The physical region situating just above the right cut defines the physical sheet of the Riemann surface for S . By combining the unitarity condition in the physical region

$$S_{ij}^{kl}(s)[S_{lk}^{nm}(s)]^* = \delta_i^n \delta_j^m \quad (1.13)$$

with the real analyticity property

$$S_{ij}^{kl}(s^*) = [S_{ij}^{kl}(s)]^* \quad (1.14)$$

we can show that the two cuts are of square-root type [107]. In principle, analytically continuing S through one cut might end up on a different sheet than the one obtained through the other

cut. Hence, the Riemann surface of the S-matrix consists in general of several sheets, possibly infinite.

The structure of this Riemann surface turns out to be more transparent if we map the s-plane to the rapidity plane

$$\theta_{12} = \operatorname{arccosh}\left(\frac{s^2 - m_1^2 - m_2^2}{2m_1m_2}\right) = \log \frac{s^2 - m_1^2 - m_2^2 + \sqrt{[s - (m_1 + m_2)^2][s - (m_1 - m_2)^2]}}{2m_1m_2}.$$

The right (left) cut is mapped into $\mathbb{R} + 2i\pi\mathbb{Z}$ and $\mathbb{R} + i\pi + 2i\pi\mathbb{Z}$ respectively. The physical sheet of the s-plane corresponds to the strip $0 \leq \Im(\theta_{12}) \leq \pi$ in the theta-plane. Furthermore, the original cuts are opened up and $S(\theta)$ is analytic at the images $i\pi\mathbb{Z}$ of the branch points. In conclusion, $S(\theta)$ is a meromorphic function of θ . Unitarity (1.13) and crossing (1.12) are written in rapidity variable as

$$S_{ij}^{kl}(\theta)S_{lk}^{nm}(-\theta) = \delta_i^n \delta_j^m, \quad S_{ij}^{kl}(\theta) = S_{ji}^{\bar{k}\bar{l}}(i\pi - \theta). \quad (1.15)$$

The real analyticity in the s-plane (1.14) implies that $S(\theta)$ is real when θ is purely imaginary. Multiplying the S-matrix by any function $F(\theta)$ which satisfies $F(\theta)F(-\theta) = 1$ and $F(i\pi - \theta) = F(\theta)$ will give an S matrix still obeying the Yang-Baxter equation, crossing and unitarity. Such function F is called a CDD factor.

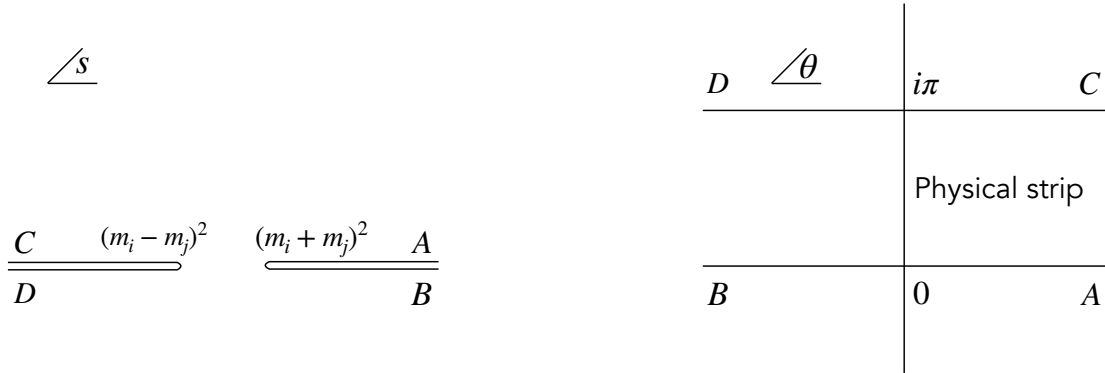


Figure 1.3: Analytic structure of the two particle S-matrix on the s and θ plane.

The two-particle S-matrix can also have simple poles related to bound states. In the s-plane, these poles are found between the two-particle thresholds i.e. $(m_i - m_j)^2$ and $(m_i + m_j)^2$. This interval is mapped into the interval $(0, i\pi)$ in the θ -plane. Denote by iu_{ij}^n a simple pole corresponding to a bound state n formed by two particles i and j . The mass of this bound state is given by

$$m_n^2 = m_i^2 + m_j^2 + 2m_i m_j \cos u_{ij}^n. \quad (1.16)$$

This identity admits a simple geometric interpretation: the three masses are three sides of a triangle and the real part of the pole is one of its outside angles, see figure 1.4.

This geometric point of view also hints at a democracy between bound states and elementary particles. For instance, one can regard i and j themselves as bound states formed respectively by j, n and i, n particles. If one can even find the scattering matrix between these particles, then the corresponding poles in the physical strip u_{jn}^i and u_{in}^j must satisfy

$$u_{ij}^n + u_{jn}^i + u_{ni}^j = 2\pi. \quad (1.17)$$

One can proceed and scatter this bound state with other particles and other bound states, looking for poles and new bound states. Consistency of the theory requires that this procedure closes upon itself, namely one should always end up with a finite set of particles. This is the idea of S-matrix bootstrap principle [95]. The problem of finding S-matrix of bound states can be solved by the so-called fusion method [108–110]. In the following section we will bootstrap the S-matrix of the $SU(N)$ chiral Gross-Neveu model.

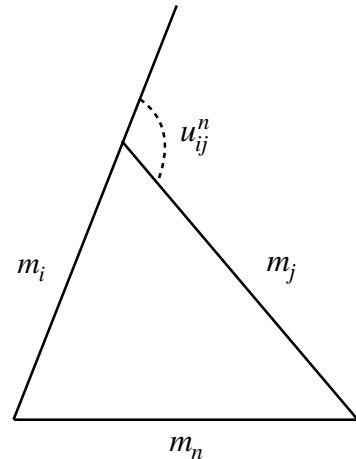


Figure 1.4: The mass triangle

1.1.4 Finding the two-particle S-matrix: an example

In many integrable models [110–115], the S-matrix can often be fixed by a variety of constraints: the Yang-Baxter equation (1.8), unitarity and crossing symmetry (1.15), global symmetries, the consistency of bound states and finally, by requiring that the bootstrap procedure closes. One can then check that the obtained S-matrix is indeed the correct one by computing the free energy of the model (for instance by the Thermodynamic Bethe Ansatz method that will be described in the next sections) and ensuring that it agrees with the correct results in various limits. We illustrate this idea for the $SU(N)$ chiral Gross-Neveu model.

To remind, each particle of the theory is in one-to-one correspondence with fundamental representations of the $SU(N)$ group. The particle corresponding to the Young tableau of one column and a rows is a bound state of a vector particles. According to the previous section, S-matrices between bound states can be referred from those between elementary particles. The S-matrix between vector particles is therefore all we need to find.

Invariance under the $SU(N)$ group implies that the S-matrix can be expressed as linear combinations of projection operators. In the case of vector particles, only the symmetric and antisymmetric representation appear in their tensor product. The S-matrix of two vector particles can thus be written as

$$S_{VV}(\theta) = f_{VV}^S(\theta)\mathcal{P}_S + f_{VV}^A(\theta)\mathcal{P}_A, \quad (1.18)$$

where the projection operators on the symmetric (S) and antisymmetric (A) tensors are given by

$$\begin{aligned} \mathcal{P}_S[a_i(\theta_a)b_j(\theta_b)] &= \frac{1}{2}[a_i(\theta_a)b_j(\theta_b) + a_j(\theta_a)b_i(\theta_b)], \\ \mathcal{P}_A[a_i(\theta_a)b_j(\theta_b)] &= \frac{1}{2}[a_i(\theta_a)b_j(\theta_b) - a_j(\theta_a)b_i(\theta_b)]. \end{aligned}$$

The subscripts in a_i and b_j represent the i and j particles in the vector multiplets. The advantage of expressing the S-matrix in terms of projection operators is that the Yang-Baxter equation (1.8) greatly simplifies. It can be shown that the two coefficients in (1.18) must satisfy [116]

$$\frac{f_{VV}^A(\theta)}{f_{VV}^S(\theta)} = \frac{\theta + 2\pi i \Delta}{\theta - 2\pi i \Delta}, \quad (1.19)$$

where Δ is a parameter that cannot be fixed by the Yang-Baxter equation. Unitarity and crossing symmetry then requires that

$$f_{VV}^S(\theta) = X(\theta) F_{VV}^{\min}, \quad \text{with} \quad F_{VV}^{\min} = \frac{\Gamma(1 - \frac{\theta}{2\pi i}) \Gamma(\frac{\theta}{2\pi i} + \Delta)}{\Gamma(1 + \frac{\theta}{2\pi i}) \Gamma(-\frac{\theta}{2\pi i} + \Delta)}. \quad (1.20)$$

In this expression $X(\theta)$ is a CDD phase and F_{VV}^{\min} is called the minimal solution, because the corresponding S-matrix has no pole in the physical strip.

The CDD phase can be determined by looking at the bound states structure of model. As there are bound states in the antisymmetric representation of $SU(N)$, but not in the symmetric representation, there must be a pole in f_{VV}^A but not in f_{VV}^S . The relation (1.19) tells us that this pole is situated at $\theta = 2\pi i \Delta$, corresponding to a bound-state with mass $m_A/m_V = 2 \cos \pi \Delta$. Such pole has been canceled by the minimal solution and so the CDD factor must reintroduce it into the S-matrix

$$X(\theta) = \frac{\sinh(\theta/2 + \pi i \Delta)}{\sinh(\theta/2 - \pi i \Delta)}.$$

Now that we have obtained the S-matrix of vector particles as a function of Δ , we can apply the bootstrap procedure. By requiring that the bootstrap closes, we can fix this parameter to be $\Delta = 1/N$ [117, 118]. We conclude that the vector-vector S-matrix of the chiral $SU(N)$ Gross-Neveu model is given by

$$\mathcal{S}_{VV}(\theta) = \frac{\sinh(\theta/2 + \pi i/N)}{\sinh(\theta/2 - \pi i/N)} \frac{\Gamma(1 - \frac{\theta}{2\pi i}) \Gamma(\frac{\theta}{2\pi i} + \frac{1}{N})}{\Gamma(1 + \frac{\theta}{2\pi i}) \Gamma(-\frac{\theta}{2\pi i} + \frac{1}{N})} \left(\mathcal{P}_S + \frac{\theta + 2\pi i/N}{\theta - 2\pi i/N} \mathcal{P}_A \right). \quad (1.21)$$

The S-matrices between other particles in the spectrum can be built from this S-matrix by fusion method.

1.1.5 The Bethe equation of $SU(2)$ chiral Gross-Neveu model

With the two-particle S-matrix at hand, one can find the on-shell condition of an asymptotic state living in a finite, periodic but very large (compared to the inverse mass scale) volume L . We consider as example the $SU(2)$ chiral Gross-Neveu model. There is only the vector multiplet in this theory, so the vector-vector S-matrix (1.21) is all we need

$$\mathcal{S}^{SU(2)}(\theta) = \frac{\theta - \pi i \mathcal{P}}{\theta - \pi i} S_0^{SU(2)}, \quad S_0^{SU(2)}(\theta) = -\frac{\Gamma(1 - \theta/2\pi i) \Gamma(1/2 + \theta/2\pi i)}{\Gamma(1 + \theta/2\pi i) \Gamma(1/2 - \theta/2\pi i)}. \quad (1.22)$$

The periodicity condition imposed on the wave function $|\Psi\rangle = |\theta_1, \theta_2, \dots, \theta_N\rangle$ when a particle of rapidity θ_j is brought around the circle and scatters with other particles reads

$$e^{-ip(\theta_j)L}\Psi = \prod_{k \neq j} \mathcal{S}^{\text{SU}(2)}(\theta_j, \theta_k)\Psi, \quad j = \overline{1, N}.$$

In this equation, the product runs on the index k and this rule is implicitly understood from now on. Using the fact that the scattering matrix at coinciding rapidity is exactly minus the permutation operator, one can cast the above equation in the following form

$$e^{-ip(\theta_j)L}\Psi = -T^{\text{SU}(2)}(\theta_j)\Psi, \quad j = \overline{1, N}. \quad (1.23)$$

where $T(u) = \text{Tr}_{\mathbb{C}_u^2}[\mathcal{S}(u, \theta_1) \dots \mathcal{S}(u, \theta_N)]$ is the transfer matrix. The advantage of writing Bethe equations in this form is that we can now regard the physical rapidities θ_j 's as non-dynamical impurities on a spin chain. The argument u of the transfer matrix plays the role of the rapidity of an auxiliary particle living in time direction. Up to a scalar factor, T is also the transfer matrix of the XXX spin chain with Hamiltonian

$$H = -J \sum_{i=1}^N (\vec{\sigma}_i \cdot \vec{\sigma}_{i+1} - 1),$$

where $\vec{\sigma}$ are Pauli matrices with periodicity $\sigma_{N_f+1} = \sigma_1$. For $J > 0$ this is a model of a ferromagnet where spins prefer to align, while for $J < 0$ we have an antiferromagnet where spins prefer to alternate.

As a consequence of the Yang-Baxter equation, the transfer matrices at different values of the spectral parameters commute with each other $[T(u), T(v)] = 0$. By developing the transfer matrix in powers of u , we can obtain a tower of commuting observables, one of which is the Hamiltonian. The transfer matrix can be diagonalized by the technique of algebraic Bethe ansatz [119]. Its eigenvalues are parametrized by a set of spin chain excitations u_1, \dots, u_M . Replacing these eigenvalues into (1.23) one obtains the "physical" Bethe equation for the $SU(2)$ chiral Gross-Neveu model

$$1 = e^{ip(\theta_j)L} \prod_{k \neq j}^N S_0^{\text{SU}(2)}(\theta_j - \theta_k) \prod_{m=1}^M \frac{\theta_j - u_m + i\pi/2}{\theta_j - u_m - i\pi/2}, \quad j = \overline{1, N}. \quad (1.24)$$

The spin chain rapidities themselves must satisfy an Bethe equation on the spin chain setting

$$1 = \prod_{j=1}^N \frac{u_k - \theta_j - i\pi/2}{u_k - \theta_j + i\pi/2} \prod_{l \neq k}^M \frac{u_k - u_l + i\pi}{u_k - u_l - i\pi}, \quad k = \overline{1, M}. \quad (1.25)$$

We see that in the physical perspective, the rapidities u 's correspond to auxiliary particles with vanishing energy and momentum. By construction of algebraic Bethe ansatz, their number should not exceed half the number of physical rapidities.

1.1.6 Integrability in open systems

The scattering theory of systems with a reflecting boundary was first investigated by Cherednik in [120]. In addition to the bulk two-particle S-matrix the author proposed a reflection matrix

that describes the reflection amplitudes at boundary. This matrix must satisfy unitarity and a boundary version of the Yang-Baxter equation. The boundary analogy of crossing symmetry and bootstrap equation was later found in [121] and [122]. In this subsection we consider a simple situation where both the diagonal bulk scattering matrix and the reflection matrix are diagonal. The boundary unitarity and boundary crossing-unitarity read in that case

$$R_a(\theta)R_a(-\theta) = 1, \quad (1.26)$$

$$R_a(\theta)R_{\bar{a}}(\theta - i\pi) = S_{aa}(2\theta). \quad (1.27)$$

In particular, R is $2\pi i$ periodic. The boundary bootstrap equation that describes the reflection amplitude of a bound state c of particles a and b is given by

$$R_c(\theta) = R_a(\theta + iu_{ac}^b)R_b(\theta - \bar{u}_{bc}^a)S_{ab}(2\theta + i\bar{u}_{ac}^b - iu_{bc}^a), \quad (1.28)$$

where u denotes the fusion angle and $\bar{u} = i\pi - u$. Similar to the CDD ambiguity in the bulk S-matrix, the reflection matrix cannot be uniquely fixed from these constraints. For instance, one can multiply a solution to these equations by a solution of the bulk bootstrap, unitarity and crossing equations to obtain another viable solution. Without additional requirements, the minimal solution i.e. the one with smallest possible number of poles and zeros often proves to be physically meaningful.

Let us illustrate this idea on the affine Toda theory of type A_k . This theory consists of $k-1$ particles $a = 1, \dots, k-1$ ($\bar{a} = k-a$) with mass spectrum $m_a = m \sin(\pi a/k)/\sin(\pi/k)$. Particles a and b can form bound states at fusion angle $u_{ab}^c = (a+b)\pi/k$ and $2\pi - [(a+b)\pi/k]$. The purely elastic scattering consistent with this bound state structure was bootstrapped in [112, 123]

$$S_{ab}(\theta) = F_{|a-b|}(\theta)F_{a+b}(\theta) \prod_{s=|a-b|/2+1}^{(a+b)/2-1} F_s^2(\theta), \quad F_\alpha(\theta) \equiv \sinh\left(\frac{\theta}{2} + \frac{i\pi\alpha}{2k}\right)/\sinh\left(\frac{\theta}{2} - \frac{i\pi\alpha}{2k}\right). \quad (1.29)$$

Periodicity and boundary unitarity of the reflection factors require them to be products of the building blocks F as well. One then relies on crossing-unitarity to find the smallest number of F needed. Indeed, each pole or zero of $S_{aa}(2\theta)$ on the right hand side of (1.27) must appear in one of the two factors on the left hand side of the same equation. This condition sets a lower bound on the number of poles and zeros for the reflection factor $R_a(\theta)$. The minimal reflection factor [124]

$$R_a(\theta) = \prod_{s=0}^{a-1} F_s(\theta)F_{k+1-s}^{-1}(\theta), \quad a = \overline{1, k-1}. \quad (1.30)$$

obtained this way turned out to also satisfy the boundary bootstrap equation (1.28). This solution will be relevant for our study of g-function of current-perturbed WZNW model in chapter 4.

1.2 Thermodynamic Bethe Ansatz

In this section we present a method to describe the thermodynamics of integrable models: the thermodynamic Bethe ansatz (TBA). It was discovered by Yang and Yang [7] to study the Bose gas with delta function interaction at finite temperature. It was then extended to lattice integrable models such as Heisenberg spin chain [2, 125] and Hubbard model [24]. When applied to relativistic integrable quantum field theories, the TBA free energy density is equivalent to the ground state energy in finite volume [25].

We start with a summary of the derivation of Zamolodchikov, applicable for any massive integrable quantum field theories with diagonal scattering matrix.

1.2.1 The traditional derivation

Assume that we have a relativistic, integrable QFT with a single neutral particle of mass m . The question we try to answer is whether we can compute the ground state energy $E_0(R)$ of the theory compactified on a circle of length R from its S-matrix data? The idea of Zamolodchikov is to let the theory evolve under a very large imaginary time L . The Euclidean partition function in such toroidal geometry is dominated by the ground state energy

$$Z(R, L) \approx e^{-LE_0(R)}. \quad (1.31)$$

On the other hand, relativistic invariance allows the same partition function to be computed in the other channel, where time evolution is along the R -circle

$$Z(R, L) = \text{Tr} e^{-RH(L)} = \sum_n e^{-RE_n(L)}, \quad (1.32)$$

where $H(L)$ and $E_n(L)$ are respectively the Hamiltonian of the theory in volume L and its energy levels. This means that if we succeed at extracting the free energy density at finite temperature R from expression (1.32) then the ground state energy would simply be given by

$$E_0(R) = Rf(R). \quad (1.33)$$

Why is it possible to evaluate the trace in (1.32)? The advantage of being in very large volume L is that we can construct a basis of asymptotic states in which individual particles are well separated.

Each asymptotic state is characterized by a set of rapidities $\theta_1, \dots, \theta_N$ which are subjected to Bethe equations

$$e^{im \sinh(\theta_j)L} \prod_{k \neq j} S(\theta_j - \theta_k) = 1, \quad j = 1, 2, \dots, N. \quad (1.34)$$

Once we find a solution of this system of equation, the energy of the corresponding state is given by $E_{|\vec{\theta}\rangle}(L) = m \cosh(\theta_1) + \dots + m \cosh(\theta_n)$. In this thesis, we will mostly consider *fermionic* Bethe wave functions where the rapidities take pairwise distinguishing values. This happens when $S(0) = -1$ (+1) and the particles are of Bose (Fermi) statistics. Next, we have to decide

which states appear in the sum (1.32) i.e. what is a complete basis of the Hamiltonian $H(L)$? To answer this question, let us write the Bethe equations (1.34) in their logarithmic form

$$m \sinh(\theta_j) + \frac{1}{L} \sum_{k \neq j} [-i \ln S(\theta_j - \theta_k)] = \frac{2\pi}{L} n_j, \quad j = 1, 2, \dots, N. \quad (1.35)$$

The integers n_j that appear on the right hand side are called Bethe numbers. For some specific models [7], it can be rigorously shown that for each set of pairwise distinct integers $\{n_1, \dots, n_N\}$ the system of equations (1.35) admits a unique solution. Furthermore, the entirety of these states form a complete basis of the Hamiltonian $H(L)$. Normally, we admit this as a hypothesis.

When L tends to infinity, we can characterize the thermodynamic state by a smooth distribution $\rho_p(\theta)$ of particle rapidities. In terms of this distribution, the Bethe equation (1.35) reads

$$m \sinh(\theta_j) + \int [-i \ln S(\theta_j - \theta)] \rho_p(\theta) d\theta = \frac{2\pi}{L} n_j. \quad (1.36)$$

This equation means in particular that each density in the space of rapidity induces a density on the lattice \mathbb{Z}/L of Bethe quantum numbers. Inversely, the density of unoccupied Bethe quantum numbers induces itself a density $\rho_h(\theta)$ in the space of rapidity. We refer to ρ_p and ρ_h respectively as particles and holes density.

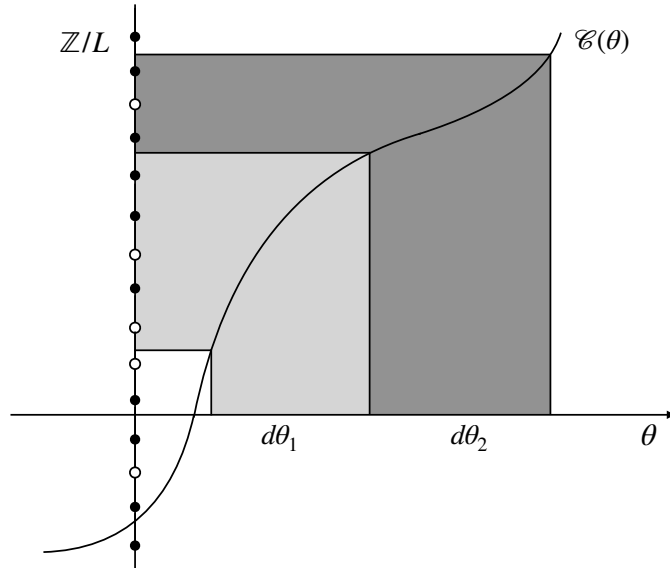


Figure 1.5: Illustration of the counting function.

To express ρ_h in terms of ρ_p we define the counting function

$$\mathcal{C}(\theta) = \frac{1}{2\pi} m \sinh(\theta) + \int \frac{d\eta}{2\pi} [-i \log S(\theta - \eta)] \rho_p(\eta). \quad (1.37)$$

It is straightforward from the definition that $\mathcal{C}(\theta_j) = n_j$. In the example shown in figure 1.5 the counting function hovers through the interval $d\theta_1$ and picks out 2 holes and 3 particles,

marking 5 sites on the lattice in total. In the interval $d\theta_2$ it encounters only 1 hole and 2 particles. This is because the counting function is steeper in $d\theta_1$ than it is in $d\theta_2$. In other words, the derivative of the counting function gives the total number of states and holes:

$$\rho_p(\theta) + \rho_h(\theta) = \mathcal{C}'(\theta) = \frac{1}{2\pi} m \cosh(\theta) + \int K(\theta - \eta) \rho_p(\eta) d\eta, \quad (1.38)$$

where $K(\theta) = -i\partial_\theta \log S(\theta)$.

We can then find the particle and hole densities of the thermodynamic state by minimizing the corresponding free energy $E - S/R$. The energy is simply given by

$$E = L \int m \cosh(\theta) \rho_p(\theta) d\theta. \quad (1.39)$$

Regarding the entropy, in an infinitesimal interval $d\theta$, the $\rho_p(\theta)d\theta$ particles and the $\rho_h(\theta)d\theta$ holes can be re-shuffled without changing the energy. The number of ways to shuffling them is equal to the number of anagrams made from $\rho_p(\theta)d\theta$ letters s and $\rho_h(\theta)d\theta$ letters h

$$\Omega(d\theta) = \frac{[\rho_p(\theta)d\theta + \rho_h(\theta)d\theta]!}{[\rho_p(\theta)d\theta]![\rho_h(\theta)d\theta]!}. \quad (1.40)$$

We can take the interval $d\theta$ to be very large compared to $1/L$ (but still very small compared to 1) so that the number of states and holes in this interval are sufficiently large. Applying the Stirling approximation, we find that the entropy of the thermodynamic state is given by

$$S = L \int_{-\infty}^{+\infty} d\theta [(\rho_p + \rho_h) \ln(\rho_p + \rho_h) - \rho_p \ln \rho_p - \rho_h \ln \rho_h]. \quad (1.41)$$

By requiring that the functional derivative of $E - S/R$ with respect to ρ_p vanishes under the constraint (1.38), we find that

$$Rm \cosh(\theta) + \ln \frac{\rho_p(\theta)}{\rho_h(\theta)} - \int \frac{d\eta}{2\pi} \ln \frac{\rho_p(\eta) + \rho_h(\eta)}{\rho_h(\eta)} K(\eta - \theta) = 0. \quad (1.42)$$

Clearly this equation involves only the relative ratio between the density of particles and holes. This is expected because at the beginning we did not have a chemical potential coupled to the number of particles. Let us define $\epsilon = -\ln(\rho_p/\rho_h)$, then equation (1.42) becomes

$$\epsilon(\theta) - Rm \cosh(\theta) + \int \frac{d\eta}{2\pi} \ln[1 + e^{-\epsilon(\eta)}] K(\eta - \theta) = 0. \quad (1.43)$$

This is called TBA equation, and ϵ is referred to as the pseudo-energy. Once we solve (1.43) for ϵ , we can plug it into (1.38) to find ρ_p and ρ_h and deduce other physical quantities from them. It turns out that the free energy can be expressed as a function of the pseudo-energy. To do this, let us multiply (1.43) with $\rho_p(\theta)$ and carry out the integration over θ

$$0 = \int d\theta [Rm \cosh(\theta) - \epsilon(\theta)] \rho_p(\theta) - \int \frac{d\eta}{2\pi} \ln[1 + e^{-\epsilon(\eta)}] \int d\theta K(\eta - \theta) \rho_p(\theta). \quad (1.44)$$

Using the density constraint (1.38), the integration over θ on the second term can be obtained

$$\int d\theta [Rm \cosh(\theta) - \epsilon(\theta)] \rho_p(\theta) = \int \frac{d\eta}{2\pi} \ln[1 + e^{-\epsilon(\eta)}] \{2\pi[\rho_p(\eta) + \rho_h(\eta)] - m \cosh(\eta)\}. \quad (1.45)$$

By using the definition of ϵ we can write the free energy in the following form

$$Rf(R) = \int d\theta [Rm \cosh(\theta) - \epsilon(\theta)] \rho_p(\theta) - \int d\theta [\rho_p(\theta) + \rho_h(\theta)] \ln[1 + e^{-\epsilon(\theta)}]. \quad (1.46)$$

By injecting equation (1.45) into the above expression, we find that the only term that survives is

$$Rf(R) = E_0(R) = - \int \frac{d\theta}{2\pi} m \cosh(\theta) \ln[1 + e^{-\epsilon(\theta)}]. \quad (1.47)$$

This is the ground-state energy of the system in volume R that we seek. It can be shown (see for instance [39]) that (1.47) is nothing but the free energy at inverse temperature R of a non-interacting theory in which the energy of particles is given by ϵ/R .

For *bosonic* Bethe equations, particle rapidities can take coinciding values and similar analysis leads to the bosonic TBA equation and free energy

$$\epsilon(\theta) = Rm \cosh(\theta) + \int \frac{d\eta}{2\pi} \ln[1 - e^{-\epsilon(\eta)}] K(\eta - \theta), \quad (1.48)$$

$$E_0(R) = \int \frac{d\theta}{2\pi} m \cosh(\theta) \ln[1 - e^{-\epsilon(\theta)}]. \quad (1.49)$$

Generalization to theories with a non-degenerate mass spectrum m_1, \dots, m_N is straightforward. Let us denote the S-matrix by $S_{ab}(\theta)$ for $a, b = 1, 2, \dots, N$ and $K_{ab}(\theta) = -i\partial_\theta \log S_{ab}(\theta)$. There is a pseudo-energy for each particle type and they are given by a system of N TBA equations

$$\epsilon_a(\theta) = Rm_a \cosh(\theta) \mp \sum_{b=1}^N \int \frac{d\eta}{2\pi} \ln[1 \pm e^{-\epsilon_b(\eta)}] K_{ba}(\eta - \theta), \quad a = 1, \dots, N. \quad (1.50)$$

The ground-state energy of the theory is given by

$$E_0(R) = \mp \sum_{a=1}^N m_a \int \frac{d\theta}{2\pi} \cosh(\theta) \ln[1 \pm e^{-\epsilon_a(\theta)}]. \quad (1.51)$$

where the upper (lower) sign corresponds to the fermionic (bosonic) case. We stress that the unconventional order of the convolution in (1.43) and (1.50) comes directly from the minimization condition of the free energy. The analysis leading to this condition is completely general (it does not rely on any property of the S-matrix) and therefore this order must always be respected in the TBA formalism. At this stage, $K_{ab}(\theta) = K_{ba}(-\theta)$ as a consequence of unitarity and this remark might seem redundant. As we shall see in section 1.2.4 however, for theories with non-diagonal scattering, the TBA formalism involves auxiliary particles which do not necessarily respect the unitary condition. In that case, it is of great importance to have the right order of convolution in the TBA equations.

1.2.2 UV limit of the ground-state energy

In this subsection we discuss the quantitative behavior of the solution of the TBA equation (1.43) as we vary the temperature $1/R$ from zero to infinity. We cite equation (1.43) here for convenience

$$\epsilon(\theta) = Rm \cosh(\theta) - \int \frac{d\eta}{2\pi} K(\eta - \theta) \ln[1 + e^{-\epsilon(\eta)}]. \quad (1.52)$$

When R tends to infinity, the driving term $Rm \cosh(\theta)$ dominates the right hand side of this expression. One can therefore perform a low-temperature limit expansion of the pseudo energy

$$\epsilon(\theta) \approx Rm \cosh(\theta) - \int \frac{d\eta}{2\pi} K(\eta - \theta) \ln[1 + e^{-Rm \cosh(\eta)}] + \dots \quad (1.53)$$

In the limit $R \rightarrow 0$, we know that the ground-state energy must become proportional to the effective central charge of the CFT describing the short-distance behavior of the theory [126]

$$\lim_{R \rightarrow 0} RE_0(R) = -\frac{\pi}{6}(c - 12\Delta - 12\bar{\Delta}), \quad (1.54)$$

where $\Delta, \bar{\Delta}$ are lowest dimensions of the CFT, these are zero for unitary theory but negative otherwise. Let us see if the finite-temperature effective central charge obtained from TBA

$$c(R) = \frac{3}{\pi^2} \int_{-\infty}^{+\infty} d\theta \log[1 + e^{-\epsilon(\theta)}] Rm \cosh(\theta) \quad (1.55)$$

can be matched with the CFT central charge in the UV limit. By taking the derivative of (1.52) with respect to θ one sees that the pseudo-energy becomes flat in the interval $|\theta| \ll \log(2/Rm)$, as $R \rightarrow 0$. Denote this constant value of ϵ by $\epsilon(\infty)$, which satisfies an algebraic equation

$$\epsilon^{\text{UV}} = -\ln(1 + e^{-\epsilon^{\text{UV}}}) \int \frac{d\theta}{2\pi} K(\theta). \quad (1.56)$$

It then turns out [127, 128] that the integral (1.55) can be expressed in terms of the so-called Roger dilogarithm function

$$\lim_{R \rightarrow 0} c(R) = \text{Li}_R([1 + e^{\epsilon^{\text{UV}}}]^{-1}) \quad \text{with} \quad \text{Li}_R(x) \equiv \frac{6}{\pi^2} [\text{Li}_2(x) + \frac{1}{2} \log(x) \log(1-x)]. \quad (1.57)$$

Two important properties of this function are

$$\text{Li}_R(x) + \text{Li}_R(1-x) = 1, \quad \text{Li}_R(x) + \text{Li}_R(y) = \text{Li}_R(xy) + \text{Li}_R\left(\frac{x(1-y)}{1-xy}\right) + \text{Li}_R\left(\frac{y(1-x)}{1-xy}\right). \quad (1.58)$$

Generalization of (1.57) to a theory with N masses takes the form

$$\lim_{R \rightarrow 0} c(R) = \sum_{a=1}^N \text{Li}_R([1 + e^{\epsilon_a^{\text{UV}}}]^{-1}) \quad \text{where} \quad \epsilon_a^{\text{UV}} = \sum_{b=1}^N -\ln[1 + e^{-\epsilon_b^{\text{UV}}}] \int \frac{d\theta}{2\pi} K_{ab}(\theta). \quad (1.59)$$

The conformal limit (1.57) of the ground-state energy provides a substantial check for the S-matrix derived in section 1.1.4. Indeed, the inclusion of extra CDD factors will modify the

kernel K appearing in TBA equation (1.52) and affect its constant solution. As a result, the high temperature limit of the ground-state energy will not match the effective central charge of the corresponding CFT. This line of idea has been extensively exploited in [129], resulting in interesting relations between the central charge, dilogarithm function and constant solutions of TBA equations. See also [130–132] for more in-depth studies on the interplay between dilogarithm and CFT.

For illustration purpose we consider the perturbation of the minimal model $\mathcal{M}_{2,2n+3}$ by its $\Phi_{1,3}$ operator of dimensions $[-(2n-1)/(2n+3), -(2n-1)/(2n+3)]$. This CFT has central charge $-2n(6n+5)/(2n+3)$ and effective central charge $2n/(2n+3)$. The perturbed theory is integrable with n masses interacting via an elastic S-matrix

$$S_{ab}(\theta) = F_{|a-b|/(2n+1)}(\theta) \left[\prod_{k=1}^{\min(a,b)-1} F_{(|a-b|+2k)/(2n+1)}(\theta) \right]^2 F_{(a+b)/(2n+1)}(\theta), \quad a, b = 1, 2, \dots, n, \quad (1.60)$$

where

$$F_\alpha(\theta) \equiv \frac{\sinh \theta + i \sin \pi \alpha}{\sinh \theta - i \sin \pi \alpha}. \quad (1.61)$$

The constant values of the pseudo-energies are given by

$$e^{\epsilon_a^{\text{UV}}} = \sin \left[a\pi/(2n+3) \right] \sin \left[(a+2)\pi/(2n+3) \right] / \sin^2 \left[\pi/(2n+3) \right]. \quad (1.62)$$

We recover from this solution the effective central charge of $\mathcal{M}_{2,2n+3}$ thanks to the identity

$$\sum_{a=1}^n \text{Li}_R \left[\frac{\sin^2(\pi/(2n+3))}{\sin^2((a+1)\pi/(2n+3))} \right] = \frac{2n}{2n+3}. \quad (1.63)$$

1.2.3 Non-diagonal scattering and string hypothesis

For theories with non-diagonal S-matrix, the TBA formalism is considerably more complicated. The analysis is usually model dependent and as an example we will derive the TBA equations for the $SU(2)$ chiral Gross-Neveu model. To remind, the spectrum of this theory contains only one particle in the vector multiplet of $SU(2)$ group. The Bethe equations for a wavefunction $|\theta_1, \theta_2, \dots, \theta_N\rangle$ in a periodic space of length L have been derived in section 1.1.5. We cite equations (1.24) and (1.25) here for the ease of following

$$1 = e^{ip(\theta_j)L} \prod_{k \neq j}^N S_0^{\text{SU}(2)}(\theta_j - \theta_k) \prod_{m=1}^M \frac{\theta_j - u_m + i\pi/2}{\theta_j - u_m - i\pi/2}, \quad j = \overline{1, N}, \quad (1.64)$$

$$1 = \prod_{j=1}^N \frac{u_k - \theta_j - i\pi/2}{u_k - \theta_j + i\pi/2} \prod_{l \neq k}^M \frac{u_k - u_l + i\pi}{u_k - u_l - i\pi}, \quad k = \overline{1, M}. \quad (1.65)$$

The next step in the TBA formalism is to find a complete set of solutions of this system. For theories with diagonal S-matrix described in the previous section, we simply took all the (physical) rapidities to be real. Here the situation is different: even if the physical rapidities are real, the auxiliary ones can take complex values. For instance, there are complex solutions for

auxiliary rapidities when $N = 5$ and $M = 2$. Let us assume the existence of these solutions when the number of physical rapidities grows arbitrarily large. Without loss of generality, suppose that there exists a state with $\Im(u_1) > 0$. Then the first product in (1.65) would vanish as N tends to infinity. The only way to compensate this zero is by having a pole in one of the terms in the second product of (1.65). In other words, there must be another auxiliary rapidity, say u_2 with $u_2 = u_1 - i\pi$.

The appearance of the rapidity u_2 has resolved the problem with the Bethe equation for u_1 , but another issue arises. By multiplying the Bethe equation for u_1 and u_2 to eliminate their singular terms and by denoting $u_{12} = (u_1 + u_2)/2$, we find that

$$1 = \prod_{j=1}^N \frac{u_{12} - \theta_j - i\pi}{u_{12} - \theta_j + i\pi} \prod_{l=3}^M \frac{u_{12} - u_l + 3i\pi/2}{u_{12} - u_l - i\pi/2} \frac{u_{12} - u_l + i\pi/2}{u_{12} - u_l - 3i\pi/2}. \quad (1.66)$$

There are two scenarios: if u_{12} is real then we can consider (1.66) as part of our system of Bethe equations, replacing the original equations of u_1 and u_2 . Once we solve it for u_{12} then u_1 and u_2 are given by $u_{1,2} = u_{12} \pm i\pi/2$. On the other hand, if the imaginary part of u_{12} is not zero then the above arguments that have been applied for u_1 can now be applied for u_{12} as well. If $\Im(u_{12}) > 0$ then there must be a pole in the second product of (1.66). This pole can not be at $u_l = u_{12} - i\pi/2$ however because in that case u_l would coincide with u_2 . Therefore there must be a rapidity, say u_3 which is equal to $u_{12} - 3i\pi/2$. Inversely, if $\Im(u_{12}) < 0$ then $u_3 = u_{12} + 3i\pi/2$. We can now repeat the above procedure, multiplying the Bethe equations for u_1, u_2, u_3 together and write it in terms of the new rapidity $u_{123} = (u_1 + u_2 + u_3)/3$. Either u_{123} is real or the procedure continues and we generate a bigger configuration.

To summarize, we have found that when the number of physical rapidities tends to infinity, if there are complex auxiliary rapidities then they must organize themselves into string patterns. A string is characterized by its real center u and its length (number of its constituents)

$$\{u_Q\} \equiv \{u - (Q + 1 - 2j)i\pi/2 \mid j = 1, 2, \dots, Q\}. \quad (1.67)$$

For the construction of string solutions in other model, see for instance [133] for the XXZ spin chain, or [134] and [135] for more sophisticated structures.

Now if we want to take the thermodynamic limit, we must send not only the number of physical particles but also the number of auxiliary magnons to infinity as well. In that regime, there is a plot hole in our analysis: the infinite product of magnon S-matrices with complex rapidities can mimic the role of a pole and our construction of magnon strings is no longer justified. Although solutions of this type (and other singular structures) can exist we might assume that they are rather uncommon. In other words, we can say that most solutions are of string type or more precisely, the dominant contribution to the free energy comes mostly from them. For example, in the XXX spin chain there exist solutions that do not approach the expected string forms in the thermodynamic limit [136–138], but the free energy is correctly recovered by taking only string configurations into consideration [139]. The process of constructing string solutions and the assumption that they are the only solutions of Bethe equations that are relevant in the thermodynamic limit is known in the literature as *the string hypothesis*. For a detailed discussion and further references on the string hypothesis, see for instance [140].

With the string hypothesis, a relevant system of Bethe equations for the $SU(2)$ chiral Gross-Neveu model involves: N_0 number of real physical rapidities θ_j with $j = \overline{1, N_0}$, N_Q number of Q -string real centers $u_{Q,l}$; $l = \overline{1, N_Q}$ for each Q from 1 to $+\infty$

$$-1 = e^{ip(\theta_j)L} \prod_{k=1}^{N_0} S_{00}(\theta_j - \theta_k) \prod_{Q=1}^{+\infty} \prod_{l=1}^{N_Q} S_{0Q}(\theta_j - u_{Q,l}), \quad j = \overline{1, N_0}, \quad (1.68)$$

$$(-1)^Q = \prod_{j=1}^{N_0} S_{Q0}(u_{Q,l} - \theta_j) \prod_{P=1}^{+\infty} \prod_{m=1}^{N_P} S_{QP}(u_{Q,l} - u_{P,m}), \quad Q = \overline{1, +\infty}, l = \overline{1, N_Q}. \quad (1.69)$$

where the scattering phases involving strings are, by construction, the products of the scattering phases of their constituents

$$\begin{aligned} S_{00}(\theta) &\equiv S_0^{\text{SU}(2)}(\theta) = -\frac{\Gamma(1 - \theta/2\pi i) \Gamma(1/2 + \theta/2\pi i)}{\Gamma(1 + \theta/2\pi i) \Gamma(1/2 - \theta/2\pi i)}, \\ S_{0Q}(\theta - u_Q) &\equiv \prod_{u_j \in \{u_Q\}} \frac{\theta - u_j + i\pi/2}{\theta - u_j - i\pi/2}, \quad S_{Q0}(u_Q - \theta) = \prod_{u_j \in \{u_Q\}} \frac{u_j - \theta - i\pi/2}{u_j - \theta + i\pi/2}, \\ S_{PQ}(u_Q - u_P) &\equiv \prod_{j \in \{u_Q\}} \prod_{k \in \{u_P\}} \frac{u_j - u_k + i\pi}{u_j - u_k - i\pi}. \end{aligned} \quad (1.70)$$

We note that the total number of auxiliary particles i.e. $\sum_Q Q N_Q$ should not exceed half the number of physical particles.

This construction is reminiscent of the S-matrix bootstrap procedure described in section 1.1.3. In the XXX spin chain language, the strings can be interpreted as bound states, having less energy than the total energy of individual real magnons. Furthermore, building the S-matrix between these bound states from the S-matrix between fundamental excitations can be regarded as spin chain equivalence of the fusion method. Despite the analogies, one should not take this idea too seriously. For instance, our choice of the "S-matrix" between physical rapidity and strings clearly violates unitarity: $S_{0Q}(\theta)S_{Q0}(-\theta) \neq 1$. As we shall explain in the next section, the reason for this choice of "S-matrix" is purely technical. With that being said, it is important to keep in mind that auxiliary particles are mathematical artifacts in the TBA formalism and they are not subjected to any physical constraint *a priori*.

1.2.4 TBA equations and Y-system for $SU(2)$ chiral Gross-Neveu model

With the Bethe equations (1.68) and (1.69) at our disposal, we can proceed to the next steps in the TBA formalism: taking logarithm of Bethe equations to find Bethe quantum numbers, passing to the continuum limit and defining the counting function for each species of particle. Most of these steps are mechanical: one basically treats the theory as having an infinite number of particles interacting via elastic S-matrices given in (1.70). There is however a subtlety in defining the counting function for auxiliary strings that is worth mentioning. To guarantee that the density of states and holes are positive, the counting function must always be monotonically increasing (see equation (1.38)). For the physical particle, this poses no problem as the particle momentum serves as the leading term for the corresponding counting function (1.37). For

auxiliary strings, the leading term is the spin chain momentum. The problem is that there are two equivalent ways of defining this quantity without modifying physically-relevant quantities. These two choices are of opposite values and only one of them ¹ is an increasing function of rapidity: the one given in (1.70). Take for instance 1-string then

$$\partial_u p(u) > 0 \quad \text{with} \quad e^{ip(u)N} \equiv \prod_{j=1}^N \frac{u - \theta_j - i\pi/2}{u - \theta_j + i\pi/2}. \quad (1.71)$$

With this remark, we are now ready to write down the TBA equations for the theory. There is an infinite number of pseudo energies: ϵ_0 for the physical rapidity and ϵ_Q for Q -string for $Q = \overline{1, \infty}$

$$\epsilon_n(\theta) = Rm \cosh(\theta) \delta_{n,0} - \sum_{m=0}^{\infty} \log[1 + e^{-\epsilon_m}] \star K_{mn}(\theta), \quad n = \overline{0, \infty}, \quad (1.72)$$

where $K_{nm}(\theta) = -i\partial_\theta \log S_{nm}(\theta)$. The free energy only depends explicitly on the physical pseudo-energy

$$Rf(R) = - \int \frac{d\theta}{2\pi} m \cosh(\theta) \log[1 + e^{-\epsilon_0(\theta)}]. \quad (1.73)$$

The system (1.72) of infinitely many coupled equations can be cast into an equivalent form called Y-system, which has the advantage of being local

$$\log Y_n + RE\delta_{n,0} = s \star [\log(1 + Y_{n+1}) + \log(1 + Y_{n-1})], \quad n = \overline{0, \infty}. \quad (1.74)$$

In this expression $Y_0 = e^{-\epsilon_0}$, $Y_n = e^{\epsilon_n}$ for $n \geq 1$, $Y_{-1} = 0$ and s is a simple kernel given in appendix A.1. The structure Y-systems can usually be represented by graphs. In our case, it is the infinite Dynkin diagram of A-type, see figure 1.6.

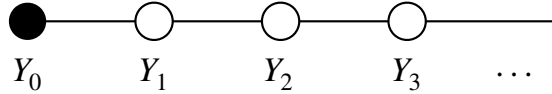


Figure 1.6: The Y-system of $SU(2)$ chiral Gross-Neveu model, the black node stands for the physical Y-function while the n^{th} white node represents that of the auxiliary n -string.

In general the Y-functions live on a direct product of two Dynkin diagrams: a finite one which represents the symmetry of the model and an infinite one which encodes the irreducible representations of this symmetry. For instance the Y-system of the $SU(N)$ chiral Gross-Neveu model is shown in figure 1.7. To make the group theoretical meaning behind these graphs more precise, we recall that auxiliary strings of $SU(2)$ model are bound states of the XXX spin chain. A bound state of Q constituents carry a spin of $Q/2$ and can be identified with an irreducible representations of $SU(2)$. The same structure holds for higher ranks: Y-functions correspond to inequivalent non-singlet irreducible representations of $SU(N)$, represented by Young diagrams of maximal height $N - 1$. The totality of these diagrams form the grid in figure 1.7 if we draw a square around every node. For an in-depth review of Y-systems, see for instance [141].

¹one could nevertheless work with the other, the price to pay is that the TBA equations cannot be written in a uniform fashion

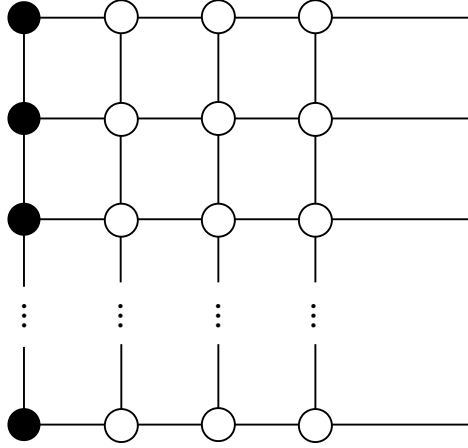


Figure 1.7: Y-system of $SU(N)$ chiral Gross-Neveu model. There are $N-1$ rows and an infinite number of columns.

Let us come back to the $SU(2)$ chiral Gross-Neveu model and look at its Y-system in more details. Two special regimes are of interest. At zero temperature the solutions of TBA equations become constants

$$Y_n^{\text{IR}} = (n+1)^2 - 1, \quad n \geq 0. \quad (1.75)$$

As we turn on the temperature, a plateau structure starts to develop for each Y-function inside the region from $-\log[2/(mR)]$ to $\log[2/(mR)]$. Outside of this region Y-functions retain their IR values while the tops of the plateaux flatten out at height

$$Y_n^{\text{UV}} = (n+2)^2 - 1, \quad n \geq 0. \quad (1.76)$$

There are two consistency checks for these stationary solutions. In the zero temperature limit one would expect the behavior of a non-interacting gas. In particular, as the physical particle belongs to the vector representation of $SU(2)$, the leading contribution to the free energy should be

$$\lim_{R \rightarrow 0} Rf(R) = -2 \int \frac{d\theta}{2\pi} m \cosh(\theta) e^{-Rm \cosh(\theta)}.$$

By replacing the leading term of the physical Y-function into the expression (1.73) we see that this is indeed the case². At the UV, the Casimir energy computed from TBA should match the central charge of the unperturbed CFT, as explained in subsection 1.2.2

$$\lim_{R \rightarrow 0} c(R) = \sum_{n \geq 0} \text{Li}_R\left(\frac{1}{1+Y_n^{\text{IR}}}\right) - \sum_{n \geq 0} \text{Li}_R\left(\frac{1}{1+Y_n^{\text{UV}}}\right) = 1. \quad (1.77)$$

The particle densities can also be easily computed in the UV limit [143]. Let us denote by $D_0 = N_0/L$ the density of physical particle and $D_a = N_a/L$ that of string of length a , then

$$\lim_{R \rightarrow 0} \pi R D_0(R) = \log(1 + Y_0^{\text{UV}}), \quad \lim_{R \rightarrow 0} \pi R D_a(R) = \log(1 + Y_a^{\text{IR}}) - \log(1 + Y_a^{\text{UV}}).$$

²For higher order matching between TBA and Luscher correction, see [142]

We find that the density of physical particle is exactly twice the total density of auxiliary particles in this limit

$$\lim_{R \rightarrow 0} \pi R D_0(R) = \log 4, \quad \lim_{R \rightarrow 0} \sum_{a=1}^{\infty} \pi R a D_a(R) = \log 2.$$

For later discussions of g-function, we will add to the TBA equations (1.72) a chemical potential coupled to the $SU(2)$ symmetry. Denote by μ the chemical potential of the physical particle. In the spin chain language, μ can be thought of as the strength of an external magnetic field. The auxiliary particle corresponds to spin flipping and is assigned a chemical potential of -2μ . A string of n auxiliary particles have chemical potential $-2n\mu$. The TBA equations of chiral $SU(2)$ Gross-Neveu now read

$$\begin{aligned} \log Y_0(\theta) &= -Rm \cosh(\theta) + \mu + \sum_{n=0}^{\infty} K_{n,0} \star \log(1 + Y_n)(\theta), \\ \log Y_n(\theta) &= -2n\mu + \sum_{m=0}^{\infty} K_{m,n} \star \log(1 + Y_m)(\theta), \quad n \geq 1. \end{aligned} \quad (1.78)$$

This inclusion of chemical potential does not affect the structure of Y system. It does affect however the asymptotic values of Y-functions. Write $2\mu = -\log \kappa$ with κ usually known as the twist parameter. The IR and UV values of Y-functions are given by (to be compared with (1.75) and (1.76))

$$1 + \mathcal{Y}_n^{\text{IR}}(\kappa) = [n+1]_{\kappa}^2, \quad 1 + \mathcal{Y}_n^{\text{UV}}(\kappa) = [n+2]_{\kappa}^2, \quad (1.79)$$

where the κ -quantum numbers are defined as

$$[n]_{\kappa} \equiv (1 + \kappa + \dots + \kappa^{n-1}) / \kappa^{(n-1)/2}.$$

We can repeat the above analysis for this twisted theory. At zero temperature, the double degeneracy of up/down spin is lifted

$$Y_0^{\text{IR}}(u) = e^{-Rm \cosh(u)} \sqrt{1 + \mathcal{Y}_1^{\text{IR}}(\kappa)} = [2]_{\kappa} e^{-Rm \cosh(u)}.$$

In the UV limit the particle densities are now given by

$$\lim_{R \rightarrow 0} \pi R D_0(R, \mu) = 2 \log(1 + \kappa) - \log \kappa, \quad \lim_{R \rightarrow 0} \sum_{a=1}^{\infty} \pi R a D_a(R, \mu) = \log(1 + \kappa).$$

The scaled free energy density

$$c(R, \mu) \equiv -\frac{6R^2 f(R)}{\pi} = \frac{3}{\pi^2} \int m R \cosh(\theta) \log[1 + Y_0(\theta)] d\theta - \frac{6}{\pi} \sum_{a=0}^{\infty} \mu_a R D_a(R, \mu),$$

where $\mu_0 = \mu$, $\mu_n = -2n\mu$ for $n \geq 1$, can again be computed in the UV limit with help of Roger dilogarithm function

$$\lim_{R \rightarrow 0} c(R, \mu) = 1 - \frac{6\mu^2}{\pi^2}. \quad (1.80)$$

The Y-system is derived from the TBA equations and as such contains *a priori* less information. This is indeed the case as we have shown that the TBA equations with and without a chemical potential give rise to the same Y-system. If one wishes to only use the Y-system to describe thermodynamic quantities then one must provide extra information on the Y-functions. As we saw above, this could be their IR values, or equivalently their large θ asymptotics.

1.2.5 Excited state energies from analytic continuation

In this subsection we discuss the extension of the TBA method to include excited state energies. This seems impossible at first regard, given the unique footing of the ground state energy in the mirror trick proposed by Zamolodchikov. In [44] Dorey and Tateo proposed an alternate route to bypass this barrier: an analytic continuation in some parameter of the theory that connects different energy levels. This approach appeared in fact earlier in the case of the quantum anharmonic oscillator [144]. Let us illustrate the idea on toy model

$$H\psi = E\psi \quad \text{with} \quad H = \begin{pmatrix} 1 & 0 \\ 0 & -1 \end{pmatrix} + \lambda \begin{pmatrix} 0 & 1 \\ 1 & 0 \end{pmatrix}. \quad (1.81)$$

The spectrum of this system is very simple: the ground state energy is $-\sqrt{1+\lambda^2}$ and the only excited state energy is $\sqrt{1+\lambda^2}$. If we allow the *coupling constant* λ to take complex values then the ground state energy has branch points at $\lambda = \pm i$. As a consequence, if we start with a real-valued coupling constant and we go around one of these branch points and come back to our starting point then the energy flips its sign and we end up with the excited state energy.

The problem is not so simple in the TBA formalism, because we do not have an explicit formula for the ground state energy. It is instead expressed in terms of the pseudo energy, which in turn is determined by an integral equation (1.43). Let us mimic such situation by rewriting the ground state energy of the toy model as an integral

$$E(\lambda) = - \int_{-1}^1 \frac{dz}{2\pi i} f(z)g(z) - 1, \quad (1.82)$$

where

$$f(z) = \frac{1}{z - i/\lambda} \quad \text{and} \quad g(z) = 2\lambda\sqrt{1-z^2} \quad (1.83)$$

respectively playing the role of $\ln(1+Y)$ and the energy in the expression of TBA ground state energy (1.47).

Let us analytically continue the expression (1.82) to complex-valued λ . The integral is well-defined as long as the pole i/λ is found outside of the integration domain. We start with a real-valued λ_0 of the coupling constant and move it around one of the branch point, for instance $\lambda = +i$. The only issue we encounter along the trajectory is when we cross the imaginary axis at second time. There, the pole enters the integration contour, drags it and wraps it around the original pole i/λ_0 . Upon coming back to our starting point, we pick up the residue at this pole and thus end up with the excited state energy

$$E^c(\lambda_0) = E(\lambda_0) + g(i/\lambda_0). \quad (1.84)$$

In this procedure the explicit expressions of f was not used. All we need to know is the relative position of its pole with respect to the integration contour of $E(\lambda)$.

The same idea can be used to find excited state energies from the ground state one

$$E_0(R) = \int \frac{d\theta}{2\pi} m \sinh(\theta) \frac{\partial_\theta Y(\theta)}{1+Y(\theta)}, \quad (1.85)$$

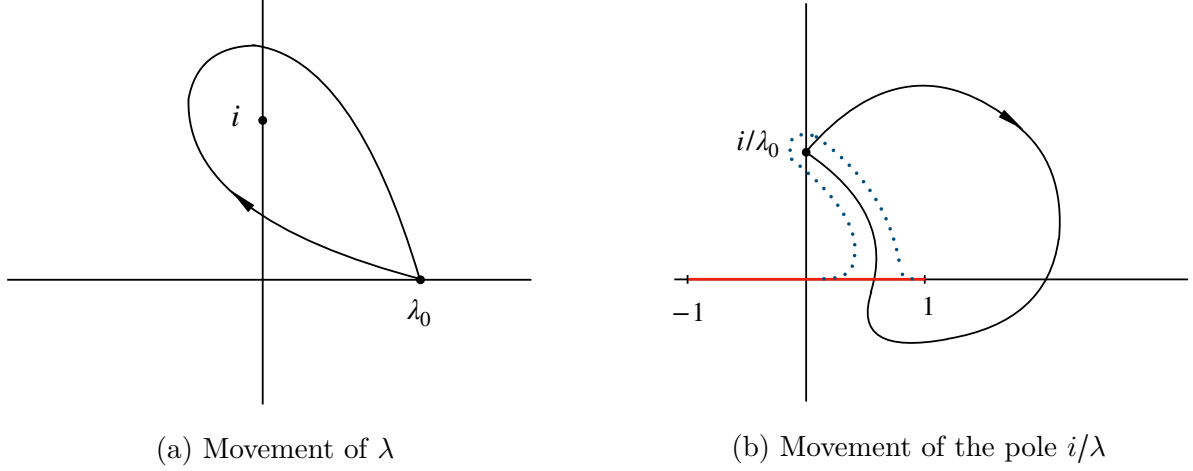


Figure 1.8: (a) When λ is analytically continued around a branch point, the energy flips its sign. (b) The corresponding movement of the pole at i/λ . At some point, it crosses the integration contour and drags it along for continuity. Once the integration contour is taken back to the real line we gain a residual contribution.

where we have performed an integration by parts. We start by parametrizing the original TBA equation by some real parameter λ , for instance the inverse temperature R or the mass scale of the theory. Let us assume that in the process of analytically continuing this variable we encounter some poles $\theta_j^*(\lambda)$ such that $Y(\theta_j^*) = -1$. If we move on the complex plane in such a way that some of these points cross the real line, then upon coming back, we will pick up their residues

$$E^c(R) = i \sum m \sinh(\theta_j^*) - \int \frac{d\theta}{2} m \cosh(\theta) \log[1 + Y^c(\theta)]. \quad (1.86)$$

The original TBA equation

$$\log Y(\theta) = -Rm \cosh(\theta) - \int \frac{d\eta}{2\pi i} \log S(\eta - \theta) \frac{\partial_\eta Y(\eta)}{1 + Y(\eta)}. \quad (1.87)$$

is likewise affected by this analytic continuation

$$\log Y^c(\theta) = -Rm \cosh(\theta) - \sum_j \log S(\theta_j^* - \theta) + \int \frac{d\eta}{2\pi} K(\eta - \theta) \log[1 + Y^c(\eta)]. \quad (1.88)$$

The interpretation of excited energy (1.86) and the excited TBA equation (1.88) will become clear if we define $\tilde{\theta}_j^* = \theta_j^* + i\pi/2$. Then $i \sinh(\theta_j^*) = \cosh(\tilde{\theta}_j^*)$ and $-\cosh(\theta_j^*) = i \sinh(\tilde{\theta}_j^*)$. The leading order in the large volume expansion of the equation $Y^c(\theta_j^*) = -1$ which determines the positions of the singular points is written in terms of these new variables as

$$e^{im \sinh(\tilde{\theta}_j^*)R} \prod_k S(\tilde{\theta}_j^* - \tilde{\theta}_k^*) = -1, \quad (1.89)$$

which is nothing but the Bethe equation (1.34) at volume R . Furthermore, in this limit, the excited state energy (1.86) is simply

$$E^c(R) = \sum_j m \cosh(\theta_j^*). \quad (1.90)$$

That is, $\tilde{\theta}_j^*$ are precisely the rapidities of some state living in the mirror theory. The convoluted terms in the excited state energy (1.86) and excited TBA equation (1.88) correspond to finite size corrections to the asymptotic expressions of this theory.

If we were to cross the real axis from the other direction then the sign in front of $im \sinh(\theta_j^*)$ and $\log S(\theta_j - \theta)$ in these equations would change. In that case, the mirror-physical conversion is defined as $\tilde{\theta}_j^* = \theta_j^* - i\pi/2$.

We note however that none of these two transformations is actually the *honest* mirror transformation. A real mirror transformation interchanges space and time via a double Wick rotation $(x, t) \rightarrow (-it, ix)$ and thus $(p, E) \rightarrow (iE, -ip)$. It reads in terms of rapidity $\theta \rightarrow i\pi/2 - \theta$. The above transformations are combinations of the honest mirror transformation with either the parity transformation or the time reversal transformation. By abuse of language and for simplicity we call them mirror transformation, however we will specify the rapidity conversion each time the terminology is used. The real mirror transformation will be used in a heuristic argument to obtain the average current in Generalized Hydrodynamics, see subsection 1.4.2.

1.3 Application of form factors in finite volume

The idea of the form factors program is construct fundamental building blocks for correlation functions in integrable quantum field theories. These building blocks can be determined from symmetry, their analytic structure and the knowledge of the two-particle S-matrix. The program was initially formulated for relativistic quantum field theories with excitations over the vacuum [145]. For the construction of form factors in $\mathcal{N} = 4$ SYM see for instance [38, 146]. More recently, there are propositions to study form factors built on top of a thermodynamic state [147, 148]. In this thesis, we focus on the applications of form factors in finite volume.

We restrict our discussion to theories with a non-degenerate mass spectrum and we use the index a to denote particle types.

1.3.1 Motivation and axioms

Facing the problem of computing a correlation function $\langle \mathcal{O}_1(x_1) \mathcal{O}_2(x_2) \dots \mathcal{O}_n(x_n) \rangle$, one can take a reductionist stance, inserting as many resolutions of identity

$$1 = \sum_n \sum_{a_1, \dots, a_n} \int \frac{d\theta_1 \dots d\theta_n}{n! (2\pi)^n} |\theta_1, \dots, \theta_n\rangle_{a_1, \dots, a_n} {}_{a_1, \dots, a_n} \langle \theta_1, \dots, \theta_n| \quad (1.91)$$

as it takes to bring the problem down to two smaller tasks. The first task is to evaluate matrix elements of the type

$${}_{a'_1, \dots, a'_m} \langle \theta'_1, \dots, \theta'_m | \mathcal{O}(0, 0) | \theta_1, \dots, \theta_n \rangle_{a_1, \dots, a_n} \equiv F^{\mathcal{O}}_{a'_1, \dots, a'_m; a_1, \dots, a_n}(\theta'_1, \dots, \theta'_m | \theta_1, \dots, \theta_n). \quad (1.92)$$

which are called the *form factors* of the operator \mathcal{O} . The second task is to perform the infinite sum involving these form factors. Some concrete examples following this line of idea can be found in [149–151] for the Ising model and in [152, 153] for the Principal chiral model at large N . In this subsection we will only present the properties of form factors that are relevant to this thesis. For an in-depth review, see [145].

As physical processes involve real rapidities, form factors are *a priori* functions of real variables. However we can consider their analytic continuation on the complex plane, like we did with the two-particle S-matrix. The first simplification we can do with (1.92) is to move some rapidity from the bra to the ket. It can be shown (see for instance [154]) that

$$\begin{aligned} & F^{\mathcal{O}}_{a'_1, \dots, a'_m; a_1, \dots, a_n}(\theta'_1, \dots, \theta'_m | \theta_1 \dots \theta_n) \\ &= F^{\mathcal{O}}_{a'_1, \dots, a'_{m-1}; a'_m, a_1, \dots, a_n}(\theta'_1, \dots, \theta'_{m-1} | \theta'_m + i\pi, \theta_1, \dots, \theta_n) + \sum_{k=1}^n \delta_{a'_m a_k} \delta(\theta'_m - \theta_k) \\ & \times \prod_{l=1}^{k-1} S_{a_l a_k}(\theta_l - \theta_k) F^{\mathcal{O}}_{a'_1, \dots, a'_{m-1}; a_1, \dots, a_{k-1}, a_{k+1}, \dots, a_n}(\theta'_1, \dots, \theta'_{m-1} | \theta_1, \dots, \theta_{k-1}, \theta_{k+1}, \dots, \theta_n), \end{aligned} \quad (1.93)$$

This is called the *crossing relation* and is illustrated in figure 1.9.

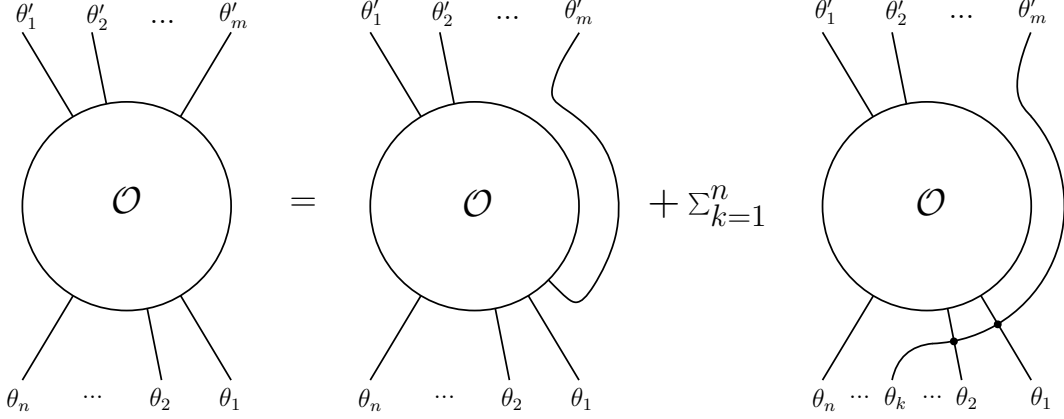


Figure 1.9: The crossing relation (1.93).

For $m = 1$ there are two equivalent ways of writing the crossing relation

$$\begin{aligned}
& F_{a'_1, a_1, \dots, a_n}^{\mathcal{O}}(\theta'_1 | \theta_1, \dots, \theta_n) \\
&= F_{a'_1, a_1, \dots, a_n}^{\mathcal{O}}(\theta'_1 + i\pi, \theta_1, \dots, \theta_n) + \sum_{k=1}^n \delta_{a'_1 a_k} \delta(\theta'_1 - \theta_k) \\
&\times \prod_{l=1}^{k-1} S_{a_l a_k}(\theta_l - \theta_k) F_{a_1, \dots, a_{k-1}, a_{k+1}, \dots, a_n}^{\mathcal{O}}(\theta_1, \dots, \theta_{k-1}, \theta_{k+1}, \dots, \theta_n), \tag{1.94}
\end{aligned}$$

$$\begin{aligned}
&= F_{a_1, \dots, a_n, a'_1}^{\mathcal{O}}(\theta_1, \dots, \theta_n, \theta'_1 - i\pi) + \sum_{k=1}^n \delta_{a'_1 a_k} \delta(\theta'_1 - \theta_k) \\
&\times \prod_{l=k+1}^n S_{a_l a_k}(\theta_l - \theta_k) F_{a_1, \dots, a_{k-1}, a_{k+1}, \dots, a_n}^{\mathcal{O}}(\theta_1, \dots, \theta_{k-1}, \theta_{k+1}, \dots, \theta_n). \tag{1.95}
\end{aligned}$$

By successively applying (1.93), we can express any form factor in terms of elementary ones

$$F_{a_1, \dots, a_n}^{\mathcal{O}}(\theta_1, \dots, \theta_n) \equiv \langle 0 | \mathcal{O}(0, 0) | \theta_1, \dots, \theta_n \rangle_{a_1, \dots, a_n}. \tag{1.96}$$

Elementary form factors that differ only in the order of their rapidities are related by the S-matrix

$$F_{a_1, \dots, a_j, a_{j+1}, \dots, a_n}^{\mathcal{O}}(\theta_1, \dots, \theta_j, \theta_{j+1}, \dots, \theta_n) = S_{a_j a_{j+1}}(\theta_j - \theta_{j+1}) F_{a_1, \dots, a_{j+1}, a_j, \dots, a_n}^{\mathcal{O}}(\theta_1, \dots, \theta_{j+1}, \theta_j, \dots, \theta_n). \tag{1.97}$$

By comparing the analytic part of (1.94) and (1.95) we obtain the *cyclic permutation* property

$$F_{a_1, \dots, a_n}^{\mathcal{O}}(\theta_1 + i\pi, \dots, \theta_n) = F_{a_2, \dots, a_n, a_1}^{\mathcal{O}}(\theta_2, \dots, \theta_n, \theta_1 - i\pi). \tag{1.98}$$

To evaluate the residue at the kinematical pole let us write

$$F_{a_1, a_2, \dots, a_n}(\theta_1 + i\pi, \theta_2, \dots, \theta_n) \approx \frac{\text{Res}_{\theta_1 = \theta_2 + i\pi} F_{a_1, \dots, a_n}^{\mathcal{O}}(\theta_1, \theta_2, \dots, \theta_n)}{\theta_1 - \theta_2 - i\epsilon}, \tag{1.99}$$

$$F_{a_2, \dots, a_n, a_1}(\theta_2, \dots, \theta_n, \theta_1 - i\pi) \approx \frac{\text{Res}_{\theta_1 = \theta_2 + i\pi} F_{a_1, \dots, a_n}^{\mathcal{O}}(\theta_1, \theta_2, \dots, \theta_n)}{\theta_1 - \theta_2 + i\epsilon}. \tag{1.100}$$

Plugging (1.99) into (1.93), (1.100) into (1.94) and comparing their δ -function parts we find

$$\text{Res}_{\theta_1=\theta_2+i\pi} F_{a_1,\dots,a_n}^{\mathcal{O}}(\theta_1,\theta_2,\dots,\theta_n) = 2i F_{a_3,\dots,a_n}^{\mathcal{O}}(\theta_3,\dots,\theta_n) \left[1 - \delta_{a_1 a_2} \prod_{j=3}^n S_{a_2 a_j}(\theta_2 - \theta_j) \right]. \quad (1.101)$$

This is usually served as a recursive relation between n - and $(n-2)$ -particle elementary form factors. Like the two-particle S-matrix, form factors also have poles related to bound states. However these poles are not relevant to this thesis.

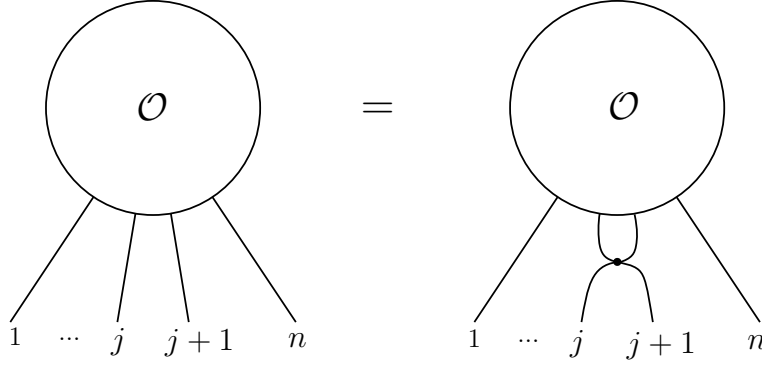


Figure 1.10: The exchange relation (1.97)

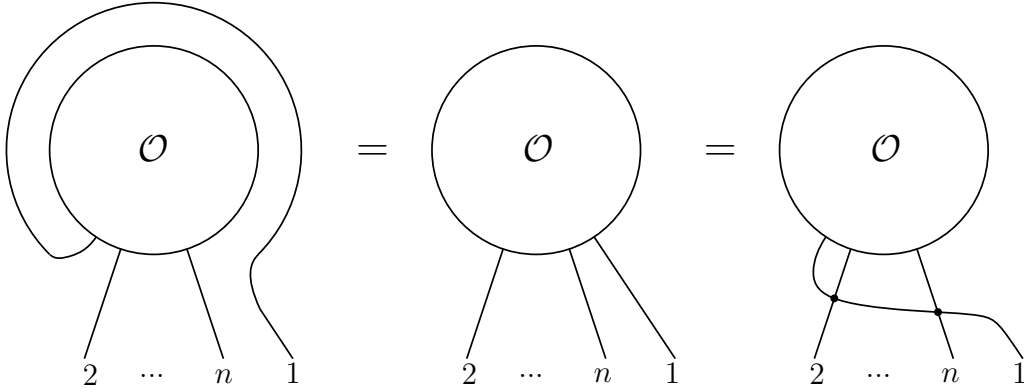


Figure 1.11: The cyclic permutation property (1.98)

Finally, we note that if \mathcal{O} carries a Lorenz charge s then under a Lorenz boost Λ the form factors of \mathcal{O} transform as $F_a^{\mathcal{O}}(\theta_1 + \Lambda, \dots, \theta_n + \Lambda) = e^{s\Lambda} F_a^{\mathcal{O}}(\theta_1, \dots, \theta_n)$. In particular, if \mathcal{O} is a scalar then $F_a^{\mathcal{O}}(\theta_1, \dots, \theta_n)$ is a function of rapidity differences.

For notational simplicity, we consider in the following theories with only one particle type. Generalization to those with more than one particle type is straightforward.

1.3.2 Connected and symmetric evaluation of diagonal form factors

Once we have obtained the elementary form factors, we can in use the crossing relation (1.93), (1.94) to write down any form factor. Subtlety arises however when some rapidities in the bra

coincide with some in the ket of (1.92). Of relevance to the following sections are the diagonal form factors $F^{\mathcal{O}}(\theta_n, \dots, \theta_1 | \theta_1, \dots, \theta_n)$.

To avoid singularity in the crossing relation, one can regularize the corresponding elementary form factor by shifting each rapidity θ_j by a small amount ϵ_j . It turns out that this limit depends on how the regulators are taken to zero. Generally one has the following structure [155]

$$F^{\mathcal{O}}(\theta_1 + i\pi + \epsilon_1, \dots, \theta_n + i\pi + \epsilon_n, \theta_n, \dots, \theta_1) = \prod_{j=1}^n \frac{1}{\epsilon_j} \sum_{j_1=1}^n \dots \sum_{j_n=1}^n a_{j_1 \dots j_n} \epsilon_{j_1} \dots \epsilon_{j_n} + \dots \quad (1.102)$$

where $a_{j_1 \dots j_n}$ is a totally symmetric tensor and the ellipsis denote terms that vanish when ϵ_i 's tend to zero. The connected evaluation of the diagonal matrix element $\langle \theta_n, \dots, \theta_1 | \theta_1, \dots, \theta_n \rangle$ is then defined as $F_c^{\mathcal{O}}(\theta_1, \dots, \theta_n) \equiv n! a_{12 \dots n}$. We will refer to it simply as the *connected form factor*. On the other hand, the *symmetric form factor* is obtained when all the regulators are equal

$$F_s^{\mathcal{O}}(\theta_1, \dots, \theta_n) = \lim_{\epsilon \rightarrow 0} F^{\mathcal{O}}(\theta_1 + i\pi + \epsilon, \dots, \theta_n + i\pi + \epsilon, \theta_n, \dots, \theta_1) = \sum_{j_1=1}^n \dots \sum_{j_n=1}^n a_{j_1 \dots j_n}. \quad (1.103)$$

To see the relation between these two form factors let us consider as an example $n = 2$ where

$$F(\theta_1 + i\pi + \epsilon_1, \theta_2 + i\pi + \epsilon_2, \theta_2, \theta_1) = \frac{1}{\epsilon_1 \epsilon_2} (a_{11} \epsilon_1^2 + 2a_{12} \epsilon_1 \epsilon_2 + a_{22} \epsilon_2^2),$$

$$F_c(\theta_1, \theta_2) = 2a_{12}, \quad F_s(\theta_1, \theta_2) = a_{11} + 2a_{12} + a_{22}.$$

The kinematical pole at fixed ϵ_2 and $\epsilon_1 = 0$ is prescribed by relation (1.101)

$$\text{Res}_{\epsilon_1=0} F(\theta_1 + i\pi + \epsilon_1, \theta_2 + i\pi + \epsilon_2, \theta_2, \theta_1) = i[1 - S(\theta_1 - \theta_2)S(\theta_1 - \theta_2 - i\pi - \epsilon_2)]F(\theta_2 + i\pi + \epsilon_2, \theta_2)$$

Developing the right hand side to first order in ϵ_2 we obtain

$$a_{22} = K(\theta_2 - \theta_1)F_c(\theta_2) \quad \text{with} \quad K(\theta) = -i\partial_\theta \log S(\theta).$$

Similarly $a_{11} = K(\theta_1 - \theta_2)F_c(\theta_1)$ so that

$$F_s(\theta_1, \theta_2) = K(\theta_2 - \theta_1)F_c(\theta_2) + K(\theta_1 - \theta_2)F_c(\theta_1) + F_c(\theta_1, \theta_2)$$

More generally, a symmetric form factor can be expressed in terms of connected form factors with smaller numbers of particles. The exact relation was found by induction in [156]

$$F_s^{\mathcal{O}}(\theta_1, \dots, \theta_n) = \sum_{\alpha \subset \{1, 2, \dots, n\}} \mathcal{L}(\alpha | \alpha) F_c^{\mathcal{O}}(\{\theta_j\}_{j \in \alpha}). \quad (1.104)$$

In this equation the sum runs over non-empty subsets of $\{1, 2, \dots, n\}$ and $\mathcal{L}(\alpha | \alpha)$ denotes the principal minor obtained by deleting the α rows and columns of the following matrix

$$L(\theta_1, \dots, \theta_n)_{jk} = \delta_{jk} \sum_{l \neq j} K(\theta_j - \theta_l) - (1 - \delta_{jk})K(\theta_j - \theta_k). \quad (1.105)$$

1.3.3 Finite volume matrix elements

The form factor formalism is plagued with divergences and we see an example in the previous subsection. The existence of divergences is due to the fact that form factors are constructed in infinite volume. As a mean to regularize these divergences, one can first define and study form factors in finite volume, before sending the volume to infinity. This approach has proven to be not only a physically meaningful regularization but also a suitable method to obtain thermal observables as the TBA formalism itself is constructed in finite volume.

In volume L , multi-particle states are labeled by a set of Bethe quantum numbers I_1, \dots, I_n . The particle rapidities are related to the quantum numbers through Bethe equations

$$2\pi I_j = \Phi_j(\vec{\theta}) \equiv mL \sinh(\theta_j) - i \sum_{k \neq j} \log S(\theta_j - \theta_k) \quad \text{for } j = \overline{1, n}. \quad (1.106)$$

The Gaudin matrix corresponding to this state is defined as the Jacobian matrix of the change of variables from quantum numbers to rapidities

$$G(\vec{\theta})_{jk} \equiv \frac{\partial \Phi_j(\vec{\theta})}{\partial \theta_k} = \delta_{jk} [mL \cosh(\theta_j) + \sum_{k \neq j} K(\theta_j - \theta_k)] - (1 - \delta_{jk}) K(\theta_j - \theta_k). \quad (1.107)$$

Notice that this is the sum of a diagonal matrix and the Laplacian matrix (1.105) that appeared in the previous section, relating connected and symmetric form factors in infinite volume. In some spin chains, the determinant of this matrix is proportional to the norm of Bethe wave function [157].

Our aim is to relate the finite matrix element $\langle I'_1, \dots, I'_m | \mathcal{O} | I_1, \dots, I_n \rangle$ to its infinite counterpart (1.92). If the two sets $\{\theta'_1, \dots, \theta'_m\}$ and $\{\theta_1, \dots, \theta_n\}$ are disjoint then there is no singularity in the crossing relation and their relation is quite simple [158]

$$\langle \vec{I}' | \mathcal{O}(0) | \vec{I} \rangle_L = \frac{F^\mathcal{O}(\theta'_m + i\pi, \dots, \theta'_1 + i\pi, \theta_1, \dots, \theta_n)}{\sqrt{\det G(\vec{\theta}') \det G(\vec{\theta})}} + O(e^{-mL}). \quad (1.108)$$

This expression directly follows the comparison of two point functions in finite and infinite volume. When the two sets of rapidities are identical, Saleur [40] conjectured that

$$\langle \vec{I}' | \mathcal{O} | \vec{I} \rangle_L = \frac{1}{\det G(\vec{\theta})} \sum_{\alpha \in \{1, 2, \dots, n\}} F_c^\mathcal{O}(\{\theta_j\}_{j \in \alpha}) \det G(\vec{\theta})_{\alpha|\alpha} + O(e^{-mL}), \quad (1.109)$$

where $\det G(\vec{\theta})_{\alpha|\alpha}$ is the principal minor obtained by selecting the α -indexed rows and columns of the full Gaudin matrix (1.107). This formula is physically intuitive if we interpret $\det G(\vec{\theta})_{\alpha|\alpha}$ as the norm of the partial state $\{\theta_j\}_{j \in \alpha}$ in the presence of other particles.

Using the relation (1.104) between connected and symmetric form factors, Pozsgay and Takacs showed [156] that (1.109) is equivalent to

$$\langle \vec{I}' | \mathcal{O} | \vec{I} \rangle_L = \frac{1}{\det G(\vec{\theta})} \sum_{\alpha \subset \{1, 2, \dots, n\}} F_s^\mathcal{O}(\{\theta_j\}_{j \in \alpha}) \det G(\{\tilde{\theta}_j\}_{j \in \bar{\alpha}}) + O(e^{-mL}), \quad (1.110)$$

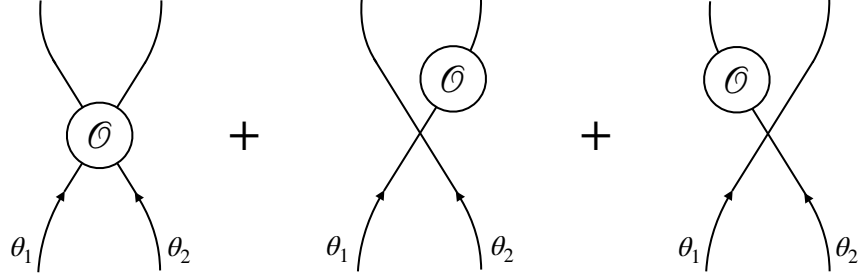


Figure 1.12: Saleur's interpretation of the connected form factors. His proposal reads in the case of two particles $\langle \theta_2, \theta_1 | \mathcal{O} | \theta_1, \theta_2 \rangle = F_c^{\mathcal{O}}(\theta_1, \theta_2) + F_c^{\mathcal{O}}(\theta_1) \langle \theta_2 | \theta_2 \rangle_{\theta_1} + F_c^{\mathcal{O}}(\theta_2) \langle \theta_1 | \theta_1 \rangle_{\theta_2}$.

where $G(\{\tilde{\theta}_j\}_{j \in \bar{\alpha}})$ is the Gaudin matrix of the subset of rapidities $\theta_j, j \in \bar{\alpha}$. The expression (1.109) was rigorously proven by Bajnok and Wu [42]. Their idea is to add a probe rapidity to the diagonal matrix element to make it non-diagonal and thus the formula (1.108) applies. When this rapidity is sent to infinity, one can use the asymptotic of the S-matrix and the clustering property of form factors to recover (1.109).

1.3.4 Leclair-Mussardo formula

Despite its success in computing zero-temperature correlation functions, the form factor formalism faces serious challenges when it comes to finite-temperature observables. If one wishes to use the formalism to evaluate the following correlation function

$$\langle \mathcal{O}_1(x_1) \mathcal{O}_2(x_2) \dots \mathcal{O}_n(x_n) \rangle_R = \frac{1}{Z} \text{Tr}[e^{-RH} \mathcal{O}_1(x_1) \mathcal{O}_2(x_2) \dots \mathcal{O}_n(x_n)] \quad (1.111)$$

then after the insertions of identity (1.91), one has to carry out an infinite sum over form factors along with their respective thermal weight. Even without the form factors, summing over the thermal weight i.e. computing the partition function Z itself is already a non-trivial task. While Z can be computed using TBA, the traditional derivation relies on a thermodynamic state that minimizes the free energy rather than an honest summation. Due to this difficulty, only one point functions have so far been obtained by form factors. The expression goes under the name of Leclair-Mussardo series [39]

$$\langle \mathcal{O} \rangle_R = \sum_{n=0}^{\infty} \frac{1}{n!} \int \frac{d\theta_1}{2\pi} \dots \frac{d\theta_n}{2\pi} \prod_{j=1}^n f(\theta_j) F_c^{\mathcal{O}}(\theta_1, \dots, \theta_n), \quad (1.112)$$

where $f = 1/(1 + e^\epsilon)$ is the TBA filling factor. In practice, the formula is used with truncating after some terms, if excitation is small enough, this provides a fairly good approximation of the one point function. The validity of (1.112) was first confirmed for non-interacting theories in [159]. The authors of [39] then argued that the effect of interaction can be mimicked by a mere replacement of bare energy by the TBA pseudo-energy and thus (1.112) was conjectured to also hold for interacting theories. They also proposed a similar expression for two point functions, but given the daring nature of their argument, it is not surprising that their proposal was proven to be wrong [40, 160–163].

Saleur gave a simple and yet convincing evidence [40] to support (1.112). He considered the case where the operator is given by the density of some conserved charge $\mathcal{Q} = \int dx Q(x, t)$. In this situation the corresponding one point function is well-known in the TBA formalism (see subsection 1.4.2 for more details)

$$\langle Q \rangle = \int \frac{dp(\theta)}{2\pi} f(\theta) q^{\text{dr}}(\theta), \quad (1.113)$$

where $q(\theta)$ is the one-particle eigenvalue of \mathcal{Q} : $\mathcal{Q}|\theta\rangle = q(\theta)|\theta\rangle$ and the dressing operation is defined for any function F as

$$F^{\text{dr}}(\theta) = F(\theta) + \int \frac{d\eta}{2\pi} K(\theta - \eta) f(\eta) F^{\text{dr}}(\eta). \quad (1.114)$$

On the other hand, as \mathcal{Q} acts diagonally on the multi-particle basis, the right hand side of (1.109) is proportional to the Gaudin determinant. By some simple matrix manipulations, it can be shown that the connected form factors of Q are given by

$$F_c^Q(\theta_1, \dots, \theta_n) = q(\theta_1) K(\theta_1 - \theta_2) \dots K(\theta_{n-1} - \theta_n) p'(\theta_n) + \text{perms}, \quad (1.115)$$

where perms. is understood as permutations with respect to the integer set $\{1, \dots, n\}$. Putting this into (1.112), we find complete agreement with the TBA result (1.113). For generic operators, one could also use (1.109) to verify (1.112) up to arbitrary order.

The first full-order proof of the Leclair-Mussardo series was given by Pozsgay [41]. The idea is quite interesting: applying (1.109) to the thermodynamic state that minimizes the TBA free energy. The ratio of the Gaudin determinants turns out to be simply proportional to the product of TBA filling factors in this limit and (1.112) directly follows. This method works equally well if one starts with (1.110) instead of (1.109). The end result is

$$\langle \mathcal{O} \rangle_R = \sum_{n=0}^{\infty} \frac{1}{n!} \int \frac{d\theta_1}{2\pi} \dots \frac{d\theta_n}{2\pi} \prod_{j=1}^n f(\theta_j) w(\theta_j) F_s^{\mathcal{O}}(\theta_1, \dots, \theta_n), \quad (1.116)$$

where $w(\theta) = \exp[-\int \frac{d\eta}{2\pi} K(\theta - \eta) f(\eta)]$.

Concerning two point functions, although there have been multiple low-temperature expansions [164–168], no general structure has been extrapolated. Another strategy is to use form factors with excitations over the thermodynamic state. This approach has been applied for free theories in [161–163] and for interacting theories in a recent work [147]. In yet another direction, the authors of [169] proposed a Leclair-Mussardo formula for two point functions with space-like separation. They argued that in that case the product of the two operators can be considered as a composite object and it is the Leclair-Mussardo series for this bi-local operator that gives the two point function. The common point of [147] and [169] is that they do not focus on the structure of the series itself but rather on the quantity that appears in the series. For [147] this is form factors built on top of a thermodynamic state, while it is form factors of the composite operator that [169] tries to compute. Although these form factors were argued to obey a set of axioms, the task of bootstrapping them proves to be challenging.

1.4 Generalized hydrodynamics

In this section we introduce the most basic concepts of GHD: a hydrodynamics description of integrable models. Let us start the discussion by reminding where hydrodynamics fits in the typical time evolution of a generic many-body system with short-range interaction. There are four time scales

- *Microscopic regime*: at short time, individual particles of the gas propagate ballistically between collisions. This description is exact and the dynamics is reversible.
- *Boltzmann equation*: after sufficiently many collisions, the individual trajectories start to fill the single-particle phase space. One can then effectively describe the dynamics of the system using a probability distribution of particle position and momentum. The change from microscopic description to a density of states amounts to the irreversibility of this stage.
- *Hydrodynamics*: at larger time, relaxation occurs and the system tends to maximize its entropy. Before this maximization of entropy takes place in the entire system, it can develop in sub-regions of mesoscopic size called *fluid cells*. Inside each fluid cell resides a local thermodynamic states with maximum local entropy. There are different scales within hydrodynamics corresponding to different orders in derivatives: the lowest order is called Euler scale, while second order gives rise to Navier-Stokes terms that describe diffusion.
- *Thermodynamics*: the spatial dependence of local states finally disappears and entropy maximization is realized in the entire system.

This picture serves as a guide on how to build a hydrodynamics theory of integrable system. First, we need to understand the characteristics of entropy-maximised states in the presence of an infinite number of conserved quantities. Maximal entropy states and their general properties will be discussed in subsection 1.4.1. In subsection 1.4.2 we will employ the TBA machinery to provide explicit expressions of quantities that characterize these states. Second, we need to know how the states of neighboring fluid cells differ from one another. This is described in subsection 1.4.3, where we present Euler hydrodynamic equations³. Finally we will solve the so-called partitioning protocol problem as an application of the constructed formalism,

1.4.1 Maximal entropy states

Let us denote by \mathcal{Q}_i the set of conserved charges present in the system and let us assume that they can be expressed as integrals of charge densities satisfying conservation laws

$$\mathcal{Q}_i = \int dx Q_i(x, t), \quad \partial_t Q_i(x, t) + \partial_x J_i(x, t) = 0. \quad \partial_t \mathcal{Q}_i = 0. \quad (1.117)$$

Looking at a subsystem of mesoscopic size, if the picture of hydrodynamics holds, we expect it to relax to some state while the rest of the system acts as an external bath. We would

³Diffusive effect is outside the scope of this thesis

like to characterize this state by a density matrix ρ such that the expectation value of any observable \mathcal{O} is given by $\langle \mathcal{O} \rangle = \text{Tr}[\rho \mathcal{O}]$. The maximization of the entropy $S(\rho) = -\text{Tr}[\rho \log \rho]$ must be subjected to the conservation laws. Let us denote by β^i and α the Lagrange parameters corresponding to the conserved charges Q_i and the normalization of ρ , the entropy maximization condition then reads

$$\delta \text{Tr}[\rho(\log \rho + \sum \beta^i Q_i + \alpha)] = 0 \Rightarrow \text{Tr}[\delta \rho(\log \rho + 1 + \alpha + \sum \beta^i Q_i)] = 0. \quad (1.118)$$

As a result, maximal entropy states are of generalized Gibbs form $\rho \propto e^{-\sum \beta^i Q_i}$. The generalized inverse temperatures β^i serve as a system of coordinates in the infinite-dimensional manifold of maximal entropy states. The average $\langle \dots \rangle_{\vec{\beta}}$ evaluated in these states satisfies the following property

$$-\frac{\partial}{\partial \beta^i} \langle \mathcal{O} \rangle_{\vec{\beta}} = \int dx \langle \mathcal{O} Q_i(x, 0) \rangle_{\vec{\beta}}^c, \quad (1.119)$$

where the upper-script c denotes connected correlation functions. In the following, we will use (1.119) as a definition of the inverse temperatures β^i instead of the explicit Gibbs form. It is therefore constructive to define an inner product on the space of local observables

$$(\mathcal{O}_1, \mathcal{O}_2) \equiv \int dx \langle \mathcal{O}_1(0, 0) \mathcal{O}_2(x, 0) \rangle_{\vec{\beta}}^c. \quad (1.120)$$

This inner product is positive semidefinite, since

$$\int dx \langle \mathcal{O}(0, 0) \mathcal{O}(x, 0) \rangle_{\vec{\beta}}^c = \lim_{L \rightarrow \infty} \frac{1}{L} \langle \Delta_{\mathcal{O}}^2 \rangle_{\beta} \geq 0, \quad \Delta_{\mathcal{O}} \equiv \int_0^L dx [\mathcal{O}(x, 0) - \langle \mathcal{O}(0, 0) \rangle_{\vec{\beta}}],$$

with L being the system size. We define the *static covariance matrix*, denoted by C_{ij} as the product between conserved densities. It is nothing but the Hessian matrix of the free energy density $F(\vec{\beta}) = \lim_{L \rightarrow \infty} \log \text{Tr}[e^{-\sum \beta^i Q_i}]/L$

$$\frac{\partial F}{\partial \beta^i} = -\langle Q_i(0, 0) \rangle_{\vec{\beta}} \Rightarrow C_{ij} = (Q_i, Q_j) = \frac{\partial^2 F}{\partial \beta^i \partial \beta^j} = (Q_j, Q_i) = C_{ji}. \quad (1.121)$$

The positivity of C implies that F is a strictly convex function of $\vec{\beta}$. Let us denote by

$$\mathbf{Q}_i \equiv \langle Q_i(0, 0) \rangle_{\vec{\beta}}, \quad \mathbf{J}_i \equiv \langle J_i(0, 0) \rangle_{\vec{\beta}}. \quad (1.122)$$

Due to the convexity of F , the map $\vec{\beta} \rightarrow \vec{\mathbf{Q}}$ from inverse temperatures to averages of conserved charge densities is a bijection. This means, the set of averages of densities can also be used as a system of coordinates on the manifold of maximal entropy states. In view of the conservation laws (1.117), this new coordinates system is particularly useful in describing the currents carried by the state. The dependence of the average currents on the average charge densities is referred to as the *equations of state* of the model

$$\mathbf{J}_i = \mathbf{J}_i(\vec{\mathbf{Q}}). \quad (1.123)$$

We will find the explicit form of these equations in the next subsection using the ingredients of TBA. Before that, there is a general property satisfied by the average currents that can be

derived from nothing but the conservation laws. Considering the average currents as functions of the inverse temperatures, let us define the following matrix

$$B_{ij} \equiv \partial \mathbf{J}_i / \partial \beta^j = (J_i, Q_j). \quad (1.124)$$

Just like the static covariance matrix C , B is also a symmetric [61, 170]. To prove this property, we note that the conservation laws (1.117) implies the existence of a height field $\varphi_i(x, t)$ such that

$$d\varphi_i(x, t) = Q_i(x, t)dx - J_i(x, t)dt. \quad (1.125)$$

Then $\langle J_i(0, 0)Q_j(x, t) \rangle_{\vec{\beta}}^c = -\langle [\partial_t \varphi_i](0, 0)[\partial_x \varphi_j](x, t) \rangle_{\vec{\beta}}^c = \langle \varphi_i(0, 0)[\partial_x \partial_t \varphi_j](x, t) \rangle_{\vec{\beta}}^c$ due to time-translation invariance $= -\langle (\partial_x \varphi_i)(0, 0)(\partial_t \varphi_j)(x, t) \rangle_{\vec{\beta}}^c$ due to space-translation invariance $= \langle Q_i(0, 0)J_j(x, t) \rangle_{\vec{\beta}}^c$. By integrating over x , we obtain the desired property.

The symmetry of B has an important consequence on the equations of state (1.123). Introducing the flux Jacobian matrix

$$A_i^j = \partial \mathbf{J}_i / \partial \mathbf{Q}_j. \quad (1.126)$$

According to the chain rule and the symmetry of the matrix C

$$\sum_k \frac{\partial \mathbf{J}_i}{\partial \mathbf{Q}_k} \frac{\partial \mathbf{Q}_k}{\partial \beta^j} = \sum_k \frac{\partial \mathbf{J}_j}{\partial \mathbf{Q}_k} \frac{\partial \mathbf{Q}_k}{\partial \beta^i} \quad \Leftrightarrow \quad AC = CA^t. \quad (1.127)$$

This means that A is symmetric under the inner product induced by the inverse matrix of C (note that C is positive) $\langle \vec{v}, \vec{w} \rangle \equiv \vec{v}C^{-1}\vec{w}$. Indeed $\langle \vec{v}, A\vec{w} \rangle \equiv \vec{v}C^{-1}A\vec{w} = \vec{v}A^tC^{-1}\vec{w} = A\vec{v}C^{-1}\vec{w} \equiv \langle A\vec{v}, \vec{w} \rangle$. As a result, A is diagonalizable and has real eigenvalues. We will discuss the physical interpretations of its eigenvectors and eigenvalues in the following subsections.

1.4.2 Equations of state and hydrodynamic matrices

We continue our discussion of maximal-entropy states. Using TBA, we present in this subsection the explicit expression for the average charge densities. We also sketch the heuristic derivation [61] of the average densities using mirror transformation. A more rigorous proof based on form factors will be delivered in section 5.1. Once we have obtained the average charge densities and average currents, the hydrodynamic matrices A, B, C directly follow.

The TBA for generalized Gibbs ensemble [66] is almost identical to the traditional TBA. The only modification is that the source term in the TBA equation

$$\epsilon(\theta) = w(\theta) - \int \frac{d\eta}{2\pi} K(\theta - \eta) \log[1 + e^{-\epsilon(\eta)}] \quad (1.128)$$

is now given by $w(\theta) = \sum \beta^i q_i(\theta)$ with q_i being the one-particle eigenvalue of the conserved charge Q_i : $Q|\theta\rangle = q_i(\theta)|\theta\rangle$. The free energy density is again given by

$$F(\vec{\beta}) = \frac{1}{L} \log \text{Tr}[e^{\sum_j -\beta^j Q_j}] = \int \frac{d(\theta)}{2\pi} p'(\theta) \log[1 + e^{-\epsilon(\theta)}] \quad (1.129)$$

The average charge densities are obtained by differentiating F with respect to β^i , as per (1.121)

$$\mathbf{Q}_i = -\frac{\partial F}{\partial \beta^i} = \int \frac{dp}{2\pi} f(\theta) \partial_{\beta_j} \epsilon(\theta), \quad \text{with} \quad f = 1/(1 + e^\epsilon). \quad (1.130)$$

The derivative of the pseudo-energy is the dressed charge eigenvalue q_j^{dr} , where the dressing operation was defined in (1.114). The notion of TBA-dressed quantities will appear repeatedly in our discussion of GHD. In particular, the *density of particles* and *density of holes* can be written as

$$\rho_p(\theta) = (p')^{\text{dr}}(\theta) f(\theta) / (2\pi), \quad \rho_p(\theta) + \rho_h(\theta) = (p')^{\text{dr}} / (2\pi). \quad (1.131)$$

There is a simple property satisfied by the dressing operation

$$\int d\theta \psi(\theta) f(\theta) \chi^{\text{dr}}(\theta) = \int d\theta \psi^{\text{dr}}(\theta) f(\theta) \chi(\theta) \quad (1.132)$$

Using this symmetry relation we can write the average charge densities in two equivalent forms

$$\mathbf{Q}_i = \int \frac{d\theta}{2\pi} p'(\theta) f(\theta) q_i^{\text{dr}}(\theta) = \int d\theta \rho_p(\theta) q_i(\theta). \quad (1.133)$$

The TBA technique does not provide however (at least not directly) the average currents. In the following we present a trick based on mirror transformation to obtain them.

In relativistic quantum field theories, the mirror transformation γ interchanges space and time through a double Wick rotation $(x, t) \rightarrow (-it, ix)$. It reads in terms of rapidity $\theta \rightarrow i\pi/2 - \theta$ and as a result, momentum and energy $p(\theta) = m \sinh \theta$, $E(\theta) = m \cosh \theta$ becomes $(p, E) \rightarrow (iE, -ip)$. Under mirror transformation, one can expect charge densities and currents to be likewise exchanged. As we already know the average charge densities, it suffices to apply the mirror transformation to the state to obtain the average currents. Let us make this statement more precise.

The expectation value of an observable \mathcal{O} in the state characterized by a source term $w(\theta)$ transforms as $\langle \mathcal{O}^\gamma \rangle_w = \langle \mathcal{O} \rangle_{w^\gamma}$ where $w^\gamma(\theta) \equiv w(i\pi/2 - \theta)$. Denoting by $Q[q]$ and $J[q]$ the average charge density and average current as functions of the one particle eigenvalue $q(\theta)$. In the mirror theory, the average current becomes the average charge density

$$(J[q])^\gamma = iQ[q^\gamma]. \quad (1.134)$$

Using the fact the mirror transformation squares to identity, we can write

$$\langle J[q] \rangle_w = \langle \{ (J[q])^\gamma \}^\gamma \rangle_w = \langle iQ[q^\gamma] \rangle_{w^\gamma}. \quad (1.135)$$

It then follows from (1.133) that

$$\mathbf{J}_i = \int \frac{d\theta}{2\pi} E'(\theta) f(\theta) q_i^{\text{dr}}(\theta). \quad (1.136)$$

We can also rewrite this expression in the following form

$$\mathbf{J}_i = \int d\theta v^{\text{eff}}(\theta) \rho_p(\theta) q_i(\theta) \quad \text{where} \quad v^{\text{eff}}(\theta) \equiv \frac{(E')^{\text{dr}}(\theta)}{(p')^{\text{dr}}(\theta)}. \quad (1.137)$$

Although we have obtained this result by mean of an heuristic argument, the form (1.137) is rather convincing. At a fixed rapidity θ the density of particles is by definition $\rho_p(\theta)$. Each particle of this rapidity carries a charge $q_i(\theta)$ and propagates at bare velocity $E'(\theta)/p'(\theta)$. Undergoing collisions with other particles in the gas, it acquires an effective velocity, which is given by the dressed version of the bare velocity.

Let us now derive the matrices A, B, C previously introduced. To remind, B and C are obtained by differentiating the average currents and average charge densities, respectively, as per (1.124) and (1.121). Their computations are similar and we will carry out the case of C

$$C_{ij} = \frac{\partial^2 F}{\partial \beta^j \partial \beta^k} = \int \frac{dp}{2\pi} \left\{ f(\theta)[1 - f(\theta)] \partial_{\beta^k} \epsilon(\theta) \partial_{\beta^j} \epsilon(\theta) + f(\theta) \partial_{\beta^k} \partial_{\beta^j} \epsilon(\theta) \right\}. \quad (1.138)$$

One can eliminate the second derivative of the pseudo energy

$$\partial_{\beta^k} \partial_{\beta^j} \epsilon(\theta) = \int \frac{d\eta}{2\pi} K(\theta, \eta) \{ f(\eta)[1 - f(\eta)] \partial_{\beta^k} \epsilon(\eta) \partial_{\beta^j} \epsilon(\eta) + f(\eta) \partial_{\beta^k} \partial_{\beta^j} \epsilon(\eta) \}, \quad (1.139)$$

by integrating this expression with the particle density measure. Using the fact that $\rho_p = f(p')^{\text{dr}}/(2\pi)$ one can then write the charge covariance as compactly as [66, 171]

$$C_{ij} = \int d\theta \rho_p(\theta) [1 - f(\theta)] q_i^{\text{dr}}(\theta) q_j^{\text{dr}}(\theta). \quad (1.140)$$

The same manipulations give

$$B_{ij} = \int d\theta v^{\text{eff}}(\theta) \rho_p(\theta) [1 - f(\theta)] q_i^{\text{dr}}(\theta) q_j^{\text{dr}}(\theta). \quad (1.141)$$

Once we have obtained B and C , the flux Jacobian matrix A directly follows in view of the relation (1.127)

$$\int d\theta v^{\text{eff}}(\theta) \rho(\theta) [1 - f(\theta)] q_j^{\text{dr}}(\theta) q_j^{\text{dr}}(\theta) = \int d\theta \rho(\theta) [1 - f(\theta)] \sum_k A_i^k q_k^{\text{dr}}(\theta) q_j^{\text{dr}}(\theta). \quad (1.142)$$

By completeness on the index j , we find that A has a continuous spectrum formed by the allowed effective velocities of the particles

$$\sum_k A_i^k q_k^{\text{dr}}(\theta) = v^{\text{eff}}(\theta) q_i^{\text{dr}}(\theta). \quad (1.143)$$

1.4.3 Local entropy maximisation and Euler hydrodynamics

Consider a generic situation where the system starts with an inhomogenous and non-stationary initial state. This means the average values of observables $\langle \mathcal{O}(x, t) \rangle$ depend explicitly on space and time. The main assumption of GHD is that this average can be evaluated in a maximal entropy state with (x, t) -dependent inverse temperatures

$$\langle \mathcal{O}(x, t) \rangle \approx \langle \mathcal{O}(0, 0) \rangle_{\tilde{\beta}(x, t)}. \quad (1.144)$$

Due to homogeneity and stationarity of maximal entropy states, the position of the operator on the right hand side is inconsequential and we chose $(0, 0)$ as a point of reference. We stress that the same local state $\vec{\beta}(x, t)$ describes any local observable at (x, t) .

This assumption of local entropy maximization lying at the heart of GHD is a strong standpoint to take and is very hard to be rigorously proven for generic systems. Nevertheless one can expect that after long enough time, the scales in which significant variations in the local averages occur are infinitely large with respect to the microscopic scales and yet still infinitely small compared to laboratory scales. We will refer to these intermediate scales where local entropy maximization takes place as fluid cells. The separation between different scales is illustrated in figure 1.13.

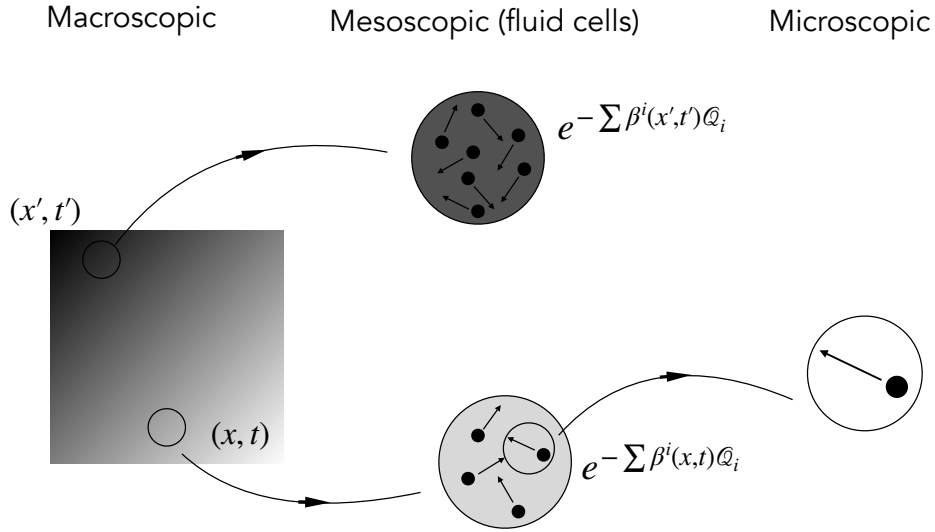


Figure 1.13: The local entropy maximization hypothesis.

Next, we want to know how the profiles of neighboring fluid cells differ from one another. Consider a contour $[X_1, X_2] \times [T_1, T_2]$ inside which the assumption of local entropy maximization is valid. The integration of the continuity equation (1.117) over this contour gives

$$\int_{X_1}^{X_2} dx [Q_i(x, T_2) - Q_i(x, T_1)] + \int_{T_1}^{T_2} dt [J_i(X_2, t) - J_i(X_1, t)] = 0. \quad (1.145)$$

Denoting $\mathbf{Q}_i(x, t) = \langle Q_i(0, 0) \rangle_{\vec{\beta}(x, t)}$, $\mathbf{J}_i(x, t) = \langle J_i(0, 0) \rangle_{\vec{\beta}(x, t)}$ and applying (1.144)

$$\int_{X_1}^{X_2} dx [\mathbf{Q}_i(x, T_2) - \mathbf{Q}_i(x, T_1)] + \int_{T_1}^{T_2} dt [\mathbf{J}_i(X_2, t) - \mathbf{J}_i(X_1, t)] = 0. \quad (1.146)$$

By reversing the logic, we can express this relation in its differential form

$$\partial_t \mathbf{Q}_i(x, t) + \partial_x \mathbf{J}_i(x, t) = 0. \quad (1.147)$$

Remember that the set of average charge densities $\vec{\mathbf{Q}}(x, t)$ encodes all information about the local state at (x, t) , just like the inverse temperatures $\vec{\beta}(x, t)$ do. Moreover, the average currents are functions of the average charge densities, which is the virtue of the equations of state (1.123). In particular, we can insert the flux Jacobian (1.126) into (1.147) and rewrite as a wave equation

$$\partial_t \mathbf{Q}_i(x, t) + \sum_j A_i^j(x, t) \partial_x \mathbf{Q}_j(x, t) = 0, \quad \text{where} \quad A_i^j(x, t) \equiv A_i^j(\vec{\mathbf{Q}}(x, t)). \quad (1.148)$$

We refer to (1.147) and equivalently (1.148) as *Euler hydrodynamic equations*. The general strategy of GHD is to solve these equations for the profile of the local state at every point (x, t) . One can then obtain the average of any observable $\mathcal{O}(x, t)$ by using $\langle \mathcal{O}(x, t) \rangle = \langle \mathcal{O}(0, 0) \rangle_{\vec{\beta}(x, t)}$.

In practice, one can exploit the fact that the flux Jacobian matrix A is diagonalizable, as per (1.143) to facilitate the solving of Euler hydrodynamic equations. Denoting by R the matrix that diagonalises A : $RAR^{-1} = v^{\text{eff}}$. If we manage to write R as the Jacobian of some function $\vec{n}(x, t)$ of $\vec{\mathbf{Q}}(x, t)$

$$\partial n_i / \partial \mathbf{Q}_j = R_i^j. \quad (1.149)$$

Then it follows from (1.148) that

$$\partial_t n_i(x, t) + v^{\text{eff}} \partial_x n_i(x, t) = 0. \quad (1.150)$$

This equation has a simple interpretation: the functions \vec{n} are normal modes being convectively transported at velocity v_i^{eff} . As R is invertible, they can be considered as new coordinates of the maximal entropy state in addition to the average charge densities and the inverse temperatures. Moreover, it turns out that equation (1.149) can be explicitly solved and the normal modes are simply given by the product of the one particle eigenvalue and the TBA filling factor

$$n_i(\theta, x, t) = q_i(\theta) f(\theta, x, t). \quad (1.151)$$

The derivation of this identity is technical and is given in appendix C.

1.4.4 The partitioning protocol

After a rather abstract formalism we present in this subsection a concrete application of GHD. We consider a situation where we bring into contact two systems initially described by two homogenous states. We then let the whole system evolve unitarily and we seek to understand its dynamics. For instance, we can ask what is the current of the steady state arising at the contact point?

Parametrizing the states by their average charge densities, we seek to solve the Euler hydrodynamic equation (1.148) with the initial condition

$$\langle Q_i(x, 0) \rangle = \begin{cases} \mathbf{Q}_i^{(l)} & x < 0 \\ \mathbf{Q}_i^{(r)} & x > 0 \end{cases} \quad (1.152)$$

As both the equation and the initial state are scale invariant, we can assume that the solution

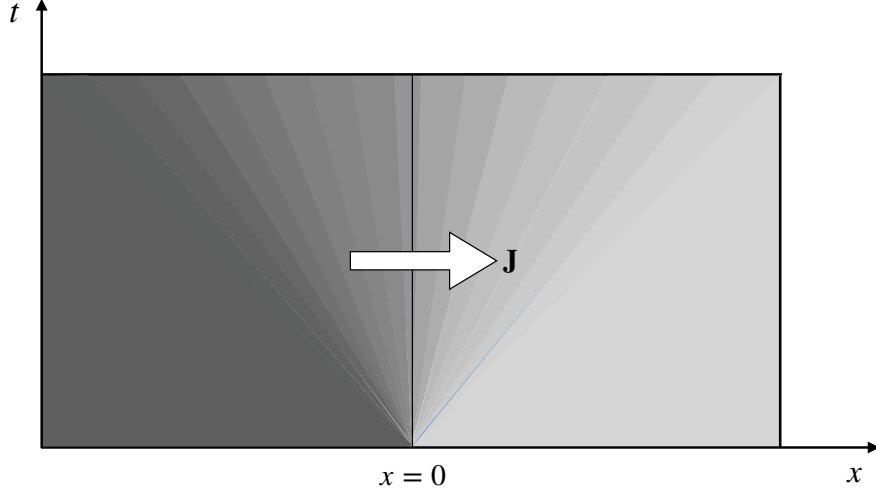


Figure 1.14: The partitioning protocol

itself depends only on the ratio $\xi = x/t$: $\mathbf{Q}_i(x, t) = \mathbf{Q}_i(\xi)$. The initial conditions translates into the asymptotics of the solution

$$\lim_{\xi \rightarrow -\infty} \mathbf{Q}_i(\xi) = \mathbf{Q}_i^{(l)}, \quad \lim_{\xi \rightarrow +\infty} \mathbf{Q}_i(\xi) = \mathbf{Q}_i^{(r)}. \quad (1.153)$$

Moreover the Euler hydrodynamic equation (1.148) is an ordinary differential equation in this parametrization

$$\sum_j [A_i^j(\xi) - \xi \delta_i^j] \frac{d\mathbf{Q}_j}{d\xi} = 0 \quad (1.154)$$

According to the discussion at the end of the previous subsection, this eigenvalue problem can be cast into diagonal form by going to the frame of normal modes. Furthermore, equation (1.151) states that normal modes are proportional to the TBA filling factor, with the proportional factor being space-time independent. Equation (1.150) therefore becomes

$$[v^{\text{eff}}(\theta, \xi) - \xi] \frac{\partial f(\theta, \xi)}{\partial \xi} = 0. \quad (1.155)$$

That is, at fixed value of the rapidity, the TBA filling factor $f(\theta, \xi)$ is constant in the light ray parameter ξ except at $\xi = \xi^*(\theta)$ satisfying

$$\xi^*(\theta) = v^{\text{eff}}(\theta, \xi^*(\theta)). \quad (1.156)$$

The asymptotic conditions (1.153) are hence fully sufficient to determine f

$$f(\theta, \xi) = \begin{cases} f^{(l)}(\theta) & \xi < \xi^*(\theta) \\ f^{(r)}(\theta) & \xi > \xi^*(\theta) \end{cases} \quad (1.157)$$

This result survives an important test. Denoting by T_L and T_R the respective temperature of the initial left and right subsystem. It was found in [172] that if we send both temperatures to

infinity with their ratio kept fixed: $T_l = \kappa T_R$ then the current of the steady state at the junction between the two halves tends to

$$\lim_{T_L \rightarrow \infty} \mathbf{J}(\xi = 0) = \frac{\pi c}{12} T_L^2 (1 - \kappa^2) \quad (1.158)$$

where c is the central charge of the CFT describing the UV limit of the theory. Equations (1.157) and (1.156) can be numerically solved using standard TBA ingredients. Once f is obtained with sufficient precision, we can compute the average current as per (1.136). For the sinh-Gordon model, the numerical result was found to be in perfect agreement with the prediction (1.158) [61].

Chapter 2

Closed systems

In this chapter we show that some thermal quantities introduced previously can be obtained in a uniform fashion. The list includes the TBA equation, the excited state energies, the Leclair-Mussardo series for one point function and the cumulants of conserved charges in a GGE. Concerning the last quantity, only the first (1.133) and second cumulant (1.140) have appeared in the literature. Our result for higher cumulants is new.

To our knowledge, the derivation of the TBA equation about to be presented here first appeared (in a slightly different form) in the work [70–72] of Kato and Wadati for the Lieb-Liniger model and the XXX Heisenberg ferromagnetic spin chain. Our derivation of TBA excited state energies and Leclair-Mussardo formula is however new.

2.1 The TBA equation

In this section we compute the partition function $Z(\vec{\beta}, L) \equiv \text{Tr}[e^{-\sum_j \beta^j Q_j}]$ of a GGE and recover the TBA equation (1.128). Here, L denotes the system volume and Q_j are conserved charges. In contrast to the traditional derivation presented in section 1.2, we approach the problem in a more straightforward manner. Namely we directly write the partition function as an infinite sum over a complete basis of the Hamiltonian. The wave functions in this basis are characterized by Bethe quantum numbers and they diagonalize all the conserved charges at once. In the thermodynamic limit the discrete sums over quantum numbers can be approximated by continuous integrals over particle rapidity. This change of variable involves the determinant of the Gaudin matrix that has been briefly mentioned in the previous chapter. These steps are standard in the low-temperature expansion and have been intensively used in the literature, both for free and interacting theories. Usually, one can only write down explicit expressions up to three or four particles. Our approach is different: instead of developing an analytic series we write the Gaudin determinant as a sum over diagrams prescribed with fixed Feynman rules. These diagrams are of tree type and their combinatorial structure allows their generating function to be determined by a simple integral equation. This equation is nothing but the TBA equation. We present these steps one by one in the following subsections.

Our method works for all theories in which the S-matrix is diagonal and is not necessarily a function of rapidities difference. We will also comment on theories with non-diagonal S-matrix at the end of this section.

2.1.1 The sum over mode numbers

The first step in computing the partition function $Z(\vec{\beta}, L) = \text{Tr}[e^{\sum_j -\beta^j Q_j}]$ is to choose a complete basis that diagonalizes all the conserved charges. We follow Bethe's hypothesis and label each multi-particle wave function by a set of quantum numbers $|n_1, n_2, \dots, n_N\rangle$. We illustrate our method for theories in which these numbers take integer values and are pairwise different. In

order to know the corresponding eigenvalue of conserved charges, one has to convert these quantum numbers into particle rapidities $\theta_1, \dots, \theta_N$. This conversion is known as Bethe-Yang equations, and is written in term of the total scattering phase Φ defined as

$$\Phi_j(\theta_1, \dots, \theta_N) \equiv Lp(\theta_j) - i \sum_{k \neq j}^N \log S(\theta_j, \theta_k) = 2\pi n_j, \quad j = \overline{1, N}. \quad (2.1)$$

If we denote by $q_j(\theta)$ the one-particle eigenvalue of the conserved charge \mathcal{Q}_j then its eigenvalue corresponding to the wave function $|n_1, n_2, \dots, n_N\rangle$ is implicitly given by

$$\mathcal{Q}_j |n_1, n_2, \dots, n_N\rangle = \sum_{k=1}^N q_j(\theta_k) |n_1, n_2, \dots, n_N\rangle. \quad (2.2)$$

By defining $w(\theta) \equiv \sum_j \beta^j q_j(\theta)$, we can write the partition function as a formal sum over Bethe quantum numbers

$$Z(\vec{\beta}, L) = \sum_{N \geq 0} \sum_{\substack{n_1, n_2, \dots, n_N \in \mathbb{Z} \\ n_1 < n_2 < \dots < n_N}} e^{-w(n_1, n_2, \dots, n_N)}. \quad (2.3)$$

In this expression, w is an implicit function of mode numbers: one has to solve the Bethe-Yang equations (2.1) for rapidities and replace $w(n_1, n_2, \dots, n_N)$ by $w(\theta_1) + w(\theta_2) \dots + w(\theta_N)$. In particular, w is a completely symmetric function of mode numbers.

In order to transform this discrete sum to an integral over phase space, we first have to remove the constraint between mode numbers. This can be done by inserting $1 - \delta$ terms which kill configurations with coinciding mode numbers. To this end we obtain an unrestricted sum

$$Z(\vec{\beta}, L) = \sum_{N \geq 0} \frac{1}{N!} \sum_{n_1, n_2, \dots, n_N \in \mathbb{Z}} e^{-w(n_1, n_2, \dots, n_N)} \prod_{j < k}^N (1 - \delta_{n_j, n_k}). \quad (2.4)$$

Once expanded, the Kronecker delta symbols glue mode numbers together into clusters of equal value. Let us see this effect in the two and three-particle sectors

$$\begin{aligned} \frac{1}{2!} \sum_{n_1, n_2} (1 - \delta_{n_1, n_2}) e^{-w(n_1, n_2)} &= \frac{1}{2!} \sum_{n_1, n_2} e^{-w(n_1, n_2)} - \frac{1}{2!} \sum_{n_1} e^{-w(n_1, n_1)} \\ \frac{1}{3!} \sum_{n_1, n_2, n_3} (1 - \delta_{n_1, n_2})(1 - \delta_{n_1, n_3})(1 - \delta_{n_2, n_3}) e^{-w(n_1, n_2, n_3)} &= \frac{1}{3!} \sum_{n_1, n_2, n_3} e^{-w(n_1, n_2, n_3)} \\ &\quad - \frac{1}{2} \sum_{n_1, n_2} e^{-w(n_1, n_1, n_2)} + \frac{1}{3} \sum_{n_1} e^{-w(n_1, n_1, n_1)}. \end{aligned}$$

In general, we have an unrestricted sum over mode numbers with multiplicities $(n_1^{(r_1)}, \dots, n_N^{(r_N)})$. Such tuple defines an (unphysical) Bethe state with $r_1 + \dots + r_N$ particles. This state is a linear combination of plane waves with momenta $r_j p(\theta_j)$, $j = 1, \dots, N$ and thermal weight $w(n_1^{r_1}, \dots, n_N^{r_N}) = r_1 w(\theta_1) + \dots + r_N w(\theta_N)$. The set of rapidities $\vec{\theta}$ is now given by Bethe-Yang equations with multiplicities. There are two modifications we need to add to the total scattering phase Φ_j in the usual Bethe-Yang equations (2.1). First, each probe particle with rapidity θ_j winds around the world and scatters r_k times with r_k particles of rapidity θ_k for each $k \neq j$.

Second, it also scatters with the $r_j - 1$ other particles with the same rapidity via the trivial S-matrix $S(\theta_j, \theta_j) = -1$

$$\Phi_j(\vec{\theta}, \vec{r}) \equiv Lp(\theta_j) - i \sum_{k \neq j}^N r_k \log S(\theta_j, \theta_k) + \pi(r_j - 1) = 2\pi n_j, \quad j = \overline{1, N}. \quad (2.5)$$

The relevance of these unphysical states and their Bethe equations has been already pointed out by Woynarovich [173] and by Dorey *et al* in [47]. In short, one replaces a sum over physical states by a sum over all possible states with proper coefficients such that in the end, unphysical states are canceled out. Finding these coefficients is a purely combinatorial exercise

$$Z(\vec{\beta}, L) = \sum_{N \geq 0} \frac{(-1)^N}{N!} \sum_{n_1, \dots, n_N \in \mathbb{Z}} \sum_{r_1, \dots, r_N \in \mathbb{N}} \prod_{j=1}^N \frac{(-1)^{r_j}}{r_j} e^{-w(n_1^{r_1}, \dots, n_N^{r_N})}. \quad (2.6)$$

One way to verify this formula is to consider the non-interacting case where the thermal weight $w(n_1^{r_1}, \dots, n_N^{r_N})$ simply decomposes into $r_1 w(n_1) + \dots + r_N w(n_N)$ and hence

$$\begin{aligned} Z(\vec{\beta}, L) &= \sum_{N \geq 0} \frac{1}{N!} \sum_{n_1, \dots, n_N \in \mathbb{Z}} \prod_{j=1}^N \sum_{r \in \mathbb{N}} \frac{(-1)^{r+1}}{r} e^{-r w(n_j)} = \sum_{N \geq 0} \frac{(-1)^N}{N!} \sum_{n_1, \dots, n_N \in \mathbb{Z}} \prod_{j=1}^N \log[1 + e^{-w(n_j)}] \\ &= \sum_{N \geq 0} \frac{1}{N!} \left[\sum_n \log[1 + e^{-w(n)}] \right]^N = \exp \left[\sum_n \log[1 + e^{-w(n)}] \right]. \end{aligned} \quad (2.7)$$

Without interaction, the mode number is nothing but $Lp/2\pi$. It suffices to perform a change of variable to bring the partition function into the known form

$$\log Z(\vec{\beta}, L) = L \int \frac{dp}{2\pi} \log[1 + e^{-w(p)}].$$

In the case of free fermions, the multiplicities r_j have obvious meaning. The vacuum energy is a sum of all fermionic loops including those winding r times around the space circle. The weight of an r -winding loop consists of a Boltzmann factor e^{-rRE} , a sign $(-1)^r$ due to the Fermi statistics and a combinatorial factor $1/r$ counting for the Z_r cyclic symmetry. It is natural to interpret the multiplicities r_j as winding, or wrapping, numbers also in the case of non-trivial scattering.

2.1.2 From mode numbers to rapidities

The discrete sum over the allowed values of the total scattering phases $\Phi_j(\vec{\theta}, \vec{r})$ for given wrapping numbers can be replaced, up to exponentially small in L terms, by an integral

$$\sum_{n_1, n_2, \dots, n_N} \approx \int \frac{d\Phi_1}{2\pi} \int \frac{d\Phi_2}{2\pi} \dots \int \frac{d\Phi_N}{2\pi}. \quad (2.8)$$

Since the thermal weight takes a simpler form as a function of rapidities, we are going to perform a change of variables from total scattering phases Φ_j to rapidities θ_j

$$Z(\vec{\beta}, L) = \sum_{N \geq 0} \frac{(-1)^N}{N!} \sum_{r_1, \dots, r_N \in \mathbb{N}} \prod_{j=1}^N \frac{(-1)^{r_j}}{r_j} \int \frac{d\theta_j e^{-r_j w(\theta_j)}}{2\pi} \det G[\theta_1^{(r_1)}, \dots, \theta_N^{(r_N)}]. \quad (2.9)$$

Aside from the Jacobian, the structure of this series is identical to that of free fermions theory (2.7). In other words, all non-trivial information about the interacting theory is encoded in this matrix

$$G_{jk}[\theta_1^{(r_1)}, \dots, \theta_N^{(r_N)}] \equiv \frac{\partial \Phi_j}{\partial \theta_k} = [Lp'(\theta_j) + \sum_{l \neq j} r_l K(\theta_j, \theta_l)] \delta_{jk} - r_k K(\theta_k, \theta_j)(1 - \delta_{kj}). \quad (2.10)$$

2.1.3 The Gaudin determinant and its diagrammatic expansion

Let us denote for brevity

$$p'_j \equiv p'(\theta_j), \quad K_{jk} = K(\theta_j, \theta_k).$$

Inspecting the expansion of the Gaudin determinant for $N = 1, 2, 3$

$$\begin{aligned} \det G[\theta^{(r)}] &= Lp', \\ \det G[\theta_1^{(r_1)}, \theta_2^{(r_2)}] &= L^2 p'_1 p'_2 + Lp'_1 r_1 K_{21} + Lp'_2 r_2 K_{12}, \\ \det G[\theta_1^{(r_1)}, \theta_2^{(r_2)}, \theta_3^{(r_3)}] &= L^3 p'_1 p'_2 p'_3 \\ &\quad + L^2 p'_2 p'_3 r_2 K_{12} + L^2 p'_2 p'_3 r_3 K_{13} + L^2 p'_1 p'_3 r_1 K_{21} \\ &\quad + L^2 p'_1 p'_3 r_3 K_{23} + L^2 p'_1 p'_2 r_1 K_{31} + L^2 p'_1 p'_2 r_2 K_{32} \\ &\quad + Lp'_1 r_1 r_3 K_{31} K_{23} + Lp'_1 r_1 r_2 K_{21} K_{32} + Lp'_1 r_1^2 K_{21} K_{31} \\ &\quad + Lp'_2 r_1 r_2 K_{31} K_{12} + Lp'_2 r_2 r_3 K_{13} K_{32} + Lp'_2 r_2^2 K_{12} K_{32} \\ &\quad + Lp'_3 r_1 r_3 K_{31} K_{23} + Lp'_3 r_2 r_3 K_{12} K_{23} + Lp'_3 r_3^2 K_{13} K_{23}, \end{aligned}$$

we see that there are no cycles of the type $K_{12}K_{21}$ or $K_{12}K_{23}K_{31}$. In order to apply the matrix-tree theorem we consider the matrix

$$\tilde{G}_{jk} = r_k G_{jk}. \quad (2.11)$$

This newly defined matrix is then the sum of a diagonal matrix and a Laplacian matrix (one in which the elements in each row or column sum up to zero): $\tilde{G}_{jk} = \tilde{D}_j \delta_{jk} + \tilde{K}_{jk}$ where

$$D_j = Lr_j p'(\theta_j), \quad \tilde{K}_{jk} = \delta_{jk} \sum_{l \neq j} r_l r_k K(\theta_j, \theta_l) - (1 - \delta_{kj}) r_j r_k K(\theta_k, \theta_j). \quad (2.12)$$

Before stating the result of the matrix-tree theorem, we need to introduce some terminologies in graph theory. A *spanning forest* of a directed graph Γ is a subgraph \mathcal{F} of Γ fulfilling the following three conditions

- \mathcal{F} contains all vertices of Γ ,
- \mathcal{F} does not contain cycles,
- for any vertex of Γ there is at most one oriented edge of \mathcal{F} ending at this vertex.

The vertices with no incoming lines are called roots. Any forest \mathcal{F} can be decomposed into connected components called directed trees. Each tree contains one and only one root. Let us prove this property, starting with the existence. Assume on the contrary that there is at least one coming edge entering every vertex of a tree \mathcal{T} . Starting with an arbitrary vertex v_0 , we can find another vertex v_1 such that $\langle v_1 \rightarrow v_0 \rangle$ is an edge of \mathcal{T} . We can then repeat the procedure to create a chain of vertices $v_n \rightarrow v_{n-1} \rightarrow \dots \rightarrow v_1 \rightarrow v_0$. Due to the finiteness of \mathcal{T} , this chain must close upon itself, creating a cycle and thus violating the second hypothesis. To prove the uniqueness of the root, assume again on the contrary that there are at least two roots r and \tilde{r} in the same tree \mathcal{T} . The connectedness of \mathcal{T} guarantees the existence of a path $(r, v_0, v_1, \dots, v_n, \tilde{r})$ joining the two roots. By definition of roots, the edge joining r and v_0 must be of direction $r \rightarrow v_0$. According to the third property, the edge connecting v_0 and v_1 must then come from v_0 to v_1 . One keeps going and finds eventually that last edge of the path is of direction v_n to \tilde{r} , contradicting the assumption that \tilde{r} is a root.

The matrix-tree theorem [48] states that the determinant of \tilde{G} can be written a sum over directed forests that span the totally connected graph with vertices labeled by $j = 1, \dots, N$

$$\det \tilde{G} = \sum_{\mathcal{F}} \prod_{v_j \text{ roots}} D_j \prod_{\langle jk \rangle \text{ branches}} r_j r_k K(\theta_k, \theta_j). \quad (2.13)$$

That is, the weight of a forest \mathcal{F} is a product of factors D_j associated with the roots and factors K_{kj} associated with the oriented edges $\langle jk \rangle = \langle v_j \rightarrow v_k \rangle$ of \mathcal{F} . The expansion in spanning forests for $N = 1, 2, 3$ is depicted in Fig. 1

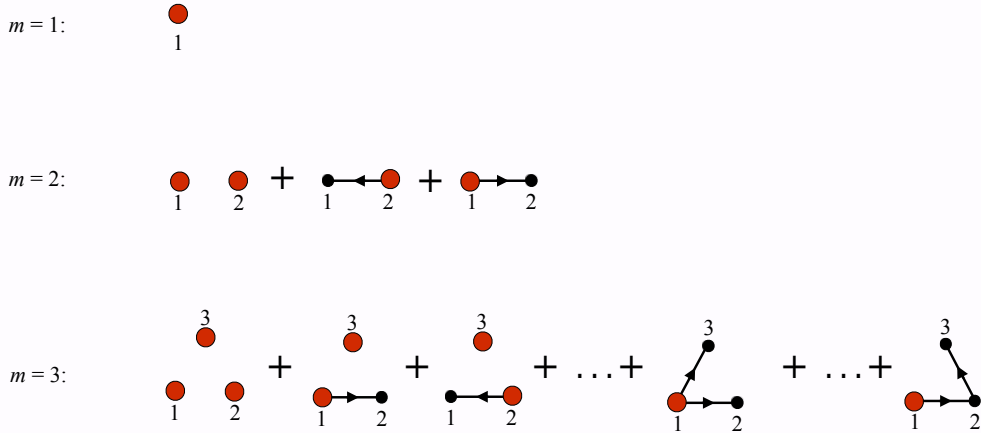


Figure 2.1: The expansion of the determinant of the matrix \tilde{G} in directed spanning forests for $N = 1, 2, 3$. Ellipses mean sum over the permutations of the vertices of the preceding graph. Each vertex of a directed tree, except for the root, has exactly one incoming edge and an arbitrary number of outgoing edges. The root can have only outgoing edges. A factor $r_k r_j K_{kj}$ is associated with each edge $\langle jk \rangle$. A factor D_j is associated with the roots of each connected tree, which is symbolised by a red dot.

With this expansion of the Gaudin determinant, can now write the partition function as

$$Z(\vec{\beta}) = \sum_{N \geq 0} \frac{(-1)^N}{N!} \sum_{r_1, \dots, r_N \in \mathbb{N}} \prod_{j=1}^N \int \frac{(-1)^{r_j}}{r_j^2} \frac{d\theta_j}{2\pi} e^{-r_j w(\theta_j)} \sum_{\mathcal{F}} \prod_{j \text{ roots}} L r_j p'(\theta_j) \prod_{\langle jk \rangle} r_j r_k K(\theta_k, \theta_j). \quad (2.14)$$

The next step is to invert the order of the sum over graphs and the integral/sum over the coordinates (θ_j, r_j) assigned to the vertices. As a result we obtain a sum over the ensemble of tree graphs, with their symmetry factors, embedded in the space $\mathbb{R} \times \mathbb{N}$ where the coordinates (θ, r) of the vertices take values. The embedding is free, in the sense that the sum over the positions of the vertices is taken without restriction. One can think of these graphs as tree level Feynman diagrams obtained by applying the following Feynman rules

$$\begin{array}{ll}
 \begin{array}{c} \bullet \\ (\theta, r) \end{array} & = \frac{(-1)^{r-1}}{r^2} e^{-rw(\theta)} \\
 \begin{array}{c} \bullet \\ (\theta, r) \end{array} & = Lp'(\theta) \frac{(-1)^{r-1}}{r} e^{-rw(\theta)} \\
 \begin{array}{c} \xrightarrow{\hspace{1cm}} \\ (\theta_1, r_1) \quad (\theta_2, r_2) \end{array} & = r_1 r_2 K(\theta_2, \theta_1).
 \end{array} \quad (2.15)$$

2.1.4 Summing over the trees

The sum over the embedded graphs is the exponential of the sum over connected ones. In this way we can write the free energy density as

$$F(\vec{\beta}) = \int \frac{d(\theta)}{2\pi} p'(\theta) \sum_{r \geq 1} r Y_r(\theta), \quad (2.16)$$

where $Y_r(\theta)$ is the sum of all trees rooted at the point (θ, r) , see figure 2.2.

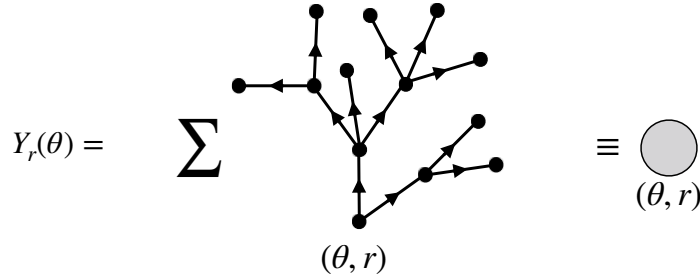


Figure 2.2: The sum over all trees growing out of a fixed root. In defining $Y_r(\theta)$, we have extracted a factor $Lp'(\theta)r$ out of the weight (2.15) of the root. Thus, all vertices appearing in this diagram have the same weight.

As any partition sum of trees, it satisfies a simple non-linear equation (a Schwinger-Dyson equation in the QFT language), illustrated in figure 2.3

$$Y_r(\theta) = \frac{(-1)^r}{r^2} [e^{-w(\theta)} \exp \sum_s \int \frac{d\eta}{2\pi} s K(\eta, \theta) Y_s(\eta)]^r. \quad (2.17)$$

$$Y_r(\theta) = \text{diagram 1} + \text{diagram 2} + \frac{1}{2!} \text{diagram 3} + \frac{1}{3!} \text{diagram 4} + \dots$$

Figure 2.3: Diagrammatic representation of the TBA equation.

By comparing this equation for arbitrary r and for $r = 1$ we find that $Y_r(\theta) = (-1)^r Y_1^r(\theta)/r^2$. The Schwinger-Dyson equation (2.17) for $r = 1$ is then the well-known TBA equation if we identify $Y_1(\theta) = Y(\theta) = e^{-\epsilon(\theta)}$

$$Y(\theta) = e^{-w(\theta)} \exp \int \frac{d\eta}{2\pi} K(\eta, \theta) \log[1 + Y(\eta)]. \quad (2.18)$$

Furthermore, the free energy density (2.16) also takes its familiar form

$$F(\vec{\beta}) = \int \frac{d(\theta)}{2\pi} p'(\theta) \log[1 + Y(\theta)]. \quad (2.19)$$

Our machinery works equally well for *bosonic* theories in which the mode numbers of a multi-particle state can take coinciding values. In this case, we simply need to remove all the minus signs in the combinatorial coefficients that appear in the expansion of the partition function

$$Z(\vec{\beta}, L) = \sum_{N \geq 0} \frac{1}{N!} \sum_{n_1, \dots, n_N \in \mathbb{Z}} \sum_{r_1, \dots, r_N \in \mathbb{N}} \prod_{j=1}^N \frac{1}{r_j} e^{-w(n_1^{r_1}, \dots, n_N^{r_N})}. \quad (2.20)$$

The Feynman rules for vertices are modified accordingly

$$\begin{aligned} \text{black dot } (\theta, r) &= \frac{1}{r^2} e^{-rw(\theta)}, \\ \text{red dot } (\theta, r) &= L p'(\theta) \frac{1}{r} e^{-rw(\theta)}. \end{aligned}$$

while the rule for propagators remain unchanged. It follows that $Y_r(\theta) = Y^r(\theta)/r^2$ and we recover the bosonic TBA equation

$$Y(\theta) = e^{-w(\theta)} \exp \left\{ - \int \frac{d\eta}{2\pi} K(\eta, \theta) \log[1 - Y(\eta)] \right\}, \quad F(\vec{\beta}) = - \int \frac{d(\theta)}{2\pi} p'(\theta) \log[1 - Y(\theta)].$$

2.1.5 A comment on theories with non-diagonal S-matrix

We have provided a new derivation of the TBA equation for theories with diagonal S-matrix. Can we extend our method for theories in which the S-matrix is not diagonal, for instance the chiral $SU(2)$ Gross-Neveu model? Unfortunately we encounter a serious problem at the very

first step of our formalism: the sum over mode numbers. For the chiral $SU(2)$ Gross-Neveu model, there are Bethe equations for the physical rapidity (1.24) and there are also Bethe equations for auxiliary rapidity (1.25). In deriving these equations, we have used the fact that the auxiliary rapidities correspond in fact to dynamical excitations on a spin chain where the physical rapidities are impurities. In particular the number of the auxiliary particles can never exceed half the number of physical particles. This constraint prohibits us from carrying out the infinite sum over mode numbers.

However, we saw above that the combinatorial structure of the trees is equivalent to the TBA equation. Therefore, we can reverse the logic and translate the TBA equations of the chiral $SU(2)$ Gross-Neveu model (which are obtained by the traditional method) into a sum over trees. These trees involve an infinite number of vertex types: they correspond to either the physical rapidity or the auxiliary strings. Going back further, we can say that if instead of summing over two species of mode number with constraint, we consider a free sum over an infinite number of mode number species then at the end, we would end up with the correct TBA equations. That is, if we deliberately commit two errors: first, removing the constraint between auxiliary and physical particles and second, including auxiliary strings in our summation then the net result turns out to be accurate.

At this point, this is nothing more than a mere interpretation of the TBA equations with string solutions. In chapter 4 however, this line of thought will provide some useful information for the boundary entropy of a theory with non-diagonal scattering.

2.2 The charge statistics in GGE

In this section we use our diagrammatic formalism to obtain the cumulants of conserved charges in a GGE. As the results of this subsection will later be applied in the context of GHD, we restrict our consideration to S-matrices that depend on the difference of rapidities. In particular, the scattering kernel is symmetric: $K(\theta_1, \theta_2) = K(\theta_2, \theta_1)$ and the resulting graphs are unoriented. The relevance of this symmetry will be explained at the end of subsection 2.2.2.

The first two cumulants, namely the charge average and the charge covariance matrix has been obtained in subsection (1.4.2) directly from the free energy. For the convenience of following we repeat here their expressions. The charge average is given by

$$\frac{1}{L}\langle \mathcal{Q}_j \rangle = -\frac{\partial F(\vec{\beta})}{\partial \beta^j} = \int \frac{d\theta}{2\pi} p'(\theta) f(\theta) q_j^{\text{dr}}(\theta). \quad (2.21)$$

where the dressing operation was defined in (1.114). The charge covariance matrix involves second derivatives of the pseudo energy which could be eliminated using the manipulation described in subsection 1.4.2

$$\frac{1}{L}\langle \mathcal{Q}_j \mathcal{Q}_k \rangle^c = \frac{\partial^2 F(\vec{\beta})}{\partial \beta^j \partial \beta^k} = \int \frac{d\theta}{2\pi} p'(\theta) f(\theta) [1 - f(\theta)] q_j^{\text{dr}}(\theta) q_k^{\text{dr}}(\theta). \quad (2.22)$$

For the third cumulants, the same trick eliminates the third derivatives of the pseudo-energy but leaves the second ones

$$\begin{aligned} \frac{1}{L}\langle \mathcal{Q}_j \mathcal{Q}_k \mathcal{Q}_l \rangle^c = & \int \frac{d\theta}{2\pi} p'(\theta) f(\theta) [1 - f(\theta)] \times \left\{ [1 - 2f(\theta)] q_j^{\text{dr}}(\theta) q_k^{\text{dr}}(\theta) q_l^{\text{dr}}(\theta) \right. \\ & \left. + q_j^{\text{dr}}(\theta) \partial_{\beta_l} \partial_{\beta_k} \epsilon(\theta) + q_j^{\text{dr}}(\theta) \partial_{\beta_l} \partial_{\beta_k} \epsilon(\theta) + q_j^{\text{dr}}(\theta) \partial_{\beta_l} \partial_{\beta_k} \epsilon(\theta) \right\}. \end{aligned} \quad (2.23)$$

This direct computation from the free energy is clearly impractical for higher cumulants. There is no general rule to write the obtained expression in terms of fundamental TBA quantities like the particle density, the filling factor or simple dressing operators.

2.2.1 Charge average

As the conserved charges act diagonally on the basis of multi-particle states, we can calculate their averages by following the exact same steps as before. The only point we need to pay attention to is their action on multi-wrapping states. In view of the interpretation of these states as linear combinations of plane waves, we propose a natural generalization of (2.2)

$$\mathcal{Q}_j |n_1^{r_1}, \dots, n_N^{r_N}\rangle = \sum_{i=1}^N r_i q_j(\theta_i) |n_1^{r_1}, \dots, n_N^{r_N}\rangle, \quad (2.24)$$

Consequently, the unnormalized charge average is given by

$$\begin{aligned} \text{Tr}[e^{-\sum \beta^i \mathcal{Q}_i} \mathcal{Q}_j] &= \sum_{N \geq 0} \frac{(-1)^N}{N!} \sum_{n_1, \dots, n_N \in \mathbb{Z}} \sum_{r_1, \dots, r_N \in \mathbb{N}} \prod_{i=1}^N \frac{(-1)^{r_i}}{r_i} e^{-w(n_1^{r_1}, \dots, n_N^{r_N})} \sum_{i=1}^N r_i q_j(\theta_i), \\ &= \sum_{N \geq 0} \frac{(-1)^N}{N!} \sum_{r_1, \dots, r_N \in \mathbb{N}} \prod_{j=1}^N \frac{(-1)^{r_j}}{r_j^2} \int \frac{d\theta_j e^{-r_j w(\theta_j)}}{2\pi} \det \tilde{G}[\theta_1^{(r_1)}, \dots, \theta_N^{(r_N)}] \sum_{i=1}^N r_i q_j(\theta_i). \end{aligned}$$

Expanding the Gaudin determinant, we obtain a sum over forests with the same Feynman rules as (2.15) except for one modification: each forest now contains a vertex, the coordinate of which denoted by (θ, r) , that is marked with a charge insertion and carries an extra weight of $r q_j(\theta)$ coming from (2.24). Contribution coming from un-inserted trees (vacuum diagrams) cancel with the partition function. As a result, the average of \mathcal{Q}_j is a sum over trees with a vertex marked with charge insertion. In order to perform the sum over these trees, we note that from

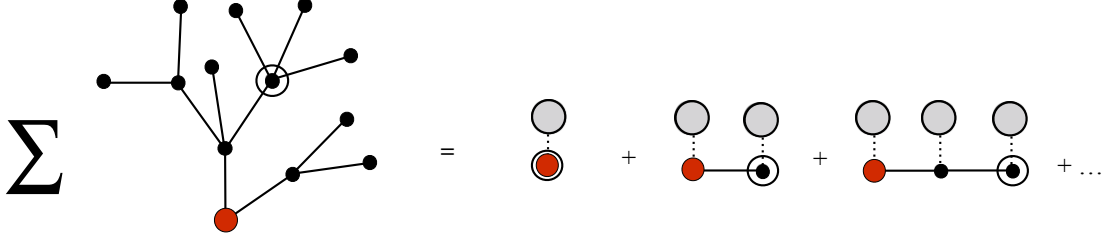


Figure 2.4: Diagrammatic representation of the charge average. Circled vertex stands for the charge insertion.

the inserted vertex we can always trace a unique path- a *spine* to the root of the tree¹. At each node (θ, r) inside this spine, we can sum up the trees growing out of it while absorbing the multiplicities r^2 coming from the two adjacent propagators. The nodes at the two ends of the spine receive a multiplicity from the charge (or momentum derivative) insertion and a residual multiplicity from one propagator. This results in the TBA filling factor on every node along the spine

$$\sum_{r \geq 1} r^2 Y_r(\theta) = \sum_{r \geq 1} (-1)^{r-1} Y^r(\theta) = \frac{Y(\theta)}{1 + Y(\theta)} = f(\theta). \quad (2.25)$$

Moreover, the sum over spines each of which carries a filling factor on its nodes is nothing but the explicit expansion of the dressing operation (1.114)

$$q_j^{\text{dr}}(\theta) = q_j(\theta) + \int \frac{d\eta}{2\pi} K(\theta - \eta) f(\eta) q_j(\eta) + \int \frac{d\eta}{2\pi} \frac{d\zeta}{2\pi} K(\theta - \eta) f(\eta) K(\eta - \zeta) f(\zeta) q_j(\zeta) + \dots$$

We thus recover the expression (2.21) of the charge average

$$\frac{1}{L} \langle \mathcal{Q}_j \rangle = \int \frac{dp}{2\pi} f(\theta) q_j^{\text{dr}}(\theta). \quad (2.26)$$

2.2.2 Charge covariance

The action of a product of two conserved charges \mathcal{Q}_j and \mathcal{Q}_k on a multi-wrapping states is factorized

$$\mathcal{Q}_j \mathcal{Q}_k |\theta_1^{r_1}, \dots, \theta_N^{r_N}\rangle = \mathcal{Q}_j \sum_{i=1}^N r_i q_k(\theta_i) |\theta_1^{r_1}, \dots, \theta_N^{r_N}\rangle = \sum_{i=1}^N r_i q_j(\theta_i) \sum_{i=1}^N r_i q_k(\theta_i) |\theta_1^{r_1}, \dots, \theta_N^{r_N}\rangle. \quad (2.27)$$

¹Existence comes from connectedness and uniqueness comes from the absence of loops in a tree.

Thus $\text{Tr}[e^{-\Sigma \beta_i Q_i} Q_j Q_k]$ is given by a sum over forests each one of which contains two vertices with charge insertions. Un-inserted diagrams again cancel with the partition function and the product average $\langle Q_j Q_k \rangle$ is the sum over inserted ones. They can be of two types: either a tree with two inserted vertices or two trees with one inserted vertex each. The sum over diagrams of second type is nothing but the product of charge averages $\langle Q_j \rangle \langle Q_k \rangle$. Therefore the charge covariance $\langle Q_j Q_k \rangle^c$ is given by the sum over trees with two charge insertions.

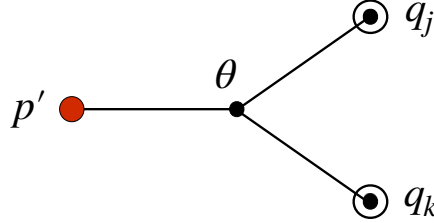


Figure 2.5: Combinatorial structure of a tree with two leaves: there exists an internal vertex connected to the three external ones. We take this vertex as a reference point to sum over the trees.

From each inserted vertex, one can find a unique path to the root of the tree. The two paths must join at some point (θ, r) : a unique vertex linked to the root and likewise to the two leaves. Except for this vertex, all other vertices receive the filling factor f as explained previously. At this vertex we can pull three multiplicities from the three adjacent propagators. This results in a special filling factor

$$\sum_{r \geq 1} r^3 Y_r(\theta) = \frac{Y(\theta)}{[1 + Y(\theta)]^2} = f(\theta)[1 - f(\theta)].$$

The charge covariance involves three dressed quantities corresponding to the three spines coming out of this intersection point. We recover the expression (2.22)

$$\frac{1}{L} \langle Q_j Q_k \rangle^c = \int \frac{d\theta}{2\pi} f(\theta)[1 - f(\theta)] (p')^{\text{dr}}(\theta) q_j^{\text{dr}}(\theta) q_k^{\text{dr}}(\theta). \quad (2.28)$$

We can see here the reason why we chose to work with symmetric scattering kernels in this section. If that was not the case then we would need to define two dressing operations corresponding to the two directions on a spine. In this particular case, there is one spine coming toward θ and two spines coming outward. For higher cumulants, there are more propagators (spines) and it is tedious to specify their direction. We want to avoid this unnecessary complication by restricting our discussion to relativistically-invariant theories.

2.2.3 Higher cumulants

After understanding the explicit examples of the charge average and charge covariance, generalization to higher cumulants is straightforward. The n^{th} cumulant is given by a sum over all tree-diagrams with $n + 1$ external vertices : a root with p' inserted and n leaves carrying the n

conserved charges. Their internal vertices live in phase space and will be integrated over. An external propagator connecting an internal vertex θ and an external vertex inserted with an operator ψ has a weight $\psi^{\text{dr}}(\theta)$, here ψ can either be the momentum derivative or the charge eigenvalues. An internal propagator connecting two internal vertices θ, η is assigned a weight $K^{\text{dr}}(\theta, \eta)$, where

$$K^{\text{dr}}(u, v) = K(u, v) + \int \frac{dw}{2\pi} K(u, w) f(w) K^{\text{dr}}(w, v). \quad (2.29)$$

The weight of an internal vertex θ of degrees d is

$$\sum_{r \geq 1} (-1)^{r-1} r^{d-1} Y^r(\theta).$$

We summarize these rules in the following

$$\begin{aligned} \theta \bullet \text{---} \odot \psi &= \psi^{\text{dr}}(\theta) \\ \theta \bullet \text{---} \bullet \eta &= K^{\text{dr}}(\theta, \eta) \end{aligned} \quad (2.30)$$

$$\theta \bullet \begin{array}{c} \diagup \\ \diagdown \end{array} = \sum_{r \geq 1} (-1)^{r-1} r^{d-1} Y^r(\theta)$$

There is a simple recursive algorithm to generate all diagrams with n leaves. For each partition of n that is not the trivial one (i.e. $n = n$)

$$n = \underbrace{a_1 + \dots + a_1}_{\alpha_1} + \underbrace{a_2 + \dots + a_2}_{\alpha_2} + \dots + \underbrace{a_j + \dots + a_j}_{\alpha_j}, \quad a_1 < a_2 < \dots < a_j \quad (2.31)$$

we choose α_1 trees with a_1 leaves, ..., α_j trees with a_j leaves. We then remove their roots and join them to a new common root. This algorithm translates into the following equation that determines the number d_n of diagrams with n leaves

$$d_n = \sum_{\substack{p \in \mathcal{P}_n, |p| > 1 \\ p = (a_1^{\alpha_1}, \dots, a_j^{\alpha_j})}} \prod_{i=1}^j \binom{d_{a_i} + \alpha_i - 1}{\alpha_i}. \quad (2.32)$$

Some values of d_n are given in table 2.1. We also list all diagrams with up to 5 leaves in figure 2.6.

n	1	2	3	4	5	6	7	8	9	10
d_n	1	1	2	5	12	33	90	261	766	2312

Table 2.1: Number of trees as function of their leaves.

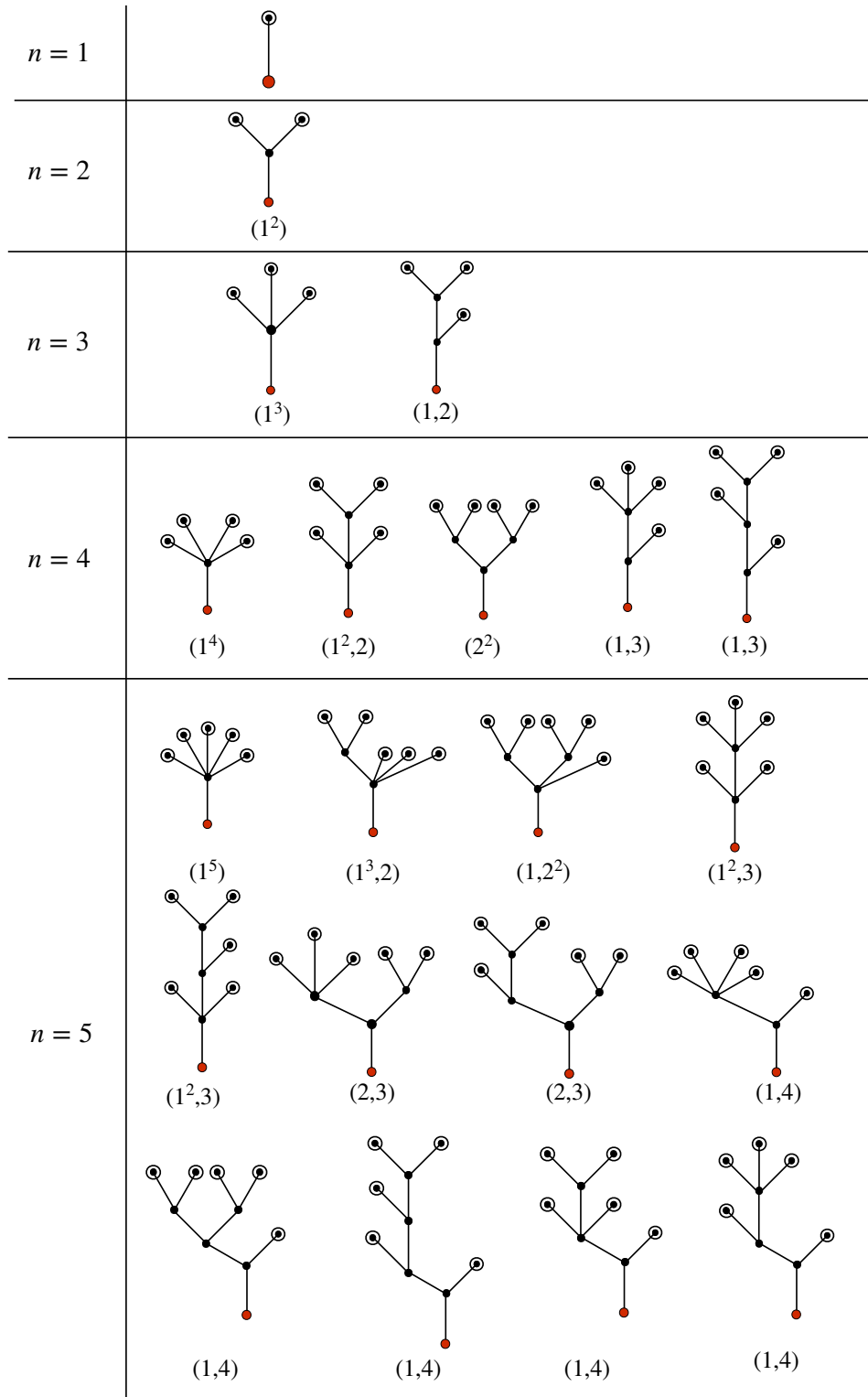


Figure 2.6: Trees up to five leaves along with the partition used to generate them.

The third cumulant $\langle \mathcal{Q}_j \mathcal{Q}_k \mathcal{Q}_l \rangle^c$ can be read directly from the two diagrams with three leaves. The one on the left gives

$$\int \frac{d\theta}{2\pi} f(\theta) [1 - f(\theta)] [1 - 2f(\theta)] (p')^{\text{dr}}(\theta) q_j^{\text{dr}}(\theta) q_k^{\text{dr}}(\theta) q_l^{\text{dr}}(\theta). \quad (2.33)$$

The one on the right involves three permutations of vertices

$$\begin{aligned} \int \int \frac{d\theta}{2\pi} \frac{d\eta}{2\pi} (p')^{\text{dr}}(\theta) f(\theta) [1 - f(\theta)] f(\eta) [1 - f(\eta)] K^{\text{dr}}(\eta, \theta) [q_j^{\text{dr}}(\theta) q_k^{\text{dr}}(\eta) q_l^{\text{dr}}(\eta) \\ + q_k^{\text{dr}}(\theta) q_j^{\text{dr}}(\eta) q_l^{\text{dr}}(\eta) + q_l^{\text{dr}}(\theta) q_j^{\text{dr}}(\eta) q_k^{\text{dr}}(\eta)]. \end{aligned} \quad (2.34)$$

This result agrees with the expression (2.23) obtained from GGE free energy. Indeed, we can write the second derivative of pseudo-energy in terms of the dressed propagator as follows

$$\partial_{\beta^l} \partial_{\beta^k} \epsilon(\theta) = \int \frac{d\eta}{2\pi} f(\eta) [1 - f(\eta)] K^{\text{dr}}(\theta, \eta) \partial_{\beta^k} \epsilon(\eta) \partial_{\beta^l} \epsilon(\eta). \quad (2.35)$$

Our formalism provides an intuitive picture of these cumulants: external vertices are the bare charges while internal vertices are virtual particles that carry anomalous corrections

2.3 The Leclair-Mussardo formula

The Pozsgay-Takacs formula provides an expansion of the diagonal matrix elements of a local operator in terms of the infinite-volume form factors with the same or lower number of particles

$$\langle n_N, \dots, n_1 | \mathcal{O} | n_1, \dots, n_N \rangle_L = \frac{1}{\det G(\theta_1, \dots, \theta_N)} \sum_{\alpha \cup \bar{\alpha} = \{1, \dots, N\}} F_c^\mathcal{O}(\alpha) \det_{j,k \in \bar{\alpha}} G(\theta_1, \dots, \theta_N). \quad (2.36)$$

where the sum goes over all partitions of the rapidities $\theta_1, \dots, \theta_N$ in to two complementary sets α and $\bar{\alpha}$ and $\det_{j,k \in \bar{\alpha}} G$ denotes the minor of the Gaudin matrix obtained by deleting the lines and the columns that belong to the subset α . With this result we will derive the Leclair-Mussardo formula from the tree expansion method. For that we will need the diagonal matrix elements also for the multi-wrapping states $|n_1^{(r_1)}, \dots, n_N^{(r_N)}\rangle$. We will make a very natural conjecture about this action namely ²

$$\begin{aligned} & \langle n_N^{(r_N)}, \dots, n_1^{(r_1)} | \mathcal{O} | n_1^{(r_1)}, \dots, n_N^{(r_N)} \rangle_L \\ &= \frac{1}{\det G[\theta_1^{(r_1)}, \dots, \theta_N^{(r_N)}]} \sum_{\alpha \cup \bar{\alpha} = \{1, \dots, N\}} \prod_{j \in \alpha} r_j F_c^\mathcal{O}(\alpha) \det_{j,k \in \bar{\alpha}} G[\theta_1^{(r_1)}, \dots, \theta_N^{(r_N)}]. \end{aligned} \quad (2.37)$$

The logic behind this conjecture is that the action of the operator on a multi wrapping particle is the same as if it were single wrapping particle. The only difference is that the r - wrapping particle appears r times in the same time slice, the operator acts on each copy, which brings an overall factor of r . We should mention here that a discussion about the “multi-diagonal” matrix elements was presented in [175].

Repeating the argument from the beginning of section 2.4, we can perform the sum over the complete set of states in the thermal expectation value of the operator \mathcal{O}

$$\langle \mathcal{O} \rangle_{\vec{\beta}} = \frac{1}{Z(\vec{\beta}, L)} \sum_{N \geq 0} \sum_{n_1 < \dots < n_N} e^{-w(n_1, \dots, n_N)} \langle n_N, \dots, n_1 | \mathcal{O} | n_1, \dots, n_N \rangle_L \quad (2.38)$$

Then, by inserting and expanding $1 - \delta$ symbols we obtain a sum over mode numbers and rapidities where the multi-wrapping matrix element (2.37) appears in each term of the sum. The Jacobian of the change of variables from mode numbers to rapidities compensates for its inverse on the right hand side of (2.37). As a result, the one point function of \mathcal{O} takes the following form

$$\begin{aligned} \langle \mathcal{O} \rangle_{\vec{\beta}} &= \frac{1}{Z(\vec{\beta}, L)} \sum_{N \geq 0} \frac{(-1)^N}{N!} \sum_{r_1, \dots, r_N \in \mathbb{N}} \prod_{j=1}^N \frac{(-1)^{r_j}}{r_j^2} \int \frac{d\theta_j e^{-r_j w(\theta_j)}}{2\pi} \\ &\times \sum_{\alpha \cup \bar{\alpha} = \{1, \dots, N\}} \prod_{j \in \alpha} r_j^2 F_c^\mathcal{O}(\alpha) \det_{j,k \in \bar{\alpha}} \tilde{G}[\theta_1^{(r_1)}, \dots, \theta_N^{(r_N)}]. \end{aligned} \quad (2.39)$$

The next step is to apply the matrix-tree theorem for the diagonal minors of the (modified) Gaudin matrix in the last factor in the integrand in (2.39). A minor obtained by removing all

²A relation between connected form factors with coinciding rapidities and those with generic rapidities was obtained in [174]. It would be interesting to study the connection between that relation and our conjecture.

edges and all columns from the subset $\alpha \in \{1, \dots, N\}$ of the matrix \tilde{G} defined in eq. has the following expansion

$$\det_{j,k \in \bar{\alpha}} \tilde{G} = \sum_{\mathcal{F} \in \mathcal{F}_{\alpha, \bar{\alpha}}} \prod_{\substack{j \in \bar{\alpha} \\ j \text{ is a root}}} D_j \prod_{\langle jk \rangle \in \mathcal{F}} r_j r_k K(\theta_k, \theta_j) \quad (2.40)$$

The spanning forests $\mathcal{F} \in \mathcal{F}_{\alpha, \bar{\alpha}}$ are subjected to the three conditions in subsection 2.1.3, with the additional restriction that all vertices belonging to α are roots. The weight of these roots is one. An example is given in fig. 2.7

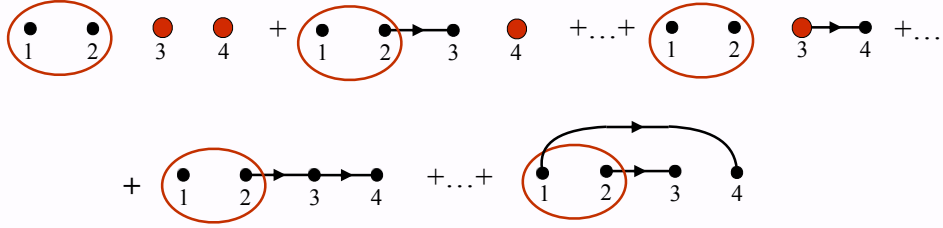


Figure 2.7: The tree expansion for a principal minor of the Gaudin matrix $\det_{j,k \in \bar{\alpha}} \tilde{G}$ for $\alpha = \{1, 2\}$ and $\bar{\alpha} = \{3, 4\}$.

The expansion (2.40) follows directly from the expansion (2.13) of the previous section which corresponds to the particular case $\alpha = \emptyset, \bar{\alpha} = \{\theta_1, \dots, \theta_N\}$. Indeed, the rhs of (2.40) by retaining only the terms in the rhs of (2.13) that contain the factor $\prod_{j \in \alpha} D_j$ and then dividing the sum by this factor.

Now we can proceed similarly to what we have done in the computation of the partition function, where rearranging of the order of summation allowed us to rewrite the sum as a series of tree Feynman diagrams. This time there will be two kinds of Feynman graphs: the “vacuum trees” and diagrams representing a vertex $F_c^\mathcal{O}$ with n lines and a tree attached to each line. The weight of such tree is the same as the weight of the vacuum trees except for a factor of r^2 associated with the root.



Figure 2.8: The tree expansion for the thermal expectation value of a local operator.

The sum over the vacuum trees cancels with the partition function and the sum over the surviving terms has the same structure as

$$\langle \mathcal{O} \rangle_{\tilde{\beta}} = \sum_{n=0}^{\infty} \frac{1}{n!} \int \frac{d\theta_1}{2\pi} \dots \frac{d\theta_n}{2\pi} \prod_{j=1}^n f(\theta_j) F_c^\mathcal{O}(\theta_1, \dots, \theta_n) \quad (2.41)$$

which is depicted in fig. 2.8. The factor $f(\theta)$ is obtained as the sum of all trees with a root at the point θ , with extra weight r^2 associated with the root, as explained in (2.25). The difference of the sum over trees in the factor $f(u)$ compared with the sum over vacuum trees (2.34) is that there is an extra factor r associated with the root reflecting the breaking of the Z_r symmetry of the corresponding wrapping process.

2.4 Excited state energies

In subsection 1.2.5 we have interpreted the singular points in the TBA equation as rapidities of some state in the mirror theory. In this subsection we will recover the excited state energy (1.86) and excited state TBA equation (1.88) by computing the partition in the presence of a mirror state $|\tilde{\theta}^*\rangle = |\tilde{\theta}_1^*, \dots, \tilde{\theta}_M^*\rangle$ propagating along the spatial direction. We carry out the computation in the physical channel, summing over physical eigenstates $|\theta\rangle = |\theta_1, \dots, \theta_N\rangle$. It is important to mention that the idea of using particles as defects and the defect TBA equations were derived in [176] while the idea of deriving the exact Bethe ansatz equation from a partition function with defects already appeared in [177].

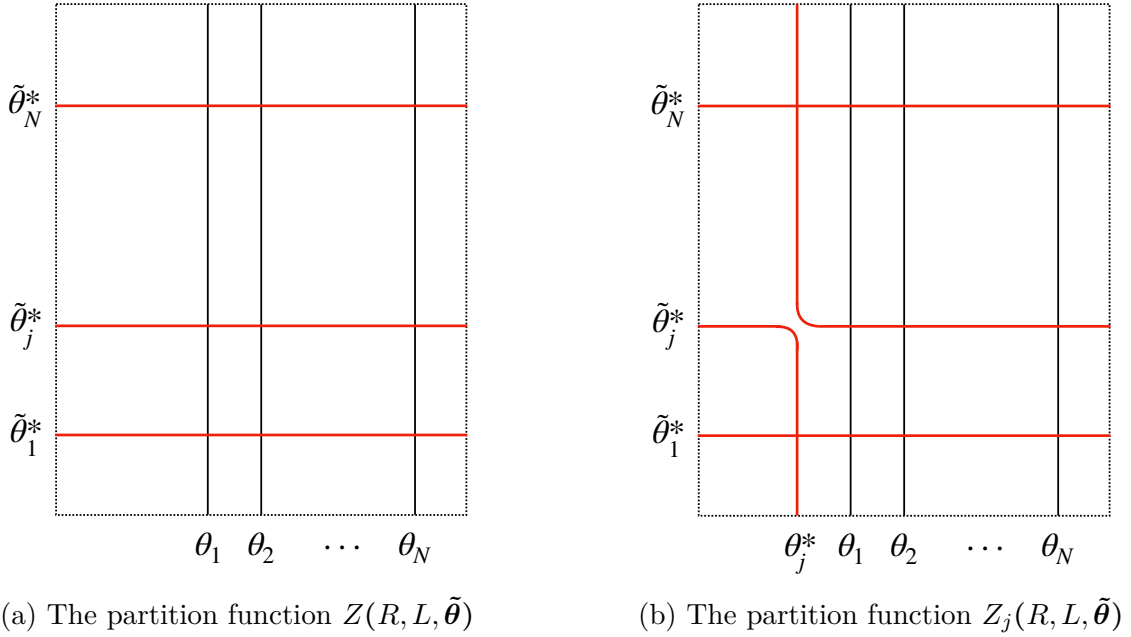


Figure 2.9: Schematic representation of the partition function under the presence of a mirror state $\tilde{\theta}^*$. A mirror particle can wrap around the time direction and acts like a physical particle. By requiring the equality between the two equivalent ways of computing the partition function, we recover the excited state TBA equation.

For consistency with section 1.2.5, we adopt the convention $\theta^{\text{mirror}} = \theta^{\text{physics}} + i\pi/2$ in the following computation. The presence of a mirror state leads to two modifications. First, the thermal weight of a physical particle now includes the interaction with mirror particles

$$e^{-w(\theta, \tilde{\theta}^*)} \equiv e^{-Rm \cosh(\theta)} \prod_{j=1}^M S(\theta, \tilde{\theta}_j^* - i\pi/2). \quad (2.42)$$

Second, the total scattering phases (2.1) also contain a similar contribution

$$\Phi_j(\theta_1, \dots, \theta_N, \tilde{\theta}^*) = Lp(\theta_j) - i \sum_{l=1}^M \log S(\theta_j, \tilde{\theta}_l^* - i\pi/2) - i \sum_{k \neq j}^N \log S(\theta_j, \theta_k). \quad (2.43)$$

This will modify the diagonal part of the corresponding Gaudin matrix. Consequently, the Feynman rules must be updated, while the rule for propagators remain unchanged

$$\begin{aligned} \bullet & (\theta, r) = \frac{(-1)^{r-1}}{r^2} e^{-rw(\theta, \tilde{\theta}^*)}, \\ \circ & (\theta, r) = [Lp'(\theta) + \sum_{l=1}^M K(\theta, \tilde{\theta}_l^* - i\pi/2)] \frac{(-1)^{r-1}}{r} e^{-rw(\theta, \tilde{\theta}^*)}. \end{aligned}$$

The combinatorial structure of the trees is also the same as before. The energy of the mirror state is obtained by adding to the free energy the contribution from the mirror particles that go around the spatial direction without scattering

$$\begin{aligned} E(\tilde{\theta}^*) &= \sum_{l=1}^M m \cosh(\tilde{\theta}_l^*) - \lim_{L \rightarrow \infty} \frac{1}{L} \int \frac{d\theta}{2\pi} [Lp'(\theta) + \sum_{l=1}^M K(\theta, \tilde{\theta}_l^* - i\pi/2)] \log[1 + Y^c(\theta)] \\ &= \sum_{l=1}^M m \cosh(\tilde{\theta}_l^*) - \int \frac{d\theta}{2\pi} Lp'(\theta) \log[1 + Y^c(\theta)], \end{aligned} \quad (2.44)$$

where Y^c solves for the excited state TBA equation

$$Y^c(\theta) = e^{-w(\theta, \tilde{\theta}^*)} \exp \int \frac{d\eta}{2\pi} K(\eta, \theta) \log[1 + Y^c(\eta)]. \quad (2.45)$$

The exact Bethe equations for the mirror state are obtained by the following requirement. Let $Z_j(R, L, \tilde{\theta}^*)$ be the partition function with the j -th mirror particle winding once around the time circle before winding around the space circle. The configurations that contribute to $Z(R, L)$ and $Z_j(R, L)$ are depicted in Figs. 2.9a and 2.9b. In order to compute the partition function $Z_j(R, L)$ we notice that the configurations in Fig. 2.9b can be simulated by pulling one of the mirror particles out of the thermal ensemble giving to its rapidity a physical value $\theta_j^* = \tilde{\theta}_j^* - i\pi/2$. Indeed, since $S(\theta_j^*, \theta_j^*) = -1$, the partition function in presence of such extra mirror particle is $-Z_j(R, L, \tilde{\theta}^*)$. In this way $Z_j(R, L, \tilde{\theta}^*)$ is given by the sum over all trees, with one extra tree having a root θ_j^* and $r = 1$. The generating function for such trees is $Y^c(\theta_j^*)$, while the contribution of the “vacuum” trees give the partition function: $Z_j = -Y^c(\theta_j^*)Z$. The periodicity in the space direction requires that $Z_j = Z$, which gives the exact Bethe-Yang equation

$$Y^c(\theta_j^*) = -1, \quad j = 1, 2, \dots, M. \quad (2.46)$$

Chapter 3

Open systems with diagonal scattering

In the previous chapter we have applied our diagrammatic formalism to re-derive some well-known thermal quantities in periodic integrable systems (and also obtain a new result). In this chapter we will investigate the extension of our method to systems with integrable boundaries. We restrict our discussion to $1+1$ dimensional field theories with a single massive excitation above the vacuum. The analysis of theories with non-diagonal bulk scattering matrix will be presented in the next chapter.

3.1 Finite temperature g-function: definition

Consider the theory in an open interval of length L , with two boundaries a and b . The theory is integrable with a two-to-two bulk scattering phase $S(\theta, \eta)$ and reflection factors $R_a(\theta), R_b(\theta)$ at the boundaries. They satisfy a set of conditions (see subsection 1.1.6), among which the unitarity condition

$$S(\theta, \eta)S(\eta, \theta) = R_a(u)R_a(-u) = R_b(u)R_b(-u) = 1. \quad (3.1)$$

Following the spirit of the previous chapter, we consider a general scenario where the bulk S-matrix does not necessarily depend on the difference between rapidities. We however assume a milder condition

$$S(\theta, -\eta)S(-\theta, \eta) = 1. \quad (3.2)$$

The relevance of this identity will become clear shortly. The partition function of the theory at inverse temperature R is given by the thermal trace

$$Z_{ab}(R, L) = \text{Tr } e^{-H_{ab}(L)R}, \quad (3.3)$$

where $H_{ab}(L)$ denotes the Hamiltonian defined on a segment of length L with boundary conditions a and b . If the two boundaries are removed then we recover the partition function of the periodic theory

$$Z(R, L) = \text{Tr } e^{-H(L)R}. \quad (3.4)$$

which was computed in the previous chapters. The boundary entropy of the open system is given by the difference between the two free energies

$$\mathcal{F}_{ab}(R, L) \equiv \log Z_{ab}(R, L) - \log Z(R, L). \quad (3.5)$$

The g-function is defined as the contribution of a *single* boundary to the free energy. To obtain it, we pull the two boundaries far away from each other to avoid interference

$$\log g_a(R) \equiv \frac{1}{2} \lim_{L \rightarrow \infty} \mathcal{F}_{aa}(R, L). \quad (3.6)$$

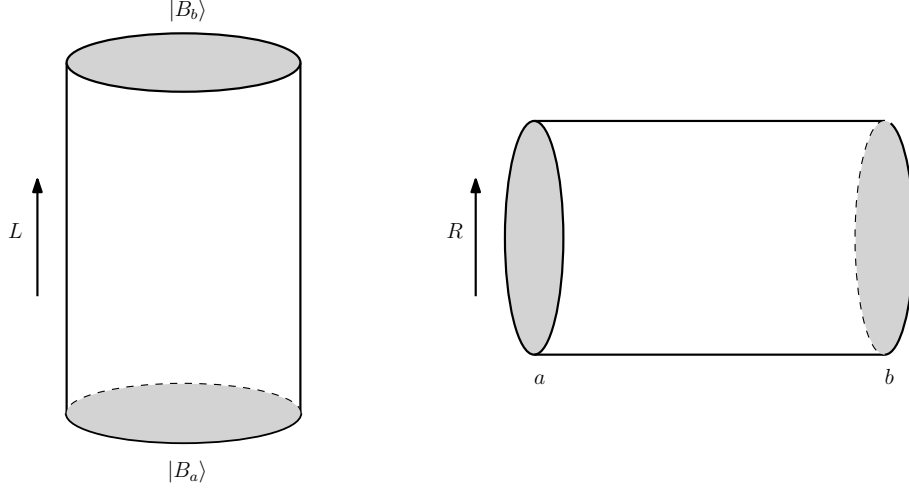


Figure 3.1: Two equivalent ways of evaluating the partition function on a cylinder.

From the perspective of the mirror theory, defined on a circle with circumference R , the partition function with periodic boundary conditions (3.4) takes a similar form

$$Z(R, L) = \text{Tr} e^{-\tilde{H}(R)L}, \quad (3.7)$$

where the trace is in the Hilbert space of the mirror theory. In contrast, after a mirror transformation the thermal partition function with open boundary conditions becomes the overlap of an initial state $\langle B_a|$ and a final state $|B_b\rangle$ defined on a circle of circumference R after evolution at mirror time L [121]. Evaluated in the mirror theory, the partition function (3.3) reads

$$Z_{ab}(R, L) = \langle B_a|e^{-\tilde{H}(R)L}|B_b\rangle. \quad (3.8)$$

Although the partition function is the same, the physics is rather different in the two channels. In the mirror theory, the g -function provides information about overlapping of the boundary state and the ground state at finite volume. To see this, we write (3.8) as a sum over eigenstates $|\psi\rangle$ of the periodic Hamiltonian $\tilde{H}(R)$

$$\langle B_a|e^{-\tilde{H}(R)L}|B_b\rangle = \sum_{|\psi\rangle} \frac{\langle B_a|\psi\rangle}{\sqrt{\langle\psi|\psi\rangle}} e^{-L\tilde{E}(|\psi\rangle)} \frac{\langle\psi|B_b\rangle}{\sqrt{\langle\psi|\psi\rangle}}. \quad (3.9)$$

In the large L limit, this sum is dominated by a single term corresponding to the ground state $|\psi_0\rangle$. The g -function is then given by the overlap between this state and the boundary state

$$g_a(R) = \frac{\langle B_a|\psi_0\rangle}{\sqrt{\langle\psi_0|\psi_0\rangle}}. \quad (3.10)$$

3.2 Known results

The first attempt to compute the g -function (3.6) was carried out by LeClair, Mussardo, Saleur and Skorik [45], using the traditional TBA saddle point approximation. They obtained an

expression similar to the bulk TBA free energy

$$\log(g_a g_b)^{\text{saddle}}(R) = \frac{1}{2} \int_{-\infty}^{+\infty} \frac{d\theta}{2\pi} \Theta_{ab}(\theta) \log[1 + e^{-\epsilon(\theta)}], \quad (3.11)$$

where ϵ is the pseudo-energy at inverse temperature R given by the familiar TBA equation

$$\epsilon(\theta) = E(\theta)R - \int_{-\infty}^{\infty} \frac{d\eta}{2\pi} K(\eta, \theta) \log(1 + e^{-\epsilon(\eta)}). \quad (3.12)$$

and the source term Θ involves the bulk scattering and the boundary reflection matrices

$$\Theta_{ab}(\theta) \equiv K_a(\theta) + K_b(\theta) - 2K(\theta, -\theta) - 2\pi\delta(u), \quad \text{where} \quad K_{a,b}(\theta) = -i\partial_\theta \log R_{a,b}(\theta). \quad (3.13)$$

It was later shown by Woynarovich [46] that another volume-independent contribution is produced by the fluctuation around the TBA saddle point. The result can be written as a Fredholm determinant

$$\log(g_a g_b)^{\text{fluc}}(R) = -\log \det(1 - \hat{K}^+), \quad (3.14)$$

where the kernel \hat{K}^+ has support on the positive real axis and its action is defined by

$$\hat{K}^+ F(\theta) = \int_0^\infty \frac{d\eta}{2\pi} [K(\theta, \eta) + K(\theta, -\eta)] \frac{1}{1 + e^{\epsilon(\eta)}} F(\eta). \quad (3.15)$$

In particular, the fluctuation (3.14) around the saddle point is boundary independent. One can say its presence is of pure geometric origin. A major problem of Woynarovich's computation is that it also predicts a similar term for periodic systems, while it is known that there is no such correction.

Dorey, Fioravanti, Rim and Tateo [47] took a different approach towards this problem. They started with the definition of the partition function as a thermal sum over a complete set of states labelled by mode numbers. In the infinite volume limit, this sum can be replaced by integrals over rapidities. The integrands were explicitly worked out for small number of particles. Based on these first terms and the structure of TBA saddle point result (A.6), the authors advanced a conjecture about the boundary-independent part of g -function. Their proposal has the structure of a Leclaire-Mussardo type series

$$\begin{aligned} \log(g_a g_b)(R) &= \log(g_a g_b)^{\text{saddle}}(R) \\ &+ \sum_{n \geq 1} \frac{1}{n} \prod_{j=1}^n \int_{-\infty}^{+\infty} \frac{d\theta_j}{2\pi} \frac{1}{1 + e^{\epsilon(\theta_j)}} K(\theta_1 + \theta_2) K(\theta_2 - \theta_3) \dots K(\theta_n - \theta_1) \end{aligned} \quad (3.16)$$

Pozsgay [178] (see also Woynarovich [173]) argued that the same expression for g -function could be obtained from a refined version of TBA saddle point approximation. He noticed that the mismatch between (3.14) and the series in (3.16) is resolved if one uses a non-flat measure for the TBA functional integration. This non-trivial measure comes from the Jacobian of the change of variables from mode number to rapidity, and represents the continuum limit of the Gaudin determinant.

The fluctuation around the saddle point involves only diagonal elements of this Gaudin matrix, resulting in the inverse power of the Fredholm determinant $\det(1 - \hat{K}^+)$. On the other hand, the functional integration measure contains the off-diagonal elements as well, which constitute another Fredholm determinant $\det(1 - \hat{K}^-)$. The kernel K^- is defined in a similar way as K^+

$$\hat{K}^- F(\theta) = \int_0^\infty \frac{d\eta}{2\pi} [K(\theta, \eta) - K(\theta, -\eta)] \frac{1}{1 + e^{\epsilon(\eta)}} F(\eta). \quad (3.17)$$

Pozsgay rewrote the result (3.16) in terms of these two Fredholm determinants

$$\log(g_a g_b)(R) = \log(g_a g_b)^{\text{saddle}}(R) + \log \det \frac{1 - \hat{K}^-}{1 - \hat{K}^+}. \quad (3.18)$$

The two kernels \hat{K}^\pm can be read off from the asymptotic Bethe equations. For a periodic system, they happen to be the same and the effects from the fluctuation and the measure cancel each other.

It is important to distinguish the Jacobians in [47] from the one in [178]. The former appear in each term of the cluster expansion while the latter is obtained from the thermodynamic state that minimizes the TBA functional action. Put it simply, the Jacobian in [178] is the thermal average of all the Jacobians in [47].

In the next sections we will derive the expression (3.18) by evaluating the partition function in the R -channel, namely equation (3.3), in the limit when L is large. In order to do that, we will insert a decomposition of the identity in a complete basis of eigenstates of the Hamiltonian $H_{ab}(L)$ and perform the thermal trace.

3.3 New derivation

3.3.1 The sum over mode number

The g -function (3.6) is extracted by taking the limit of large volume L . In this limit, we can diagonalize the Hamiltonian $H_{ab}(L)$ using the technique of Bethe ansatz. Consider an N -particle eigenstate $|\vec{\theta}\rangle = |\theta_1, \theta_2, \dots, \theta_N\rangle$. To obtain the Bethe Ansatz equations in presence of two boundaries, we follow a particle of rapidity θ_j as it propagates to a boundary and is reflected to the opposite direction. It continues to the other boundary, being reflected for a second time and finally comes back to its initial position, finishing a trajectory of length $2L$. During its propagation, it scatters with the rest of the particles twice, once from the left and once from the right. This process translates into the quantization condition of the state $|\vec{\theta}\rangle$

$$e^{2ip(\theta_j)L} R_a(\theta_j) R_b(\theta_j) \prod_{k \neq j}^N S(\theta_j, \theta_k) S(\theta_j, -\theta_k) = 1, \quad \forall j = 1, \dots, N. \quad (3.19)$$

We can write these equations in logarithmic form by introducing a new set of variables: the total scattering phases $\Phi_1, \Phi_2, \dots, \Phi_n$ defined by

$$\Phi_j(\vec{\theta}) \equiv 2p(\theta_j)L - i \log[R_a(\theta_j) R_b(\theta_j) \prod_{k \neq j}^N S(\theta_j, \theta_k) S(\theta_j, -\theta_k)], \quad \forall j = 1, \dots, N. \quad (3.20)$$

In terms of these variables, the quantization of the state $|\vec{\theta}\rangle$ reads

$$\Phi_j(\vec{\theta}) = 2\pi n_j \quad \forall j = 1, \dots, N \quad \text{with } n_j \in \mathbb{Z}. \quad (3.21)$$

In the presence of boundary two particles having the same mode numbers but of opposite signs are indistinguishable. To avoid overcounting of states, we should put a positivity constraint on mode numbers. A basis in the N -particle sector of the Hilbert space is then labeled by all sets of strictly increasing positive integers $0 < n_1 < \dots < n_N$. The corresponding eigenvector of the Hamiltonian $H_{ab}(L)$ is characterised by a set of rapidities $0 < \theta_1 < \dots < \theta_N$, obtained by solving the Bethe equations (3.20) and (3.21).

Inserting a complete set of eigenstates we write the partition function on a cylinder as

$$Z_{ab}(R, L) = \sum_{N=0}^{\infty} \sum_{0 < n_1 < \dots < n_N} e^{-RE(n_1, \dots, n_N)}. \quad (3.22)$$

In this equation, the energy E is an implicit function of mode numbers n_1, \dots, n_N . To find its explicit form, one needs to solve the Bethe equations for the corresponding rapidities $\theta_1, \dots, \theta_N$. As a function of the rapidities, the energy is equal to the sum of the energies of the individual particles $E(n_1, \dots, n_N) = E(\theta_1) + \dots + E(\theta_N)$.

In order to write the sum (3.22) as an integral over rapidities, we first have to remove the constraint between the mode numbers. We do this by inserting Kronecker symbols to get rid of unwanted configurations

$$Z_{ab}(R, L) = \sum_{N=0}^{\infty} \frac{1}{N!} \sum_{0 \leq n_1, \dots, n_N} \prod_{j < k}^N (1 - \delta_{n_j, n_k}) \prod_{j=1}^N (1 - \delta_{n_j, 0}) e^{-RE(n_1, \dots, n_N)}. \quad (3.23)$$

The first Kronecker symbol introduces the condition that the mode numbers are all different, and the second one eliminates the mode numbers equal to zero. Let us expand in monomials the first factor containing Kronecker symbols, which imposes the exclusion principle. As shown in the previous chapter, the partition function (3.23) can be written as a sum over all sequences $(n_1^{r_1}, \dots, n_N^{r_N})$ of non-negative, but otherwise unrestricted mode numbers n_i with multiplicities r_i . Each sequence $(n_1^{(r_1)}, \dots, n_N^{(r_N)})$ in the sum corresponds to a state with r_j particles of the same mode number n_j , for $j = 1, 2, \dots, N$. The total number of particles in such a sequence is $r_1 + \dots + r_N$

$$Z_{ab}(R, L) = \sum_{N=0}^{\infty} \frac{(-1)^N}{N!} \sum_{0 \leq n_1, \dots, n_N} \prod_{j=1}^N (1 - \delta_{n_j, 0}) \sum_{1 \leq r_1, \dots, r_N} \frac{(-1)^{r_1 + \dots + r_N}}{r_1 \dots r_N} e^{-RE[n_1^{(r_1)}, \dots, n_N^{(r_N)}]}. \quad (3.24)$$

The rapidities $\theta_1, \dots, \theta_N$ of a generalised Bethe states $(n_1^{r_1}, \dots, n_N^{r_N})$ satisfy the Bethe equations

$$\Phi_j = 2\pi n_j, \quad j = 1, \dots, N, \quad (3.25)$$

where the total scattering phases $\Phi_j = \Phi_j[\theta_1^{(r_1)}, \dots, \theta_N^{(r_N)}]$ are defined by

$$e^{i\Phi_j} \equiv e^{2ip(\theta_j)L} \times R_a(\theta_j)R_b(\theta_j) \times [e^{i\pi}S(\theta_j, -\theta_j)]^{r_j-1} \times \prod_{k \neq j}^N (S(\theta_j, \theta_k)S(\theta_j, -\theta_k))^{r_k}. \quad (3.26)$$

The energy of this state is given by $r_1 E(\theta_1) + \dots + r_N E(\theta_N)$.

3.3.2 From mode numbers to rapidities

In the large L limit, we can replace a discrete sum over mode numbers n by a continuum integral over variables Φ

$$\sum_{0 \leq n_1, \dots, n_N} = \int_0^\infty \frac{d\Phi_1}{2\pi} \dots \int_0^\infty \frac{d\Phi_N}{2\pi} + \mathcal{O}(e^{-L}).$$

We can then use equation (3.26) to pass from (Φ_1, \dots, Φ_m) to rapidity variables $(\theta_1, \dots, \theta_N)$. The only subtle point compared with the periodic case is the factor excluding the mode numbers $n_j = 0$ from the sum (3.24)

$$\sum_{0 \leq n_1, \dots, n_m} \prod_{j=1}^m (1 - \delta_{n_j, 0}) = \int_0^\infty \frac{d\Phi_1}{2\pi} \dots \int_0^\infty \frac{d\Phi_m}{2\pi} \prod_{j=1}^m (1 - 2\pi\delta(\Phi_j)) + \mathcal{O}(e^{-L}).$$

We would like to incorporate this factor into the Jacobian matrix $\partial_\theta \Phi$. We can do this by first expanding the product as a sum over subsets $\alpha \subset \{1, 2, \dots, N\}$

$$\begin{aligned} \int_0^\infty \frac{d\Phi_1}{2\pi} \dots \int_0^\infty \frac{d\Phi_N}{2\pi} \sum_{\alpha} (-2\pi)^{|\alpha|} \delta(\Phi_{\alpha}) &= \sum_{\alpha} \prod_{j=1}^m \int_0^\infty \frac{d\theta_j}{2\pi} \left[\frac{\partial \Phi}{\partial \theta} \right]_{\alpha, \alpha} (-2\pi)^{|\alpha|} \delta(\theta_{\alpha}) \\ &= \prod_{j=1}^m \int_0^\infty \frac{d\theta_j}{2\pi} \det \left[\frac{\partial \Phi}{\partial \theta} - 2\pi\delta(\theta) \right]. \end{aligned}$$

Here $[\partial \Phi / \partial \theta]_{\alpha, \alpha}$ denotes the diagonal minor of the Jacobian matrix obtained by deleting its α -rows and α -columns. The sum over subsets is the expansion of the determinant of a sum of two matrices. Hence the unphysical state at $\theta = 0$ can be eliminated by adding a term equal to $-2\pi\delta(\theta)$ to the diagonal elements of the Jacobian matrix when we change variables from Φ to θ

$$\begin{aligned} G_{jk}[\theta_1^{(r_1)}, \dots, \theta_N^{(r_N)}] &\equiv \partial_{\theta_k} \Phi_j - 2\pi\delta(\theta_j)\delta_{jk} \\ &= [D_{ab}(\theta_j) + 2r_j K(\theta_j, -\theta_j) + \sum_{l \neq j}^N r_l (K(\theta_j, \theta_l) + K(\theta_j, -\theta_l))] \delta_{jk} \\ &\quad - r_k [K(\theta_k, \theta_j) - K(\theta_k, -\theta_j)] (1 - \delta_{jk}), \quad \forall j, k = 1, 2, \dots, N \end{aligned} \quad (3.27)$$

where

$$D_{ab}(\theta) \equiv 2Lp'(\theta) + \Theta_{ab}(\theta). \quad (3.28)$$

with Θ_{ab} given in (3.13). In order to apply the matrix-tree theorem, we consider the following matrix

$$\begin{aligned} \tilde{G}_{jk} \equiv r_k G_{kj} &= [r_j D_{ab}(\theta_j) + 2r_j^2 \bar{K}_{jj} + \sum_{l \neq j}^N r_j r_l (K_{jl} + \bar{K}_{jl})] \delta_{jk} \\ &\quad - r_j r_k (K_{jk} - \bar{K}_{jk}) (1 - \delta_{jk}), \quad \forall j, k = 1, 2, \dots, N, \end{aligned} \quad (3.29)$$

where we have used the notation

$$K_{jk} = K(\theta_j, \theta_k), \quad \bar{K}_{jk} = K(\theta_j, -\theta_k) = K(-\theta_j, \theta_k). \quad (3.30)$$

In terms of this matrix, the partition function is written as

$$Z_{ab}(R, L) = \sum_{m=0}^{\infty} \frac{(-1)^N}{N!} \sum_{1 \leq r_1, \dots, r_N} \prod_{j=1}^N \int_0^{\infty} \frac{d\theta_j}{2\pi} \frac{(-1)^{r_j}}{r_j^2} e^{-r_j R E(\theta_j)} \det \tilde{G}[\theta_1^{(r_1)}, \dots, \theta_N^{(r_N)}]. \quad (3.31)$$

3.3.3 Matrix-tree theorem

The matrix-tree theorem for signed graphs [48] allows us to write the determinant of the matrix (3.29) as a sum over graphs. This theorem as stated in [48] is quite technical and we provide a brief formulation in the following together with two proofs, one combinatorial and one field-theoretical in the appendices. First, let us define

$$K_{jk}^{\pm} = K_{jk} \pm \bar{K}_{jk}. \quad (3.32)$$

Then the Gaudin-like matrix (3.29) takes the form ($j, k = 1, 2, \dots, N$)

$$\tilde{G}_{jk} = [r_j D_{ab}(\theta_j) + r_j^2 (K_{jj}^+ - K_{jj}^-) + \sum_{l \neq j}^m r_j r_l K_{jl}^+] \delta_{jk} - r_j r_k K_{jk}^- (1 - \delta_{jk}). \quad (3.33)$$

The determinant of this matrix can be written as a sum over all (not necessarily connected) graphs \mathcal{F} having exactly m vertices labeled by v_j with $j = 1, \dots, m$ and two types of edges, positive and negative, which we denote by $\ell_{jk}^{\pm} \equiv \langle v_j \rightarrow v_k \rangle^{\pm}$. The connected component of each graph is either:

- A rooted directed tree with only positive edges $\ell_{kl}^+ = \langle v_k \rightarrow v_l \rangle^+$ oriented so that the edge points to the vertex which is farther from the root, as shown in fig. 3.2. The weight of such a tree is a product of a factor $r_j D_{ab}(\theta_j)$ associated with the root v_j and factors $r_l r_k K_{lk}^+$ associated with its edges ℓ_{kl}^+ .
- A positive (fig. 3.3a) or a negative (fig. 3.3b) oriented cycle with outgrowing trees. A positive/negative loop is an oriented cycle (including tadpoles which are cycles of length 1) entirely made of positive/negative edges having the same orientation. The outgrowing trees consist of positive edges only. The weight of a loop with outgrowing trees is the product of the weights of its edges, with the weight of an edge ℓ_{kl}^{\pm} given by $r_l r_k K_{lk}^{\pm}$. In addition, a negative loop carries an extra minus sign. This is why we will call the positive loop bosonic and the negative loops fermionic.

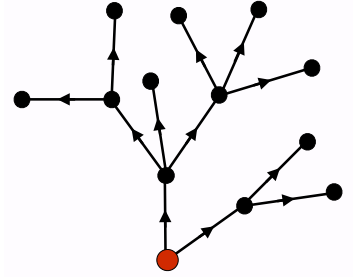


Figure 3.2: A tree with K^+ edges

Summarising, we write the determinant of the matrix (3.33) as

$$\det \hat{G}_{jk} = \sum_{\mathcal{F}} W[\mathcal{F}], \quad W[\mathcal{F}] = (-1)^{\#\text{negative loops}} \prod_{v_j \in \text{roots}} r_j D_{ab}(\theta_j) \prod_{e_{kl}^{\pm} \in \text{edges}} r_l r_k K^{\pm}(\theta_l, \theta_k) \quad (3.34)$$

with $K^{\pm}(\theta, \eta) = K(\theta, \eta) \pm K(\theta, -\eta)$. Equation (3.34) allows us to express the Jacobian for the integration measure as a sum over graphs whose weights depend only on the coordinates $\{\theta_j, r_j\}$ of its vertices. For a periodic system $K^+ = K^-$ and the two families of loops cancel each other, leaving only trees in the expansion of the Gaudin matrix.

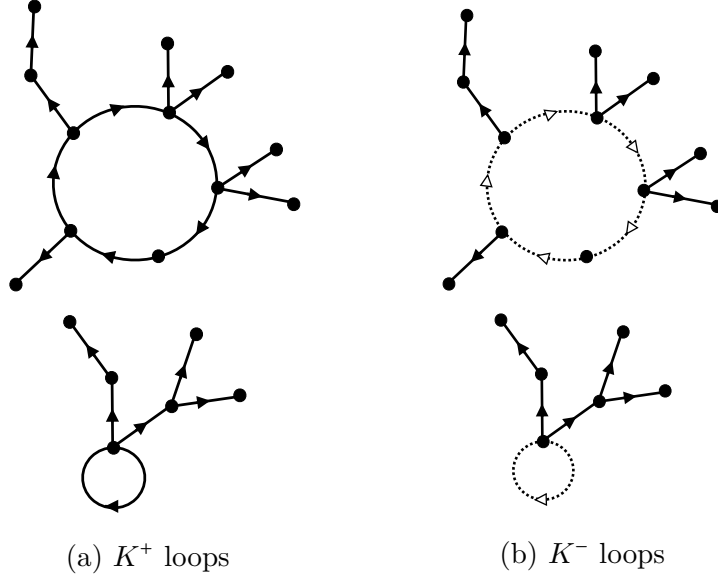


Figure 3.3: Examples of loops with out-growing trees. K^- propagators are drawn as dashed lines. They appear only in a loop and such loop comes with a factor of -1 . Tadpoles are loops of length 1.

3.3.4 Graph expansion of the partition function

Applying the matrix-tree theorem for each term in the series (3.31), we obtain a graph expansion for the partition function

$$Z_{ab}(R, L) = \sum_{N=0}^{\infty} \frac{(-1)^N}{N!} \sum_{1 \leq r_1, \dots, r_N} \prod_{j=1}^N \int_0^{\infty} \frac{d\theta_j}{2\pi} \frac{(-1)^{r_j}}{r_j^2} e^{-r_j R E(\theta_j)} \sum_{\mathcal{F}} W[\mathcal{F}], \quad (3.35)$$

where the last sum runs over all graphs \mathcal{F} with N vertices as constructed above. The next step is to invert the order of the sum over graphs and the integral/sum over the coordinates $\{\theta_j, r_j\}$ assigned to the vertices. As a result we obtain a sum over the ensemble of abstract oriented tree/loop graphs, with their symmetry factors, embedded in the space $\mathbb{R}^+ \times \mathbb{N}$ where the coordinates θ, r of the vertices take values. The embedding is free, in the sense that the sum over the positions of the vertices is taken without restriction. As a result, the sum over the embedded graphs is the exponential of the sum over connected ones. One can think of these graphs as Feynman diagrams obtained by applying the Feynman rules in Fig. 2.15.

The Feynman rules comprise three kinds of vertices: *root* vertices with only outgoing bosons, *bosonic* vertices with one incoming boson and an arbitrary number of outgoing bosons, *fermionic* vertices with one incoming and one outgoing fermion, together with an arbitrary number of outgoing bosons. The connected diagrams built from these vertices are either trees (figure 3.2) or bosonic loops (fig. 3.3a) or fermionic loops (fig. 3.3b).

$$\begin{aligned}
& \text{Red vertex with } r \text{ outgoing lines} = r D_{ab}(\theta) \frac{(-1)^{r-1}}{r^2} e^{-rRE(\theta)} \\
& \text{Black vertex with } r \text{ outgoing lines} = \frac{(-1)^{r-1}}{r^2} e^{-rRE(\theta)} \\
& \text{Solid line } \theta_1 \rightarrow \theta_2 = r_1 r_2 K^+(\theta_2, \theta_1) \\
& \text{Dashed line } \theta_1 \rightarrow \theta_2 = r_1 r_2 K^-(\theta_2, \theta_1) \\
& \text{Loop of } r \text{ dashed lines} = -1
\end{aligned} \tag{3.36}$$

The free energy is a sum over connected graphs

$$\log Z_{ab}(R, L) = \int_0^\infty \frac{d\theta}{2\pi} D_{ab}(\theta) \sum_{r \geq 1} r Y_r(\theta) + \sum_{n \geq 1} \mathcal{C}_n^\pm. \tag{3.37}$$

In this expression, $Y_r(\theta)$ denotes the sum of over all trees rooted at the point (θ, r) and \mathcal{C}_n^\pm is the sum over the Feynman graphs having a bosonic/fermionic loop of length n . We have defined $Y_r(\theta)$ in such a way that the all vertices with r outgoing lines, including the root, have the same weight.

$$Y_r(\theta) = \sum_{\text{trees rooted at } (\theta, r)} \equiv \text{Shaded circle } (\theta, r). \tag{3.38}$$

3.3.5 Summing over trees: saddle point TBA approximation

We start by analyzing the part of free energy (3.37) that comes from the tree-diagrams

$$\log Z_{ab}(R, L)^{\text{trees}} = \int_0^\infty \frac{d\theta}{2\pi} D_{ab}(\theta) \sum_{r \geq 1} r Y_r(\theta). \tag{3.39}$$

Similar to the periodic case, the combinatorial structure of trees translates into an equation satisfied by $Y_r(\theta)$. The only difference with (2.17) is that the integrals are evaluated over the

positive axis

$$\begin{aligned} Y_r(\theta) &= \frac{(-1)^{r-1}}{r^2} e^{-rRE(\theta)} \sum_{n=0}^{\infty} \frac{1}{n!} \left[\sum_{s=1}^{\infty} \int_0^{\infty} sr \frac{d\eta}{2\pi} K^+(\eta, \theta) Y_s(\eta) \right]^n \\ &= \frac{(-1)^{r-1}}{r^2} \left[e^{-RE(\theta)} \exp \sum_{s=0}^{\infty} \int_0^{\infty} \frac{d\eta}{2\pi} K^+(\eta, \theta) s Y_s(\eta) \right]^r, \end{aligned} \quad (3.40)$$

By comparing equation (3.40) for arbitrary r and for $r = 1$ we find the following simple relation between Y_r and Y_1

$$Y_r(\theta) = \frac{(-1)^{r-1}}{r^2} Y_1(\theta)^r. \quad (3.41)$$

Thanks to this simple identity, we can rewrite (3.40) for $r = 1$ as an equation involving Y_1 only

$$Y_1(\theta) = e^{-RE(\theta)} \exp \int_0^{\infty} \frac{d\eta}{2\pi} K^+(\eta, \theta) \log[1 + Y_1(\eta)]. \quad (3.42)$$

This equation starts looking like the usual TBA equation. To bring it into the desired form, we note that the integral in (3.42) can be extended to the real axis by using the parity of the kernel $K^+(v, u) = K(v, u) + K(-v, u)$. This is the reason for our assumption (3.2) on the bulk S-matrix. Without it, one cannot relate (3.42) with the periodic TBA equation (3.12) and as a result, the subtraction (3.6) cannot be carried out

$$Y(\theta) = e^{-RE(\theta)} \exp \int_{-\infty}^{\infty} \frac{d\eta}{2\pi} K(\eta, \theta) \log[1 + Y(\eta)], \quad (3.43)$$

where we have denoted $Y \equiv Y_1$ for short. In particular, we know that the free energy of a periodic system can be written in terms of Y as

$$\log Z(R, L) = L \int_{-\infty}^{\infty} \frac{d\theta}{2\pi} p'(\theta) \log[1 + Y(\theta)]. \quad (3.44)$$

Similarly, we can also extend the domain of integration in (3.39) to the real axis, using the parity of $D_{ab}(u, r)$. By subtracting the periodic free energy (3.44) from the tree part of the free energy (3.39), we obtain the tree contribution to g-function

$$g_{ab}(R)^{\text{trees}} = \frac{1}{2} \int_{-\infty}^{\infty} \frac{d\theta}{2\pi} \Theta_{ab}(\theta) \log[1 + Y(\theta)]. \quad (3.45)$$

This expression coincides with the saddle point contribution (3.11) obtained by the traditional TBA approach.

3.3.6 Summing over loops: Fredholm determinants

We now turn to the sum over loops and show that they fill the missing part of the g -function (3.18). Let us define

$$g_{ab}(R)^{\text{loops}} = \sum_{n \geq 1} \mathcal{C}_n^{\pm} \quad (3.46)$$

For each $n \geq 1$, \mathcal{C}_n^\pm is the partition sum of K^\pm loops of length n with the trees growing out of these loops which can be summed separately using the definition (3.38)

$$\mathcal{C}_n^\pm = \frac{\pm 1}{n} \sum_{1 \leq r_1, \dots, r_n} \int_0^\infty \frac{d\theta_1}{2\pi} \dots \int_0^\infty \frac{d\theta_n}{2\pi} Y_{r_1}(\theta_1) \dots Y_{r_n}(\theta_n) r_2 r_1 K^\pm(\theta_2, \theta_1) \dots r_1 r_n K^\pm(\theta_1, \theta_n).$$

In this expression, the sign comes from fermion loop and $1/n$ is the usual loop symmetry factor.

Trees growing out of a vertex (θ_j, r_j) of the loop sum up to $Y_{r_j}(\theta_j)$, by the definition (3.38). The factor $r_{j-1}r_j$ coming from the propagator linking adjacent vertices (θ_{j-1}, r_{j-1}) and (θ_j, r_j) can be pulled into trees that grow out from them. Each tree therefore receives an extra factor of r^2 at their root. We can then use the relation (3.41) to carry out the sum over r . To this end, we recover the TBA filling factor at each vertex of the loop

$$\sum_{r \geq 1} r^2 Y_r(\theta) = \frac{Y(\theta)}{1 + Y(\theta)} = f(\theta). \quad (3.47)$$

It follows that the sum over all positive (negative) loops of fixed length n is simply given by

$$\mathcal{C}_n^\pm = \frac{\pm 1}{n} \text{Tr}(\hat{K}^\pm)^n. \quad (3.48)$$

where the kernels \hat{K}^\pm are defined in (3.15) and (3.17). We recover part of the g -function (3.18) coming from fluctuations around the saddle point along with the non-trivial integration measure

$$g_{ab}(R)^{\text{loops}} = \log \det \frac{1 - \hat{K}^-}{1 - \hat{K}^+}. \quad (3.49)$$

3.4 Summary and outlook

We propose a graph theory-based method to compute the g -function of a theory with diagonal bulk scattering and diagonal reflection matrices. The idea is to apply the matrix-tree theorem to write the Jacobians in the cluster expansion of the partition function by a sum over graphs. The g -function is then written as a sum over trees and loops. The sum over trees gives TBA saddle point result while the sum over loops constitute the two Fredholm determinants.

Similar determinant structure appears in the study of *quantum quench*. In short, a quantum quench is a quantum mechanics problem where the initial state $|\Psi_0\rangle$ is not an eigenvector of the Hamiltonian H that controls the time evolution. A common way to compute time independent observables in such system is through form factor expansion

$$\langle \mathcal{O}(t) \rangle = \sum_{n,m} \langle \Psi_0 | n \rangle \langle n | \mathcal{O} | m \rangle \langle m | \Psi_0 \rangle e^{it(E_n - E_m)}, \quad (3.50)$$

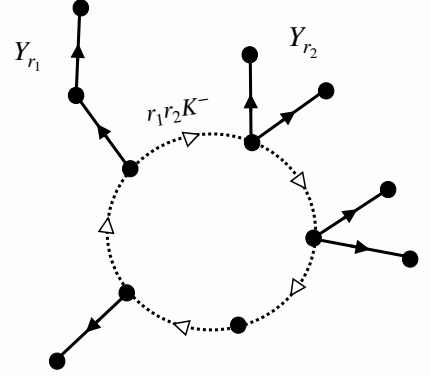


Figure 3.4: A K^- loop.

where n and m are two complete sets of normalized eigenstates of H . In order to evaluate this expression, one must know the overlap between the initial state and these eigenstates. For some families of initial states of the XXX and XXZ spin chain, it was found [179–183] that this overlap can be written in closed form: a product of some local factor and the ratio of two determinants. These determinants are precisely the finite-particle analogies of the Fredholm determinants that appear in the g-function. Similar formulae also appears in the study of one point functions in AdS/dCFT [184–188]. We note that the known expressions for the overlap are valid for any value of the length of the corresponding spin chain.

In [189] an expression for the excited state g-function was found by analytic continuation. In the large mirror volume limit (R in our notation), the authors recovered the same structure of the integrable overlaps. It would be interesting to obtain this result from our formalism, following the same lines of idea of subsection 2.4.

Chapter 4

Open systems with non-diagonal scattering

In the previous chapter we have obtained the expression (3.18) for the finite temperature g-function of a theory with a single massive excitation. The generalization to theories with more than one particle interacting via diagonal S-matrix is straightforward. If we denote the particle types by n , the scattering derivatives by $K_{nm}(\theta, \eta) \equiv -i\partial_\theta \log S_{nm}(\theta, \eta)$, the reflection derivative corresponding to a boundary condition of type a by $K_n^a(\theta) \equiv -i\partial_\theta \log R_n^a(\theta)$, the Y-functions at inverse temperature R by Y_n then

$$2 \log g_a(R) = 2 \log g_a^{\text{trees}}(R) + 2 \log g_a^{\text{loops}}(R), \quad (4.1)$$

$$2 \log g_a^{\text{trees}}(R) = \sum_n \int_{-\infty}^{\infty} \frac{d\theta}{2\pi} [K_n^a(\theta) - K_{nn}(\theta, -\theta) - \pi\delta(\theta)] \log[1 + Y_n(\theta)], \quad (4.2)$$

$$2 \log g_a^{\text{loops}}(R) = \log \det \frac{1 - \hat{K}^-}{1 - \hat{K}^+}, \quad (4.3)$$

where the kernels \hat{K}^\pm have support on \mathbb{R}^+ and their actions are given by

$$\hat{K}_{nm}^\pm(F)(\theta) = \int_0^{+\infty} \frac{d\eta}{2\pi} K_{nm}^\pm(\theta, \eta) f_m(\eta) F(\eta),$$

$$\text{with } K_{nm}^\pm(\theta, \eta) \equiv K_{nm}(\theta, \eta) \pm K_{nm}(\theta, -\eta), \quad f_m = \frac{Y_m}{1 + Y_m}.$$

A general formula as (4.1) is not known for theories in which the bulk scattering is not diagonal. Let us first spell out why the methods of Pozsgay [178] and our diagrammatic formalism are not justified in this case. The diagonalization by the Nested Bethe Ansatz technique involves particles of magnonic type, which are auxiliary particles with zero momentum and energy. The functional integration measure, as it is derived in [178], as well as the summation over multiparticle states in our formalism or in [47] treat the physical and the auxiliary particles in exactly the same way. This is justified only for states with asymptotically large number of physical particles. For states with finite number of physical particles, which dominate in the IR limit, the solutions of the Bethe Ansatz equations do not obey the string hypothesis and moreover the number of the magnons and the number of the physical particles must respect certain constraint. On the other hand, finding and summing over the exact solutions for the auxiliary magnons is of course a hopeless task.

In this chapter we demonstrate on a concrete example that assuming solutions in the form of Bethe strings and summing over unrestricted number of auxiliary particles nevertheless leads to a meaningful result for the boundary entropy, up to an infinite constant which can be subtracted. The subtraction is done by normalizing the g-function (4.1) by its zero temperature value.

The appearance of this infinite piece has an obvious explanation. When the theory is massive in the bulk, the boundary entropy must vanish at zero temperature. If the bulk scattering is

diagonal, this condition is automatically satisfied by the expression (4.1) as all Y-functions vanish in this limit. For non-diagonal bulk scattering however, magnonic particles decouple from the physical ones at zero temperature and the corresponding Y-functions retain non-zero values¹. In our diagrammatic formalism, this normalization amounts to subtracting the contribution from unphysical graphs made of these auxiliary particle. We denote in this chapter $g_{\text{IR}} \equiv g(\infty)$, $g_{\text{UV}} \equiv g(0)$

$$g(R)^{\text{ren}} = \frac{g(R)}{g_{\text{IR}}}. \quad (4.4)$$

As a test for this proposal, we show that it is possible to match the ratio $g_{\text{UV}}/g_{\text{IR}}$ with a conformal g-function under certain assumptions.

The theories under study are the current-perturbed $SU(2)$ Wess-Zumino-Novikov-Witten (WZNW) model at positive integer levels k . The bulk scattering of these theories are not diagonal, as each particle carries quantum numbers that can be nontrivially exchanged during collisions. With the Nested Bethe Ansatz technique, one can trade the nondiagonal scattering for a diagonal one with extra magnonic particles: $SU(2)$ magnon and kink magnon. In the thermodynamic limit these particles can form bound states which are strings of evenly distributed rapidities on the complex plane. In particular $SU(2)$ magnons can form strings of arbitrary lengths, effectively leading to an infinite number of particles in the TBA formalism. In the derivation of the TBA free energy one ignores that the above is true only for asymptotically large number of physical particles. The price to pay, as we will show later, is that both expressions (4.2),(4.3) are logarithmic divergent in the IR and UV limit.

We regularize these divergencies by introducing a twist or equivalently a chemical potential to the TBA equations. The chemical potential makes the sum over the auxiliary magnons finite. The twist/chemical potential is added to the TBA equations for the sole purpose of regularizing the g-function and we do not discuss its effects on the UV limit of the theory. The only change induced by this modification in the formulae (4.2) and (4.3) is the asymptotic values of Y-functions. We are then able to express the IR and UV g-function as functions of the twist parameter and evaluate their ratio in the untwisted limit. For a specific choice of boundary condition it is given by

$$\left(\frac{g_{\text{UV}}}{g_{\text{IR}}}\right)^2 = \sqrt{\frac{2}{k+2}} \times \frac{1}{\sin \frac{\pi}{k+2}}, \quad (4.5)$$

which coincides with a Cardy g-function (4.15), namely $g_{k/2}$ for even k . Equation (4.5) is the main result of this chapter.

The chapter is organized as follows. In section 1 we present the basic features of $SU(2)$ WZNW CFT at level k with emphasis on its Cardy g-functions. We also show how the boundary entropy of a massive perturbation of this CFT flows to its UV value when the temperature is sent to infinity. In section 2 we introduce the current perturbation of this CFT and its TBA equations. We show how various quantities can be extracted from solutions of the TBA equations in the UV or IR limit. We conjecture a specific set of diagonal reflection factors in

¹For periodic boundary condition, this does not lead to a problem for the ground-state energy as the auxiliary particles have vanishing energy.

section 3, fixing the values of $K_n^a(u)$ in equation (4.2). With the data from section 2 and 3, we show in section 4 that the expressions (4.2) and (4.3) diverge in the UV and IR limit. We then show using twisted TBA equations that these divergencies can be regularized, leading to (4.5) as the final result.

Although a general method for finding the g-function of a theory with non-diagonal bulk scattering is still missing, there are models with particular features that allow this quantity to be extracted via case-dependent techniques. In [190], the g-functions of perturbed unitary minimal models were studied using the roaming trajectory of the staircase model [191]. The latter is a theory with diagonal bulk scattering that depends on a free parameter. This parameter can be tuned with temperature to form a plateau RG flow with successive unitary minimal models on its steps. In another work, Pozsgay [192] computed the spin chain analogue of g-function for the XXZ spin chain using quantum transfer matrix and independent results on integrable overlaps. The TBA of this spin chain also involves an infinite number of magnon strings. Recently, the g-function of a model with supersymmetry was studied in view of its relation with a class of three point functions in planar $\mathcal{N} = 4$ SYM [189]. In contrast to our setup, the Bethe equations considered in this work have the property that only the physical rapidities come in pair. Due to this reason, the resulting g-function is free of the above-mentioned divergence. It could be observed from the results of [189, 190, 192] that the Fredholm determinant structure (4.3) of the g-function is still relevant for theories with non-diagonal bulk scattering.

4.1 The current perturbed $SU(2)_k$ WZNW theories

The Wess-Zumino-Novikov-Witten (WZNW) model for a semisimple group G is defined by the action

$$S_{\text{WZNW}} = \frac{1}{4\lambda^2} \int_{S^2} d^2x \text{Tr} \partial_\mu g \partial^\mu g^{-1} + k\Gamma,$$

where the Wess-Zumino term Γ is

$$\Gamma = \frac{1}{24\pi} \int_{B^2} d^3X \epsilon^{ijk} \text{Tr} \tilde{g}^{-1} \partial_i \tilde{g} \tilde{g}^{-1} \partial_j \tilde{g} \tilde{g}^{-1} \partial_k \tilde{g}.$$

Here g is a map from the two-sphere to G and \tilde{g} is its extension from the corresponding two-ball to the same group. Such an extension comes with an ambiguity of topological origin, leading to integer values of k .

At $\lambda^2 = 4\pi/k$ the global $G \times G$ symmetry is enhanced to a local $G(z) \times G(\bar{z})$ symmetry with two currents $J(z) = \partial_z g g^{-1}$ and $\bar{J}(\bar{z}) = g^{-1} \partial_{\bar{z}} g$ separately conserved. These currents satisfy the current algebra G_k while their bilinear satisfies the Virasoro algebra. The latter implies in particular conformal invariance and we refer to the theory at this coupling as the WZNW CFT of G at level k .

In the following we consider the case $G = SU(2)$. The left(right) moving sector of this theory consists of $k + 1$ irreducible representations \mathcal{V}_λ of $SU(2)_k$ corresponding to its $k + 1$ integrable weights. The characters $\chi_\lambda = q^{-c/24} \text{Tr}_{\mathcal{V}_\lambda} q^{L_0}$ transform to one another under the modular transformation $\tau \rightarrow -1/\tau$. This transformation is encoded in the modular S-matrix of

the theory

$$\chi_\lambda(q) = \sum_{\eta=0}^k S_{\lambda,\eta} \chi_\eta(\tilde{q}), \quad q \equiv e^{2i\pi\tau}, \tilde{q} \equiv e^{-2\pi i/\tau}.$$

It is explicitly given by

$$S_{\lambda,\eta} = \sqrt{\frac{2}{k+2}} \sin \left[\frac{\pi(\lambda+1)(\eta+1)}{k+2} \right], \quad 0 \leq \lambda, \eta \leq k, \quad (4.6)$$

which is a real, symmetric matrix that satisfies $S^2 = \mathbf{1}$. The central charge and conformal dimensions are obtained from the Sugawara construction of the energy-momentum tensor

$$c = \frac{3k}{k+2}, \quad h_\lambda = \frac{\lambda(\lambda+2)}{4(k+2)}. \quad (4.7)$$

The fusion coefficients $\mathcal{N}_{\lambda,\eta}^\kappa$ denote how many times the field ϕ_κ appears in the operator product expansion of ϕ_λ and ϕ_η . They satisfy the Verlinde formula

$$\mathcal{N}_{\lambda,\eta}^\kappa = \sum_\zeta \frac{S_{\lambda,\zeta} S_{\eta,\zeta} S_{\zeta,\kappa}}{S_{0,\zeta}}. \quad (4.8)$$

Above is our quick summary of $SU(2)_k$ WZNW CFT data. Consider now this CFT on manifolds with boundaries. Two geometries are relevant for our discussion. First let us consider the upper half complex plane. The continuity condition through the real axis requires that the underlying symmetry involves only one copy of the algebra instead of two. A particular set of boundary states which are invariant under the Virasoro algebra as well as the affine $SU(2)$ Lie algebra is called Ishibashi states [193]. These states are in one-to-one correspondence with bulk primaries and are denoted as $|\lambda\rangle\rangle$ ²

$$(L_n - \tilde{L}_{-n})|\lambda\rangle\rangle = (J_n^a + \tilde{J}_{-n}^a)|\lambda\rangle\rangle = 0. \quad (4.9)$$

Other boundary states are obtained from linear combination of Ishibashi states

$$|a\rangle = \sum_\lambda |\lambda\rangle\rangle \langle\langle \lambda|a\rangle. \quad (4.10)$$

So, on the upper half complex plane, one is quite free to choose the boundary state. The situation is greatly different if the theory is restricted on an annulus. In this geometry let us consider two boundary states $|a\rangle$ and $|b\rangle$ of the form (4.10) on its sides. Denote by $q = \exp(-\pi R/L)$ the modular parameter of this annulus. On one hand one can quantize this theory according to the Hamiltonian H_{ab} with a, b as boundary conditions

$$Z_{ab} = \sum_\lambda n_{a,b}^\lambda \chi_\lambda(q) = \sum_\lambda n_{a,b}^\lambda \sum_\eta S_{\lambda,\eta} \chi_\eta(\tilde{q}), \quad \tilde{q} = \exp(-4\pi L/R), \quad (4.11)$$

where the non-negative integers $n_{a,b}^\lambda$ denote the number of copies of \mathcal{V}_λ in the spectrum of H_{ab} . On the other hand one can consider the theory as evolving between two states $\langle a|$ and $|b\rangle$. The

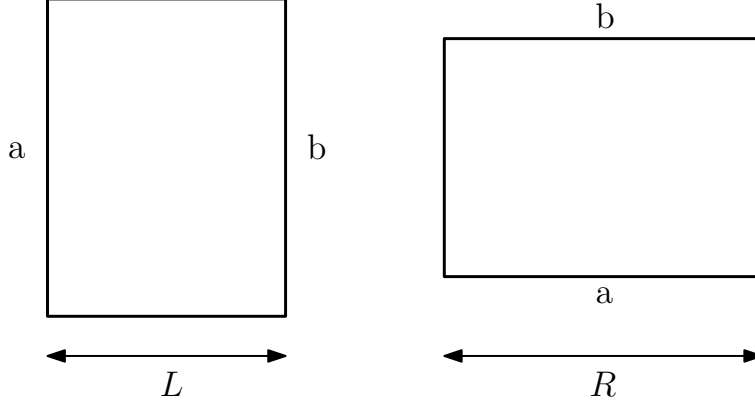


Figure 4.1: Modular invariance of the annulus partition function.

periodic Hamiltonian can be written in terms of Virasoro generators via a conformal mapping, leading to

$$Z_{ab} = \langle a | \tilde{q}^{\frac{1}{2}(L_0 + \bar{L}_0 - c/12)} | b \rangle = \sum_{\eta} \langle a | \eta \rangle \langle \eta | b \rangle \chi_{\eta}(\tilde{q}). \quad (4.12)$$

For the theory under consideration, each representation λ of the extended algebra appears only once in the spectrum. By identifying the two expressions (4.11) and (4.12) we obtain the following relation

$$\sum_{\lambda} n_{a,b}^{\lambda} S_{\lambda,\eta} = \langle a | \eta \rangle \langle \eta | b \rangle \Leftrightarrow n_{a,b}^{\lambda} = \sum_{\eta} S_{\eta,\lambda} \langle a | \eta \rangle \langle \eta | b \rangle, \quad (4.13)$$

where we have used the fact that S is real symmetric and $S^2 = \mathbf{1}$. Relation (4.13) is referred to as Cardy equation [194], which sets the constraint on admissible boundary states on an annulus. A particular solution is given by

$$\langle a | \lambda \rangle = \frac{S_{a,\lambda}}{\sqrt{S_{0,\lambda}}}, \quad n = \mathcal{N},$$

where the Cardy equation becomes the Verlinde formula (4.8). We refer to these boundary states as Cardy states and denote them by $|C_a\rangle$, $a = \overline{0, k}$.

Due to the difficulty in defining the Wess-Zumino term for a surface with boundary, our discussion of g-function should be taken at the operatorial level. We also stress that the boundary states under consideration are invariant under the extended algebra. For boundary states which are only conformal invariant, see [195].

4.1.1 Off-critical g-function

Let us now assume that there is an 1+1 dimensional integrable massive quantum field theory which admits $SU(2)_k$ WZNW CFT as its UV fixed point. We consider such a theory on a

²The plus sign for the currents come from the fact that they are of spin 1.

cylinder of length L and radius R which plays the role of periodic Euclidean time or equivalently, inverse temperature. We further assume that we can define the boundary conditions in such a way that integrability is conserved.

One would expect from integrability that, at arbitrary temperature, it is possible to compute the bulk free energy and boundary entropy densities of the theory

$$Z_{ab}(R, L) = \exp[-LRf(R)] \times g_a(R)g_b(R).$$

We also assume that in the conformal limit $R \rightarrow 0$ the two integrable boundary conditions can be identified with some CFT boundary states $|a\rangle$ and $|b\rangle$ ³. Then in this limit the modular parameter q tends to one and the contribution of vacuum state dominates other terms in the partition function (4.11)

$$\lim_{R \rightarrow 0} Z_{ab}(R, L) = \chi_0(\tilde{q}) \sum_{\lambda} n_{a,b}^{\lambda} S_{\lambda,0}.$$

Therefore the bulk free energy becomes proportional to the CFT central charge

$$\lim_{R \rightarrow 0} R^2 f(R) = -\frac{\pi C}{6} \quad (4.14)$$

while the boundary contribution to the partition function is given by the sum

$$g_a(0)g_b(0) = \sum_{\lambda} n_{a,b}^{\lambda} S_{\lambda,0}.$$

Apply now the Cardy equation (4.13), one can identify the contribution of each boundary with the corresponding overlap with the Ishibashi state $|0\rangle\rangle$. In particular, if the boundary state happens to be a Cardy state, we expect the boundary entropy to flow to

$$g_a(0) = \frac{S_{a,0}}{\sqrt{S_{0,0}}} \quad (4.15)$$

in the UV limit.

It is the purpose of this chapter to give the exact expression for the boundary entropy g_a at arbitrary temperature for a particular perturbation of $SU(2)_k$ WZNW CFT and to match its value with some Cardy g -function in the UV limit. First, we remind how to compute the bulk free energy $f(R)$ using the Thermodynamic Bethe ansatz technique. In particular we will verify the limit (4.14).

4.2 The TBA equations and Y system

The perturbation we are going to consider belongs to a larger family of perturbations of diagonal coset CFT's $G_k \times G_l / G_{k+l}$ where G is simply-laced. It was first shown in [198] that it is possible to perturb this CFT while still preserving part of its symmetry. The perturbing operator is the branching between two scalar representations and the adjoint representation in the Goddard-Kent-Olive (GKO) construction. Moreover, for negative sign of the perturbing parameter, this

³This hypothesis is usually satisfied for integrable boundary conditions, see for instance [190, 196, 197]

perturbation leads to a massive field theory. In the same paper, a factorized scattering matrix for this field theory in the particular case of $G = SU(2)$ was proposed

$$\mathcal{S} = \mathcal{S}_{[k]}^{\text{RSG}} \otimes \mathcal{S}_{[l]}^{\text{RSG}}, \quad (4.16)$$

where RSG stands for restricted sine-Gordon. Each factor in this tensor product is a S-matrix of the sine-Gordon theory at coupling $\beta^2/8\pi = (k+2)/(k+3)$ and $(l+2)/(l+3)$ respectively. The idea is to rely on the quantum group symmetry of the sine-Gordon S-matrix when the deformed parameter is a root of unity ($q = -\exp[-i\pi/(k+2)]$) to restrict the original multisoliton Hilbert space to direct sum of irreducible representations of this quantum group. As a result the infinite set of vacua of the sine-Gordon theory is truncated to $k+1$ ($l+1$) vacua and a particle of the restricted theory is defined to be a kink interpolating adjacent vacua. This case was further studied in [199] where a system of TBA equations was conjectured and shown to yield the correct central charge of the unperturbed CFT in the UV limit. It should be noted that the TBA system in [199] was not based on the scattering reported in [198] but was instead taken as generalization of several known cases. A derivation of TBA equations for $G = SU(N)$ from the basis of scattering data was later carried out in [200]. The extension to other simple Lie algebras was done in [201]. See also [202] for a lattice realization.

We are interested in the limit $l \rightarrow \infty$ and $G = SU(2)$ where the coset CFT reduces to $SU(2)_k$ WZNW and the branching operator becomes its Kac-Moody current. Moreover the second factor in the S-matrix (4.16) becomes the S-matrix of the chiral $SU(2)$ Gross-Neveu model. Each particle of the theory carries a $SU(2)$ quantum number and a kink quantum number. Each kink connects two adjacent vacua among $k+1$ vacua of the truncated sine-Gordon Hilbert space. One usually calls $(a, a+1)$ a kink and $(a+1, a)$ an anti-kink. When kinks are scattered, only the middle vacuum can be interchanged. For $k=1$ there are two vacua and the only scattering is between kink $(1, 2)$ and anti kink $(2, 1)$, which is trivial. The S-matrix for the kink scattering $K_{da}(\theta_1) + K_{ab}(\theta_2) \rightarrow K_{dc}(\theta_2) + K_{cb}(\theta_1)$ is the RSOS Boltzmann weight

$$\begin{aligned} \mathcal{S}_{[k]}^{\text{kink}}(\theta) \begin{pmatrix} a & b \\ c & d \end{pmatrix}(\theta) &= \frac{u(\theta)}{2\pi i} \left(\frac{\sinh(\pi a/p) \sinh(\pi c/p)}{\sinh \pi d/p \sinh(\pi b/p)} \right)^{-\theta/2\pi i} \\ &\times \left[\sinh \left(\frac{\theta}{p} \right) \left(\frac{\sinh(\pi a/p) \sinh(\pi c/p)}{\sinh(\pi d/p) \sinh(\pi b/p)} \right)^{1/2} \delta_{db} + \sinh \left(\frac{i\pi - \theta}{p} \right) \delta_{ac} \right], \end{aligned}$$

where $a = \overline{1, k+1}$ is the vacuum index, $p = k+2$ and

$$\begin{aligned} u(\theta) &= \Gamma\left(\frac{1}{p}\right) \Gamma\left(1 + \frac{i\theta}{p}\right) \Gamma\left(1 - \frac{\pi + i\theta}{p}\right) \prod_{n=1}^{\infty} \frac{R_n(\theta) R_n(i\pi - \theta)}{R_n(0) R_n(i\pi)}, \\ R_n(\theta) &= \frac{\Gamma(2n/p + i\theta/\pi p) \Gamma(1 + 2n/p + i\theta/\pi p)}{\Gamma((2n+1)/p + i\theta/\pi p) \Gamma(1 + (2n-1)/p + i\theta/\pi p)}. \end{aligned}$$

The scattering matrix is the tensor product of the $SU(2)$ chiral Gross-Neveu S-matrix and the kink S-matrix

$$\mathcal{S}^{\text{SU}(2)_k}(\theta) = \mathcal{S}_{[k]}^{\text{kink}}(\theta) \otimes \mathcal{S}^{\text{SU}(2)}(\theta). \quad (4.17)$$

The TBA system for perturbed $SU(2)_k$ consists of two parts. The right wing consists of $SU(2)$ magnon bound states, exactly like the Gross-Neveu model. The left wing are formed of kink magnon bound states. There are a priori k of them but the longest one does not contribute to the thermodynamic properties. This results in a reduced TBA system involving only $k-1$ kink magnons

$$\log Y_n(u) + Rm \cosh(u) \delta_{n,k} = \sum_{m=0}^{\infty} K_{mn} \star \log(1 + Y_m)(u), \quad n = \overline{1, \infty}. \quad (4.18)$$

The scattering kernels are given at the end of appendix A.2.2. For later discussion of g-function



Figure 4.2: Y system for current perturbed $SU(2)_k$ WZNW. The k 'th node is the physical rapidity. The j 'th node is kink magnon string of length $k-j$ for $1 \leq j \leq k-1$. The a 'th node is $SU(2)$ magnon string of length $a-k$ for $a \geq k+1$.

we present here their convolutions with identity

$$\begin{aligned} K_{ij} \star \mathbf{1} &= \delta_{ij} - 2 \frac{\min(i, j)[k - \max(i, j)]}{k}, & K_{ab} \star \mathbf{1} &= \delta_{ab} - 2 \min(a-k, b-k), \\ K_{kj} \star \mathbf{1} &= -K_{jk} \star \mathbf{1} = -\frac{j}{k}, & K_{ka} \star \mathbf{1} &= -K_{ak} \star \mathbf{1} = -1, \quad i, j \in \overline{1, k-1}, a, b \in \overline{k+1, \infty}, \\ K_{kk} \star \mathbf{1} &= 1 - \frac{1}{2k}. \end{aligned}$$

The TBA equations (4.18) can be transformed into an equivalent Y system. The same kernel s in (A.8) connects the two wings to the physical node, despite different scattering structures on each wing. Again, we denote $\mathcal{Y}_n = Y_n^{2\delta_{n,k-1}}$

$$\log \mathcal{Y}_n + RE \delta_{n,k} = s \star [\log(1 + \mathcal{Y}_{n-1}) + \log(1 + \mathcal{Y}_{n+1})], \quad n = \overline{1, \infty} \quad (4.19)$$

The UV and IR solutions of this Y-system are given by

$$\begin{aligned} 1 + \mathcal{Y}_n^{\text{UV}} &= (n+1)^2, \quad n = \overline{1, \infty}, \\ 1 + \mathcal{Y}_n^{\text{IR}} &= \frac{\sin^2[(n+1)\pi/(k+2)]}{\sin^2[\pi/(k+2)]}, \quad n = \overline{1, k-1}, \quad 1 + \mathcal{Y}_n^{\text{IR}} = (n-k+1)^2, \quad n = \overline{k, \infty}, \end{aligned}$$

From these values we can recover the central charge of the unperturbed CFT using Roger dilogarithm function

$$\sum_{n=1}^{\infty} \text{Li}_R\left(\frac{1}{1 + \mathcal{Y}_n^{\text{IR}}}\right) - \text{Li}_R\left(\frac{1}{1 + \mathcal{Y}_n^{\text{UV}}}\right) = \frac{3k}{k+2}. \quad (4.20)$$

For a proof of this identity, see for instance [131]. We can add to the TBA equations (4.18) a chemical potential coupled to the $SU(2)$ symmetry only. The Y system (4.19) is again

protected. In the IR limit the left wing decouples from the right wing and is immune to the $SU(2)$ chemical potential. The IR values on the left wing is therefore unchanged, while on the right wing we have

$$1 + \mathcal{Y}_n^{\text{IR}}(\kappa) = [n - k + 1]_\kappa^2, \quad n = \overline{k, \infty}.$$

In the UV limit all nodes are affected by the twist

$$1 + \mathcal{Y}_n^{\text{UV}}(\kappa) = [n + 1]_\kappa, \quad n = \overline{1, \infty}.$$

As described in chapter 1, we can compute the particle densities in this limit

$$\lim_{R \rightarrow 0} \pi R D_0(R, \mu) = 2 \log \frac{1 - \kappa^{k+1}}{1 - \kappa} - k \log \kappa, \quad \lim_{R \rightarrow 0} \sum_{a=1}^{\infty} \pi R a D_a(R, \mu) = 2 \log \frac{1 - \kappa^{k+1}}{1 - \kappa} \quad (4.21)$$

as well as the scaled free energy density

$$\lim_{R \rightarrow 0} c(R, \mu) = \frac{3k}{k+2} - \frac{6k\mu^2}{\pi^2}. \quad (4.22)$$

4.3 The reflection factors

Due to the factorization property of the S-matrix (4.17), we can study the reflection factors for kink magnons and $SU(2)$ magnons independently.

After the maximum string reduction procedure (see appendix (A.2.2)), the effective scattering between $k - 1$ kink magnon strings are very similar to the scattering of the A theories in the ADE family [129]. The scattering phase between a kink magnon string of length n and another one of length m , for $n, m = \overline{1, k-1}$ is given by

$$S_{nm}(\theta) = \frac{\sinh\left(\frac{\theta}{k} + i\pi \frac{|n-m|}{2k}\right) \sinh\left(\frac{\theta}{k} + i\pi \frac{n+m}{2k}\right)}{\sinh\left(\frac{\theta}{k} - i\pi \frac{|n-m|}{2k}\right) \sinh\left(\frac{\theta}{k} - i\pi \frac{n+m}{2k}\right)} \prod_{s=\frac{|n-m|}{2}+1}^{\frac{n+m}{2}-1} \left[\frac{\sinh\left(\frac{\theta}{k} + i\pi \frac{s}{k}\right)}{\sinh\left(\frac{\theta}{k} - i\pi \frac{s}{k}\right)} \right]^2 \quad (4.23)$$

where θ is the rapidity difference between the two string centers. On the other hand, the A_{k-1} S-matrix describes the purely elastic scattering of the coset CFT $SU(k)_1 \times SU(k)_1 / SU(k)_2$ (\mathbb{Z}_k parafermions) perturbed by its $(1, 1, \text{adj})$ operator⁴. This massive perturbation consists of $k-1$ particles $n = 1, \dots, k-1$ where $\bar{n} = k - n$ with mass spectrum

$$m_n = m \sin\left(\frac{\pi n}{k}\right) / \sin\left(\frac{\pi}{k}\right).$$

The purely elastic scattering between these particles is

$$S_{nm}(\theta) = \frac{\sinh\left(\frac{\theta}{2} + i\pi \frac{|n-m|}{2k}\right) \sinh\left(\frac{\theta}{2} + i\pi \frac{n+m}{2k}\right)}{\sinh\left(\frac{\theta}{2} - i\pi \frac{|n-m|}{2k}\right) \sinh\left(\frac{\theta}{2} - i\pi \frac{n+m}{2k}\right)} \prod_{s=\frac{|n-m|}{2}+1}^{\frac{n+m}{2}-1} \left[\frac{\sinh\left(\frac{\theta}{2} + i\pi \frac{s}{k}\right)}{\sinh\left(\frac{\theta}{2} - i\pi \frac{s}{k}\right)} \right]^2 \quad (4.24)$$

⁴The central charge of this CFT is exactly the central charge of $SU(2)_k$ minus 1 : parafermion \mathbb{Z}_k can be represented as $SU(2)_k / U(1)$.

So indeed, despite the different underlying physics, the two scattering phases (4.23) and (4.24) are identical up to a redefinition of rapidity variable

$$\theta^{\text{kink magnon}} = \frac{k}{2} \times \theta^{\text{A series}}.$$

This suggests that we can use the minimal reflection factor already derived for A series [124], [197] for the kink magnons. It is the solution of the boundary unitarity, crossing and bootstrap equations with a minimal number of poles and zeros

$$R_j(\theta) = \prod_{s=0}^{j-1} \frac{\sinh\left(\frac{\theta}{2} + i\pi \frac{s}{2}\right) \sinh\left(\frac{\theta}{2} - i\pi \frac{k-s+1}{2}\right)}{\sinh\left(\frac{\theta}{2} - i\pi \frac{s}{2}\right) \sinh\left(\frac{\theta}{2} + i\pi \frac{k-s+1}{2}\right)}, \quad j = \overline{1, k-1}.$$

It satisfies in particular the following identity

$$K_j \star \mathbf{1} - \frac{1}{2} K_{jj} \star \mathbf{1} - \frac{1}{2} = 0, \quad j = \overline{1, k-1}. \quad (4.25)$$

where $K_j = -i\partial \log R_j$, which greatly simplifies the form of the corresponding g-function in the next section. For parafermions, this set of reflection factors is assigned with the fixed boundary condition or equivalently the vacuum representation of both $SU(k)_1$ and $SU(k)_2$. The g-function was found to be

$$g_0^2 = \frac{2}{\sqrt{k+2}\sqrt{k}} \sin \frac{\pi}{k+2}. \quad (4.26)$$

On the other hand, we consider trivial reflection factors on the $SU(2)$ magnons. We do not aim at proving this point but we merely conjecture it based on the result of non linear $O(N)$ sigma model with boundary [203], [204], where similar magnon structure arises. What we are doing is to first diagonalize the bulk theory by nested Bethe Ansatz technique. We then treat the theory as one with diagonal scattering and find the reflection factors based on this bulk diagonal scattering. The standard way to do it would be to start with a set of reflection factors that satisfy the boundary Yang-Baxter equation. One then writes Bethe equations with these reflection factors and diagonalizes the corresponding two-row transfer matrix.

To summarize, we conjecture the following set of TBA equations for current perturbed $SU(2)_k$ theories in the presence of boundaries

$$\begin{aligned} \text{physical rapidity} \quad & e^{iLm \sinh(\theta_{k,n})} R_k^2(\theta_{k,n}) \prod_{j=1}^{\infty} \prod_m S_{kj}(\theta_{k,n} - \theta_{j,m}) S_{kj}(\theta_{k,n} + \theta_{j,m}) = -1 \\ \text{Kink magnons} \quad & R_j^2(\theta_{j,n}) \prod_{l=1}^k \prod_m S_{jl}(\theta_{j,n} - \theta_{l,m}) S_{jl}(\theta_{j,n} + \theta_{l,m}) = -1, \quad j = \overline{1, k-1} \\ \text{SU(2) magnons} \quad & \prod_{l=k}^{\infty} \prod_m S_{jl}(\theta_{j,n} - \theta_{l,m}) S_{jl}(\theta_{j,n} + \theta_{l,m}) = -1, \quad j = \overline{k+1, \infty} \end{aligned}$$

We denote from now on the convolution of the boundary reflections with identity by $B_j = K_j \star \mathbf{1}$. They are given by (4.25) for kink magnons and are zero for $SU(2)$ magnons. For the physical rapidity, we leave it as a parameter.

4.4 The divergence and the normalized g-function

We now have all the necessary ingredients to study the UV and IR limit of the g-function of the current-perturbed $SU(2)_k$ theories. For convenience we repeat here the result (4.1)-(4.3) , with an equivalent form of the loop part that is more adapted to actual computation

$$2 \log g(R) = 2 \log g^{\text{trees}}(R) + 2 \log g^{\text{loops}}(R), \quad (4.27)$$

$$2 \log g^{\text{trees}}(R) = \sum_n \int_{-\infty}^{\infty} \frac{d\theta}{2\pi} [K_n(\theta) - K_{nn}(\theta, -\theta) - \pi \delta(\theta)] \log[1 + Y_n(\theta)], \quad (4.28)$$

$$2 \log g^{\text{loops}}(R) = \sum_{n \geq 1} \frac{1}{n} \sum_{a_1, \dots, a_n \geq 0} \left[\prod_{j=1}^n \int_{-\infty}^{+\infty} \frac{du_j}{2\pi} f_{a_j}(u_j) \right] K_{a_1 a_2}(\theta_1 + \theta_2) K_{a_2 a_3}(\theta_2 - \theta_3) \dots K_{a_n a_1}(\theta_n - \theta_1). \quad (4.29)$$

The goal of this section is to support to our proposition (4.4) by proving that it is possible to match the normalized UV g-function, namely $g_{\text{UV}}/g_{\text{IR}}$ with a conformal g-function (4.15) in some cases. While carrying out this normalization we encounter divergence in both IR and UV limit. We illustrate this phenomenon for the Gross-Neveu model and show how an appropriate regularization could lead to a finite ratio.

4.4.1 Level 1- Gross Neveu model

At zero temperature, the tree part (4.28) of the g-function can be exactly evaluated. With the Y-functions given by constants in (1.75), the reflection kernels for $SU(2)$ magnons being zero and the scattering kernels K_{nn} given in (A.4), it turns out to be divergent in this limit

$$2 \log g_{\text{IR}}^{\text{trees}} = \sum_{n=1}^{\infty} (n-1) \log \left[1 + \frac{1}{n(n+2)} \right]. \quad (4.30)$$

The tadpole (the $n = 1$ term in the series (4.29)) suffers from a similar divergence

$$2 \log g_{\text{IR}}^{\text{tadpole}} = \sum_{n=1}^{\infty} \frac{Y_n^{\text{IR}}}{1 + Y_n^{\text{IR}}} \int_{-\infty}^{+\infty} \frac{du}{2\pi} K_{nn}(2u) = \sum_{n=1}^{\infty} \frac{1-2n}{2(n+1)^2}. \quad (4.31)$$

This logarithmic divergence is present for higher order terms and for the infinite temperature limit alike. We believe it is a common feature among models with an infinite number of string magnons.

As a regularization, we propose to use the twisted TBA solutions (1.79). The tree part of the IR g-function can now be expressed in terms of the twist parameter κ

$$2 \log g_{\text{IR}}^{\text{trees}}(\kappa) = \sum_{n=1}^{\infty} (n-1) \log \left(1 + \frac{1}{[n+1]_{\kappa}^2 - 1} \right) = -\log(1 - \kappa^2). \quad (4.32)$$

To evaluate the loop part, we remark that for constant Y-functions the series (4.29) can be written as a determinant

$$2 \log g_{\text{IR}}^{\text{loops}}(\kappa) = -\frac{1}{2} \log \det[1 - \hat{K}^{\text{IR}}(\kappa)], \quad (4.33)$$

where

$$\hat{K}_{ab}^{\text{IR}}(\kappa) \equiv \sqrt{\frac{Y_a^{\text{IR}}(\kappa)}{1 + Y_a^{\text{IR}}(\kappa)} \frac{Y_b^{\text{IR}}(\kappa)}{1 + Y_b^{\text{IR}}(\kappa)}} \int_{-\infty}^{+\infty} \frac{d\theta}{2\pi} K_{ab}(\theta), \quad (4.34)$$

The factor $1/2$ comes from the change of variables $(\theta_1 + \theta_2, \theta_2 - \theta_3, \dots, \theta_n - \theta_1) \rightarrow (\tilde{\theta}_1, \tilde{\theta}_2, \dots, \tilde{\theta}_n)$. We show in appendix B.0.1 that

$$\det[1 - \hat{K}^{\text{IR}}(\kappa)] = (1 - \kappa)^{-1}. \quad (4.35)$$

By combining the two contributions (4.32) and (4.35), we obtain the IR g-function of Gross-Neveu model as a function of the twist parameter. In the untwisted limit $\kappa \rightarrow 1$ it behaves as

$$\lim_{\kappa \rightarrow 1} 2 \log g_{\text{IR}}(\kappa) = -\log 2 - \frac{1}{2} \log(1 - \kappa). \quad (4.36)$$

We can repeat the same analysis for the UV limit, using the corresponding twisted constant solution (1.79). Compared to the IR limit we also get contribution from the physical rapidity. The loop part can again be written as a determinant by replacing the IR by UV values in the matrix (4.34). We show in appendix B.0.2 that this determinant is again a very simple function of the twist parameter

$$2 \log g_{\text{UV}}^{\text{trees}}(\kappa) = (B_0 - \frac{3}{4}) \log \frac{(1 + \kappa)^2}{\kappa} - \log(1 - \kappa^3), \quad (4.37)$$

$$2 \log g_{\text{UV}}^{\text{loops}}(\kappa) = \frac{1}{2} \log[2(1 - \kappa)]. \quad (4.38)$$

The UV value of g-function exhibits the same divergence as the IR one in the untwisted limit

$$\lim_{\kappa \rightarrow 1} 2 \log g_{\text{UV}}(\kappa) = (2B_0 - 1) \log 2 - \log 3 - \frac{1}{2} \log(1 - \kappa) \quad (4.39)$$

In particular their ratio is well defined

$$\left(\frac{g_{\text{UV}}}{g_{\text{IR}}} \right)^2 = 2^{2B_0}/3. \quad (4.40)$$

The two Cardy g-functions (4.15) of $SU(2)_1$ CFT take the same value $g_1^2 = g_2^2 = 1/\sqrt{2}$. For integrable boundary conditions, the reflection factor usually gives rational value for B_0 and our proposition (4.40) could not be matched with a Cardy g-function. We carry on our analysis to higher levels.

4.4.2 Higher levels

We first consider the IR limit, in which the left and right wing are decoupled. The former is not affected by the twist while the latter is identical to the IR of the Gross-Neveu model. Our choice of reflection factors with the property (4.25) eliminates the left wing from the tree part

of the g-function. As a consequence we get the same result as the IR tree part of Gross-Neveu model (4.32)

$$2 \log g_{\text{IR}}^{\text{trees}}(\kappa) = -\log(1 - \kappa^2). \quad (4.41)$$

The loop part is factorized into two determinants

$$2 \log g_{\text{IR}}^{\text{loops}} = -\frac{1}{2} \log \det(1 - \hat{K}_{1 \rightarrow k-1}) - \frac{1}{2} \log \det(1 - \hat{K}_{k+1 \rightarrow \infty}). \quad (4.42)$$

The finite determinant involving the trigonometric Y-functions has been computed in [197] while the infinite determinant is exactly the same as that of IR Gross-Neveu

$$\det(1 - \hat{K}_{1 \rightarrow k-1}) = \left[\frac{4k}{k+2} \sin^2 \frac{\pi}{k+2} \right]^{-1}, \quad \det(1 - \hat{K}_{k+1 \rightarrow \infty}) = (1 - \kappa)^{-1}.$$

By summing the two parts, we obtain the IR g-function. Its behavior in the untwisted limit is

$$\lim_{\kappa \rightarrow 1} 2 \log g_{\text{IR}}(\kappa) = -\log 2 + \frac{1}{2} \log \frac{4k}{k+2} + \log \sin \frac{\pi}{k+2} - \frac{1}{2} \log(1 - \kappa). \quad (4.43)$$

In the UV limit all Y-functions are twisted. Again only the right wing contributes to the tree part of g-function

$$2 \log g_{\text{UV}}^{\text{trees}}(\kappa) = (B_k - 1 + \frac{1}{4k}) \log[k+1]_{\kappa}^2 - \log(1 - \kappa^{k+2}). \quad (4.44)$$

The loop contribution is given by a determinant that connects the two wings. We compute this determinant in appendix B.0.2. Despite its complicated form, as the structure of scattering kernels on the left and right wing are different, the result is simple

$$2 \log g_{\text{UV}}^{\text{loops}}(\kappa) = \frac{1}{2} \log 2k + \frac{1}{2} \log(1 - \kappa). \quad (4.45)$$

The UV g-function is obtained by summing (4.44) and (4.45)

$$\lim_{\kappa \rightarrow 1} 2 \log g_{\text{UV}}(\kappa) = (2B_k - 2 + \frac{1}{2k}) \log(k+1) - \log(k+2) + \frac{1}{2} \log 2k - \frac{1}{2} \log(1 - \kappa). \quad (4.46)$$

We see that the IR (4.43) and UV (4.46) values of g-function exhibit the same divergence in the untwisted limit. We can therefore extract their ratio

$$\left(\frac{g_{\text{UV}}}{g_{\text{IR}}} \right)^2 = (k+1)^{2B_k - 2 + \frac{1}{2k}} \times \sqrt{\frac{2}{k+2}} \times \frac{1}{\sin \frac{\pi}{k+2}}. \quad (4.47)$$

To remind, the Cardy g-functions are given by

$$g_{\lambda}^2 = \sqrt{\frac{2}{k+2}} \times \frac{1}{\sin \frac{\pi}{k+2}} \times \sin^2 \frac{(\lambda+1)\pi}{k+2}, \quad 0 \leq \lambda \leq k \quad (4.48)$$

Therefore we can match our normalized UV g-function (4.47) with $g_{k/2}$ for even k as long as the reflection factor of the physical rapidity satisfies $B_k = 1 - 1/(4k)$. Let $k = 2m$ then the corresponding bulk primary has conformal dimension

$$\Delta = \frac{m(m+2)}{8(m+1)}.$$

4.5 Conclusion

In this chapter we propose the following procedure to study the g-function of a massive integrable theory with non-diagonal bulk scattering

- Diagonalize the theory using the Nested Bethe Ansatz technique.
- Treat the newly obtained theory as diagonal with extra magnonic particles and apply the results (4.1)-(4.3) to compute its g-function.
- Normalize the g-function by its zero temperature limit value.

We test our proposition for the current-perturbed $SU(2)$ WZNW CFTs. The TBA of these theories involves an infinite tower of magnon strings. As a consequence both the tree (4.2) and loop (4.3) part of the g-function diverge at zero and infinite temperature. This phenomenon is illustrated for the Gross-Neveu model in (4.30),(4.31). We conjecture that such divergence is present at arbitrary temperature. By considering the twisted TBA, we are able to compute these two limits of g-function as functions of the twist parameter κ . It is found that they exhibit the same divergence $-\frac{1}{2}\log(1-\kappa)$ in the untwisted limit $\kappa \rightarrow 1$ (4.43),(4.46). The normalized UV g-function is then well defined (4.47) and can be identified with a Cardy g-function of the unperturbed CFT under some assumption on the reflection factor of the physical rapidity and for even levels.

This normalization has a diagrammatical interpretation. At zero temperature the boundary entropy is given by the sum of all graphs made exclusively of auxiliary magnons. The contribution of these graphs does not depend on the temperature and can be absorbed into the normalization of the partition function. No physical observable will involve such graphs.

Chapter 5

Applications in Generalized Hydrodynamics

In this chapter we present two applications of our diagrammatic formalism in the context of GHD. The first is a rigorous derivation based on form factors [205] of the average currents. As we saw in section 1.4 this quantity is a cornerstone in the GHD formalism: all transport-related observables are derived from it. The second is a conjecture [206] that allows the cumulants of time-integrated currents to be expressed as a sum over simple tree diagrams. They are almost the same diagrams that represent the cumulants of conserved charges in section 2.2. Our conjecture thus highlights a remarkably simple duality between time-integrated currents and conserved charges, one that could potentially be extended to other transport properties as well.

5.1 Equations of state from form factors

GHD is a framework to study the dynamics of integrable systems at the Euler scale¹. At such scale, generically, many-body systems are expected to be in a state where local entropy maximization is realized. In such a state, physics is dominated by macroscopic processes protected by conserved charges, and the state potentially carry a current. In practice, this scale can be accessed by taking a scaling limit of infinitely many degrees of freedom (i.e. the ratio between a typical microscopic scale l_{mic} , say the inter-particle length, and a typical macroscopic scale l_{mac} becomes zero: $\epsilon = l_{\text{mic}}/l_{\text{mac}} \rightarrow 0$) while scaling the space-time simultaneously $(x, t) \rightarrow (\epsilon^{-1}x, \epsilon^{-1}t)$, which amounts to focusing on physics occurring at an emergent large scale called the fluid cell. Note that depending on the exponent α of the scaling of x , $\epsilon^{-\alpha}x$, a different scaling limit can be obtained (e.g. diffusive scaling for $\alpha = 1/2$ and super diffusive scaling for $1/2 < \alpha < 1$). The assumption of local entropy maximization provides us an efficient way to evaluate correlation functions at the Euler scale. In particular, the expectation value of a given local operator \mathcal{O} is computed by $\langle \mathcal{O}(x, t) \rangle_{\text{Eul}} = \text{Tr}[\rho(x, t)\mathcal{O}]$ with $\rho(x, t) \propto \exp[-\sum_i \beta_i(x, t)\mathcal{Q}_i]$, where $\mathcal{Q}_i = \int dx Q_i(x, 0)$ are the conserved charges. This suggests that, at the Euler scale, in order to solve the macroscopic continuity equations $\partial_t \langle Q_i(x, t) \rangle_{\text{Eul}} + \partial_x \langle J_i(x, t) \rangle_{\text{Eul}} = 0$, one only has to know the equilibrium form of the averages of densities $\langle Q_i \rangle_{\vec{\beta}}$ and currents $\langle J_i \rangle_{\vec{\beta}}$ as functions of Lagrange multipliers $\vec{\beta}$. The density average of a conserved charge can be written as

$$\langle Q_i \rangle = \int \frac{dp(\theta)}{2\pi} f(\theta) q_i^{\text{dr}}(\theta), \quad (5.1)$$

where f is the TBA filling factor, q_i is the one-particle eigenvalue of \mathcal{Q}_i and the dressing operation was defined in (1.114). Now, we need to know how $\langle J_i \rangle$ looks like in order to solve

¹Diffusive effect is outside the scope of this thesis

the macroscopic continuity equations. In [61,62], the exact expression of $\langle J_i \rangle$ was proposed that

$$\langle J_i \rangle = \int \frac{dE(\theta)}{2\pi} f(\theta) q_i^{\text{dr}}(\theta) = \int d\theta \rho_p(\theta) v^{\text{eff}}(\theta) q_i(\theta), \quad (5.2)$$

where $v^{\text{eff}} = (E')^{\text{dr}}/(p')^{\text{dr}}$ is the velocity of excitation over an equilibrium state. The form of v^{eff} can be in fact considered as equations of state for GHD. Recall that equations of state are relations that relate the density averages $\langle Q_i \rangle$ and the current averages. Since it is precisely what v^{eff} is doing, making (5.2) different from (5.1) by its very appearance in (5.2), the functional form of the effective velocity determines the relation between the density and current averages.

The proof in [61] exploits mirror transformation and has been sketched in subsection 1.4.2. We note however that this proof is in fact incomplete as the assumed analyticity of the TBA source term is not necessarily true for some GGEs. In [62], the expression was extended to the XXZ spin- $\frac{1}{2}$ chain where strings are present without proof but with numerical verifications. Thus a full proof of the equations of state is still needed in GHD. So far, the validity of GHD, which is equivalent to that of the effective velocity, has been numerically confirmed for spin chains such as the XXZ spin- $\frac{1}{2}$ chain [207–212] and the Fermi-Hubbard model [213], and it is believed that GHD correctly captures the long-wavelength dynamics of any Bethe solvable systems. Nonetheless, a down-to-earth proof of $v^{\text{eff}}(\theta)$ is still highly-desired to complete the program of GHD, and it is the purpose of this section to report such a proof for relativistic integrable field theories with diagonal S-matrix. With minor modifications, this proof has been shown to work equally well for integrable spin chains [67]. Very recently, there is yet another proof that does not require explicit use of relativistic invariance [214].

Our strategy relies on form factor expansions by means of the LeClair-Mussardo series (1.112). This series is universal in the sense that the expectation values of two operators differ only in their connected form factors. As a result, the task of establishing the equations of state boils down to a direct comparison between the connected form factor of the charge densities and that of the currents. Such comparison can be done with help of the Pozsgay-Takacs relation (1.104) between the connected form factors and the symmetric ones. This relation involves principal minors of a Laplacian matrix and naturally admits a diagrammatic interpretation.

5.1.1 The connected and the symmetric form factors

The connected and the symmetric evaluation of diagonal matrix elements play a pivotal role in our proof. For the convenience of following, we repeat here the Pozsgay-Takacs relation already introduced in subsection 1.3.2

$$F_s^{\mathcal{O}}(\theta_1, \dots, \theta_n) = \sum_{\alpha \subset \{1, \dots, n\}, \alpha \neq \emptyset} \mathcal{L}(\alpha|\alpha) F_c^{\mathcal{O}}(\{\theta_i\}_{i \in \alpha}) \quad (5.3)$$

where $\mathcal{L}(\alpha|\alpha)$ is the principal minor obtained by deleting the α rows and columns of the Laplacian matrix

$$L(\theta_1, \dots, \theta_n)_{jk} = \delta_{jk} \sum_{l \neq j} K(\theta_j - \theta_l) - (1 - \delta_{jk}) K(\theta_j - \theta_k). \quad (5.4)$$

Let us also repeat the LeClair-Mussardo formula for the one point function of a local operator

$$\langle \mathcal{O} \rangle = \sum_{n=0}^{\infty} \left(\prod_{j=1}^n \int \frac{d\theta_j}{2\pi} f(\theta_j) \right) F_c^{\mathcal{O}}(\theta_1, \dots, \theta_n). \quad (5.5)$$

In the particular case of a conserved charge density Q_j , the corresponding connected form factor is given by

$$F_c^{Q_i}(\theta_1, \dots, \theta_n) = q_i(\theta_1)K(\theta_1 - \theta_2) \cdots K(\theta_{n-1} - \theta_n)p'(\theta_n) + \text{perm}, \quad (5.6)$$

where perm. is understood as permutations with respect to the integer set $\{1, \dots, n\}$.

We observe that the same structure holds for the current operator J as well. Recalling (5.2), we can also recast it into the similar form and expand as

$$\langle J_i \rangle = \sum_{n=0}^{\infty} \left(\prod_{k=1}^n \int \frac{d\theta_k}{2\pi} f(\theta_k) \right) q_i(\theta_1)K(\theta_1 - \theta_2) \cdots K(\theta_{n-1} - \theta_n)E'(\theta_n), \quad (5.7)$$

This suggests that if the connected form factor of J takes the following form, then (5.2) follows:

$$F_c^{J_i}(\theta_1, \dots, \theta_n) = q_i(\theta_1)K(\theta_1 - \theta_2) \cdots K(\theta_{n-1} - \theta_n)E'(\theta_n) + \text{perm}, \quad (5.8)$$

which is the actual statement we are going to prove in order to establish (5.2).

The relation (5.3) between the symmetric and connected form factors can be understood graphically. The matrix L whose minors appear in this relation is a Laplacian matrix. It is the discretized Laplacian operator on a graph in which a weight $K(\theta_j - \theta_k)$ is assigned to the edge connecting j and k . Although L has a vanishing determinant, as the elements on each row sum up to zero, its principal minors can be expressed as a sum over forests.

As our discussion in this chapter is restricted only to relativistically invariant theories, the scattering kernel K is symmetric. Consequently, the expansion of the principal minors of L result in undirected graphs, in contrast to the previous chapters. Let α be a subset of vertices $\{1, 2, \dots, n\}$. Then we have

$$\mathcal{L}(\alpha|\alpha) = \sum_{F \in \mathcal{F}_\alpha} \prod_{e \in F} K_e, \quad (5.9)$$

where the summation is performed over all forests of n vertices each tree of which contains exactly one vertex from α . The product runs over all edges of the forests. The result (5.9) is exactly equivalent to (2.40) and (2.13) presented in previous chapters. The only difference is that we cannot refer to vertices of α as roots, due to the lack of direction on the edges.

This is known as the all-minor version of the matrix-tree theorem. A particular case is given by considering principal minors of rank $n - 1$ i.e. by taking α to be one-element subsets. The forests would then become trees.

Let us illustrate the theorem in the case of three particles, where (5.4) is given by

$$L = \begin{pmatrix} K_{12} + K_{13} & -K_{12} & -K_{13} \\ -K_{21} & K_{21} + K_{23} & -K_{23} \\ -K_{31} & -K_{32} & K_{31} + K_{32} \end{pmatrix}, \quad K_{ij} \equiv K(\theta_i - \theta_j).$$

All the principal minors of rank 2 are equal: $\mathcal{L}(1|1) = \mathcal{L}(2|2) = \mathcal{L}(3|3) = K_{21}K_{31} + K_{21}K_{32} + K_{23}K_{31}$. These terms are exactly the three trees spanning three vertices, see Fig.5.1. Note that we are referring to **labelled** trees. In particular, the trees in Fig.5.1 are considered as being distinguished, despite their similar combinatorial structure. The principal minors of rank 1 are written as forests with two trees. For example, when $\alpha = \{2, 3\}$ we have $\mathcal{L}(\alpha|\alpha) = K_{12} + K_{13}$, as in Fig.5.2.

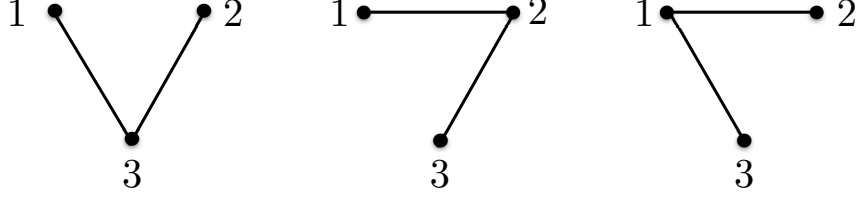


Figure 5.1: Trees associated with a minor of rank 2.



Figure 5.2: Forests associated with a minor $\mathcal{L}(\{2, 3\}|\{2, 3\})$.

The matrix-tree theorem provides a simple interpretation of the relation (5.3) between symmetric and connected form factors. For each subset α of $\{1, 2, \dots, n\}$ we decorate the connected form factor $F_c^{\mathcal{O}}(\{\theta_i\}_{i \in \alpha})$ by trees growing out of the elements of α . The decorations must guarantee that all n vertices are covered. By summing over α and over all the possible decorations for each α , we obtain the symmetric form factor $F_s^{\mathcal{O}}(\theta_1, \dots, \theta_n)$.

5.1.2 Establishing the equations of state

We are at the position to present a graph theoretic proof for the equations of state (5.8). Our proof consists of three steps

- Obtain the symmetric form factor of the charge $F_s^Q(\theta_1, \dots, \theta_n)$ from the connected one (5.6) and the relation (5.3).
- Compute the symmetric form factor of the current $F_s^J(\theta_1, \dots, \theta_n)$ from that of the charge, by using the continuity equation.
- Find the connected form factor of the current from the symmetric one, by going from the left hand side to the right hand side of equation (5.3).

The first and the last step are done with help of the matrix-tree theorem. In the first step, we represent the connected form factor of the charge

$$F_c^Q(\theta_1, \dots, \theta_n) = q(\theta_1)K(\theta_1 - \theta_2) \cdots K(\theta_{n-1} - \theta_n)p'(\theta_n) + \text{perm}, \quad (5.10)$$

as $n!$ spines of length n with the charge eigenvalue q on one end and the momentum derivative p' at the other end. Spines of length 1 with coinciding ends are allowed.

The corresponding symmetric form factor is obtained by decorating the spines with the trees, see Fig.5.3. Because the trees have different labelings and the spines come from different

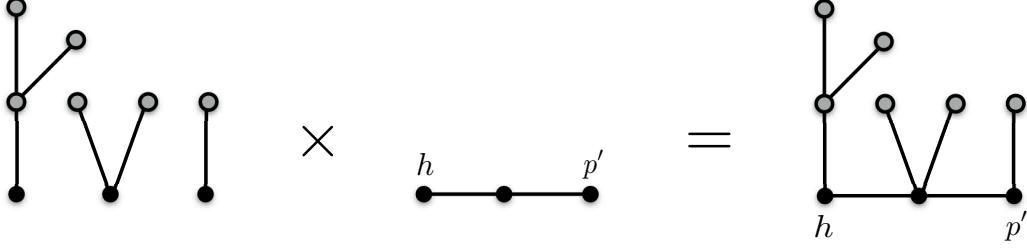


Figure 5.3: Pictorial representation of one of terms in the RHS of (5.3) when \mathcal{O} is a conserved density. Each term (forest) of $\mathcal{L}(\alpha|\alpha)$ and each term in $F_c(\{\theta_i\}_{i \in \alpha})$ form a spanning tree by merging together at vertices α represented by black dots.

permutations, each term in the symmetric form factor is a (labelled) tree with two marked points, no tree appears more than once. Vice versa, each tree with two marked points can be decomposed to a spine and a forest. Indeed, the connectedness guarantees the existence of a path between the two marked points. Moreover, the uniqueness of this path is ensured by the non-existence of cycles. We conclude that the symmetric form factor of the charge is given by the sum over all the trees of n vertices, with the weights q and p' inserted at two arbitrary vertices. This sum factorizes into the sum over the weights and the sum over the unmarked trees

$$F_s^Q(\theta_1, \dots, \theta_n) = \sum_{j=1}^n q(\theta_j) \sum_{k=1}^n p'(\theta_k) \sum_{T \in \mathcal{T}} \prod_{e \in \text{edges of } T} K_e, \quad (5.11)$$

Here, \mathcal{T} denotes the set of all trees of n vertices. The sum over these trees are exactly given by the principal minor of rank $n-1$ of the matrix (5.4). For instance, in the case of three particles

$$F_s^Q(\theta_1, \theta_2, \theta_3) = [q(\theta_1) + q(\theta_2) + q(\theta_3)][p'(\theta_1) + p'(\theta_2) + p'(\theta_3)](K_{21}K_{31} + K_{21}K_{32} + K_{23}K_{31}).$$

We now turn to the second step. In order to relate (5.11) to the symmetric form factor of the current $F_s^J(\theta_1, \dots, \theta_n)$, where J satisfies the continuity equation $\partial_t Q + \partial_x J = 0$, we note that there is a relation between $F_s^Q(\theta_1, \dots, \theta_n)$ and $F_s^J(\theta_1, \dots, \theta_n)$ which is a simple consequence of the continuity equation

$$F_s^J(\theta_1, \dots, \theta_n) = \frac{\sum_{k=1}^n E'(\theta_k)}{\sum_{k=1}^n p'(\theta_k)} F_s^Q(\theta_1, \dots, \theta_n), \quad (5.12)$$

where we recall $E(\theta) = m \cosh \theta$ and $p(\theta) = m \sinh \theta$. To see this, we first observe

$$\langle \text{vac} | J(x, t) | \vec{\theta}, \overleftarrow{\theta'} \rangle = e^{-im \sum_{k=1}^n [(\cosh \theta_k + \cosh \theta'_k)t - (\sinh \theta_k + \sinh \theta'_k)x]} \langle \text{vac} | J(0, 0) | \vec{\theta}, \overleftarrow{\theta'} \rangle \quad (5.13)$$

and thus,

$$\langle \text{vac} | \partial_x J(x, t) | \vec{\theta}, \overleftarrow{\theta'} \rangle = im \sum_{k=1}^n (\sinh \theta_k + \sinh \theta'_k) \langle \text{vac} | J(x, t) | \vec{\theta}, \overleftarrow{\theta'} \rangle. \quad (5.14)$$

Using this, it then follows that

$$\begin{aligned}
F_s^J(\theta_1, \dots, \theta_n) &\equiv \lim_{\delta \rightarrow 0} \langle \text{vac} | J(x, t) | \vec{\theta}, \overleftarrow{\theta'} \rangle \\
&= \lim_{\delta \rightarrow 0} \frac{-i}{m \sum_k (\sinh \theta_k + \sinh \theta'_k)} \langle \text{vac} | \partial_x J(x, t) | \vec{\theta}, \overleftarrow{\theta'} \rangle \\
&= \lim_{\delta \rightarrow 0} \frac{i}{m \sum_k (\sinh \theta_k + \sinh \theta'_k)} \langle \text{vac} | \partial_t Q(x, t) | \vec{\theta}, \overleftarrow{\theta'} \rangle \\
&= \lim_{\delta \rightarrow 0} \frac{\sum_k (\cosh \theta_k + \cosh \theta'_k)}{\sum_k (\sinh \theta_k + \sinh \theta'_k)} \langle \text{vac} | Q(x, t) | \vec{\theta}, \overleftarrow{\theta'} \rangle \\
&= \frac{\sum_k E'(\theta_k)}{\sum_k p'(\theta_k)} F_s^Q(\theta_1, \dots, \theta_n),
\end{aligned} \tag{5.15}$$

where we used the continuity equation when passing from the second line to the third line, and noted

$$\langle \text{vac} | \partial_t Q(x, t) | \vec{\theta}, \overleftarrow{\theta'} \rangle = -im \sum_{k=1}^n (\cosh \theta_k + \cosh \theta'_k) \langle \text{vac} | Q(x, t) | \vec{\theta}, \overleftarrow{\theta'} \rangle, \tag{5.16}$$

when moving from the third to the fourth line. Here, δ is defined as before in order to take the uniform limit $\theta'_j = \theta_j + \pi i + \delta$ of the symmetric evaluation.

Now, applying this relation to (5.11), it immediately follows that

$$F_s^J(\theta_1, \dots, \theta_n) = \sum_{k=1}^n q(\theta_k) \sum_{k=1}^n E'(\theta_k) \sum_{T \in \mathcal{T}} \prod_{e \in \text{edges of } T} K_e, \tag{5.17}$$

which is nothing but the summation over all the trees of n vertices, this time with q and E' inserted at two arbitrary points. By reversing the logic of the first step, we can write this as a sum over spines and decorating trees

$$F_s^J(\theta_1, \dots, \theta_n) = \sum_{\alpha \subset \{1, \dots, n\}, \alpha \neq \emptyset} \mathcal{L}(\alpha | \alpha) F_c^J(\{\theta_i\}_{i \in \alpha}), \tag{5.18}$$

where the spines now have q and E' on two ends

$$F_c^J(\theta_1, \dots, \theta_n) = q(\theta_1) K(\theta_1 - \theta_2) \cdots K(\theta_{n-1} - \theta_n) E'(\theta_n) + \text{perms}. \tag{5.19}$$

This is the desired formula for the current connected form factor. \square

Our proof makes use of the matrix-tree theorem to express all the determinants and minors in the relation (5.3) between connected and symmetric form factors as sums over trees. We believe this is the natural language to understand this relation, as shown by the simplicity of the proof. One can of course argue that, because the matrix-tree theorem is two-fold, quantities which are expressed in terms of trees can be written as determinants of some matrices as well. As mentioned above, this is indeed true for the symmetric form factor of the charge or the current. For instance, (5.11) can be equivalently written as

$$F_s^Q(\theta_1, \dots, \theta_n) = \mathcal{L}(1|1) \sum_{j=1}^n q(\theta_j) \sum_{k=1}^n p'(\theta_k) \tag{5.20}$$

where $\mathcal{L}(1|1)$ is the principal minor, obtained by deleting the first row and column of the $n \times n$ matrix (5.4). One could try to derive (5.20), starting from (5.6) and (5.3) with pure matrix manipulation instead of using the matrix-tree theorem.

5.1.3 Conclusion

In this section, we provided a graph theoretic proof of the equations of state used in GHD in the case of relativistic integrable quantum field theories without bound states. The proof applies to purely elastic scattering theories with one or multiple types of particles for which the corresponding LeClair-Mussardo formulae are known. Having the proofs for those cases, an obvious question would be if our approach can be applicable for theories where bound states and/or particles with internal degrees of freedom are present, such as the sine-Gordon model. This would be possible once we are able to extend the notion of connected form factor, or equivalently the LeClair-Mussardo formula for such theories.

We exemplified the graph theoretic idea using relativistic integrable quantum field theories, but it also works for the nonrelativistic case, such as the Lieb-Liniger model, through taking appropriate non-relativistic limits [215]. Extension to integrable spin chains can be found in [67].

5.2 Full counting statistics

After having the average current of the non-equilibrium state, one can go further and ask whether it is possible to obtain the probabilities of rare events with significant deflection from this mean value? In the large deviation theory [216], these probabilities are encoded in a rate function the Legendre transform of which is the generating function (also called the *full counting statistics*) of the scaled cumulants

$$\lim_{t \rightarrow \infty} \frac{1}{t} \int_0^t dt_1 \dots \int_0^t dt_n \langle J_1(0, t_1) \dots J_n(0, t_n) \rangle^c. \quad (5.21)$$

A functional equation satisfied by the full counting statistics was obtained in [68] using linear fluctuating hydrodynamics. Although the individual cumulants can be in principal extracted from this equation, their expressions quickly become cumbersome as n grows larger. We conjecture that these cumulants are simply given by the same diagrams that represent the cumulants of conserved charges, with only two modifications: the operator at the root is the energy derivative E' (instead of the momentum derivative) and each internal vertex θ of odd degree carries an extra sign of the effective velocity $\text{sign}[v^{\text{eff}}(\theta)]$. We confirm our conjecture by a non-trivial matching with the result of [69] up to the fourth cumulant.

This section is structured as follows: in the first part we remind how the second cumulant was derived in [217] using hydrodynamics approximation. The derivation in [68, 69] of higher cumulants is beyond the scope of this thesis. In the second part we compare our diagrammatic proposal with the known analytic expressions of [68]. In the third part we present several directions in which the conjecture could possibly be proven. Finally we discuss the impacts of this conjecture on other transport properties of GHD.

5.2.1 Hydrodynamics approximation

The second cumulant or the covariance matrix was first studied in [217] and named the *Drude self-weight*

$$D_{ij}^s \equiv \lim_{t \rightarrow \infty} \int_0^t ds \langle J_i(0, s) J_j(0, 0) \rangle^c. \quad (5.22)$$

The name comes from its resemblance with the conventional Drude weight, a quantity that if is non-vanishing, signals a dissipationless transport in the system

$$D_{ij} \equiv \lim_{t \rightarrow \infty} \int dx \langle J_i(x, t) J_j(0, 0) \rangle^c. \quad (5.23)$$

There are two ingredients in the derivation of the Drude self-weight in [217]. The first is a sum rule that expresses the Drude self-weight in terms of the charge-charge correlation function

$$D_{ij}^s = \int dx |x| \frac{1}{2} [\langle Q_i(x, t) Q_j(0, 0) \rangle^c + \langle Q_j(x, t) Q_i(0, 0) \rangle^c]. \quad (5.24)$$

For a proof of this identity and similar identities, see [218]. The second ingredient is the large distance limit of this correlator. To obtain this limit, we first note that the charge-charge correlation function $S_{ij}(x, t) \equiv \langle Q_i(x, t) Q_j(0, 0) \rangle^c$ satisfies, as a consequence of the Euler hydrodynamic equations (1.148)

$$\partial_t S_{ij}(x, t) + \sum_k A_i^k(x, t) \partial_x S_{kj}(x, t) = 0, \quad (5.25)$$

with the initial condition $S_{ij}(x, 0) \propto C$, where A is the flux Jacobian matrix (1.126) and C is the static covariance matrix (1.121). Thus, in the hydrodynamic approximation, small k , large t , the Fourier transform of the charge-charge correlation function $S_{ij}(k, t) \equiv \int dx e^{ikx} S_{ij}(x, t)$ can be approximated by

$$S_{ij}(k, t) \approx (e^{iktA} C)_{ij} = \int \frac{d\theta}{2\pi} e^{ikt v^{\text{eff}}(\theta)} (p')^{\text{dr}}(\theta) f(\theta) [1 - f(\theta)] q_i^{\text{dr}}(\theta) q_j^{\text{dr}}(\theta). \quad (5.26)$$

Replacing this into the sum rule (5.24) we obtain the Drude self-weight

$$D_{ij}^s = \int \frac{d\theta}{2\pi} (E')^{\text{dr}}(\theta) s(\theta) f(\theta) [1 - f(\theta)] q_i^{\text{dr}}(\theta) q_j^{\text{dr}}(\theta), \quad (5.27)$$

where we have denoted for short $s(\theta) = \text{sign}[v^{\text{eff}}(\theta)]$.

In [68, 69] all the diagonal cumulants were studied at once by mean of their generating function

$$F(\lambda) = \sum_{n=1}^{\infty} \frac{\lambda^n}{n!} c_n \quad \text{with} \quad c_n = \lim_{t \rightarrow \infty} \frac{1}{t} \int_0^t dt_1 \dots \int_0^t dt_n \langle J(0, t_1) \dots J(0, t_n) \rangle^c. \quad (5.28)$$

A functional equation satisfied by this function has been found by fluctuations from Euler-scale hydrodynamics. From this equation one can derive an explicit expression for each cumulant c_n for any value of n . Nevertheless, such derivation requires special manipulation for each case. It seems possible however that the individual cumulants can be derived from the same principle without considering the generating function, see the discussion at the end of this section. In the following we present the result of [68] for $c_{2,3,4}$ and show that they possess the same combinatorial structure as the cumulants of the corresponding conserved charges.

The authors of [69] also considered a generating function with different variables. Establishing a functional equation for such function would lead to non-diagonal cumulants. It would be interesting to see if this approach is in agreement with our conjecture.

5.2.2 Comparison with diagrams

Let us first remind how the cumulants of conserved charges can be written as a sum over tree diagrams. In section 2.2 we shown that the n^{th} cumulant $\langle \mathcal{Q}_1 \dots \mathcal{Q}_n \rangle^c$ is given by a sum over all tree-diagrams with $n + 1$ external vertices : a root with momentum derivative inserted and n leaves carrying the n conserved charges. The internal vertices of these diagrams live in phase space and will be integrated over. An external propagator connecting an internal vertex θ and an external vertex with an operator ψ is assigned a weight $\psi^{\text{dr}}(\theta)$, here ψ can either be the momentum derivative or the charges. An internal propagator connecting two internal vertices θ, η has a weight $K^{\text{dr}}(\theta, \eta)$, where

$$K^{\text{dr}}(u, v) = K(u, v) + \int \frac{dw}{2\pi} K(u, w) f(w) K^{\text{dr}}(w, v). \quad (5.29)$$

An internal vertex θ of degrees d has a weight

$$\sum_{r \geq 1} (-1)^{r-1} r^{d-1} Y^r(\theta). \quad (5.30)$$

We summarize these rules in the following

$$\begin{aligned} \theta \bullet \text{---} \odot \psi &= \psi^{\text{dr}}(\theta) \\ \theta \bullet \text{---} \bullet \eta &= K^{\text{dr}}(\theta, \eta) \\ \theta \bullet \text{---} \begin{array}{c} \diagup \\ \diagdown \end{array} &= \sum_{r \geq 1} (-1)^{r-1} r^{d-1} Y^r(\theta) \end{aligned} \quad (5.31)$$

We now show that the result of [68] is correctly reproduced by our diagrams with the above mentioned modifications.

The Drude self-weight is given by (5.27) and can be represented as the diagram in figure 5.4 with energy derivative at its root and the sign of the effective velocity at its internal vertex (of degree 3).

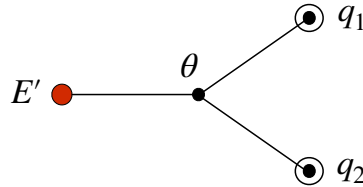


Figure 5.4: The only tree with two leaves

The third cumulant was found to be

$$\begin{aligned} c_3 = \int \frac{d\theta}{2\pi} (E')^{\text{dr}}(\theta) f(\theta) [1 - f(\theta)] s(\theta) q^{\text{dr}}(\theta) \times \\ \times \{ [1 - 2f(\theta)] [q^{\text{dr}}(\theta)]^2 s(\theta) + 3 [(q^{\text{dr}})^2 (1 - f)s]^{\text{dr}}(\theta) \}, \end{aligned} \quad (5.32)$$

where the star-dressing operator is defined as

$$\psi^{*\text{dr}}(\theta) \equiv \psi^{\text{dr}}(\theta) - \psi(\theta). \quad (5.33)$$

The first term of (5.32) is given by the left diagram in figure 5.5, again with energy derivative at the root. The internal vertex of this diagram is of degree 4 so there is no sign of the effective velocity. The second term is given by diagram on the right which comes with a symmetry factor of 3. The internal vertices are both of degrees 3 so each comes with a sign of the effective velocity. The matching is easily seen with the following writing of the star dressing operator in terms of the dressed propagator (2.29)

$$\psi^{*\text{dr}}(\theta) = \int \frac{d\eta}{2\pi} K^{\text{dr}}(\eta, \theta) f(\eta) \psi(\eta). \quad (5.34)$$

This identity also reveals the physical picture behind our diagrams: the integration over internal vertices is nothing but the contribution from virtual particles that carry anomalous corrections to the bare charges. The fourth cumulant is considerably more complicated and constitutes a

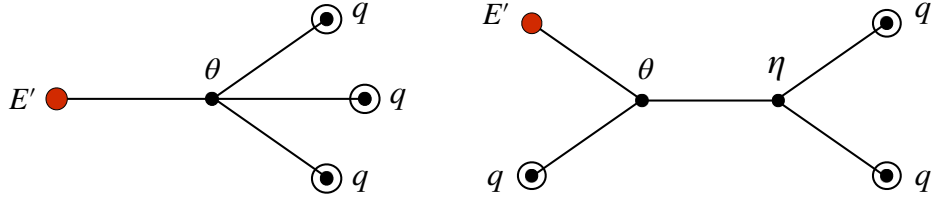


Figure 5.5: Two trees with three leaves

highly non-trivial check for our conjecture. The original formula of c_4 as it was derived in [68] is

$$\begin{aligned} c_4 = & \int \frac{d\theta}{2\pi} (E')^{\text{dr}}(\theta) f(\theta) [1 - f(\theta)] \times \left\{ \frac{Y(\theta)^2 + 6Y(\theta) + 6}{[Y(\theta) + 1]^2} s(\theta) [q^{\text{dr}}(\theta)]^4 \right. \\ & + 3s(\theta) \{[(1 - f)s(q^{\text{dr}})^2]^{\text{dr}}(\theta)\}^2 + 12s(\theta) q^{\text{dr}}(\theta) \{(1 - f)sq^{\text{dr}}[(1 - f)s(q^{\text{dr}})^2]^{\text{dr}}\}^{\text{dr}}(\theta) \\ & \left. + 6[f(\theta) - 2][q^{\text{dr}}(\theta)]^2 [s(1 - f)(q^{\text{dr}})^2]^{\text{dr}}(\theta) + 4s(\theta) q^{\text{dr}}(\theta) [(1 - f)(f - 2)(q^{\text{dr}})^3]^{\text{dr}}(\theta) \right\}. \quad (5.35) \end{aligned}$$

For convenience, we show in figure 5.6 all diagrams with four leaves.

Due to the identity (5.34), our trees are naturally expressed in terms of the star dressing operation. In order to compare them with (5.35), we repeatedly use the definition (5.33) to make appear the dressing operation. We then show that the discrepancies cancel each other. The integration variable θ in the formula (5.35) corresponds to the coordinate of the internal vertex closest to the root of each tree. These vertices are always of degree at least 3, therefore we can factorize a factor $f(\theta)[1 - f(\theta)]$ from their weights. After this factorization, the contribution from the trees are (we omit the dependence on θ)

- Tree (a)

$$\frac{Y^2 - 4Y + 1}{(Y + 1)^2} s(q^{\text{dr}})^4 = \frac{Y^2 + 6Y + 6}{(Y + 1)^2} s(q^{\text{dr}})^4 - 5(1 - f^2)s(q^{\text{dr}})^4$$

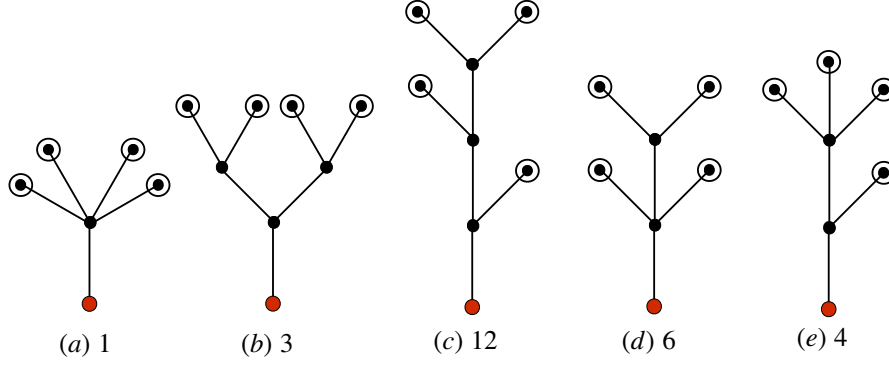


Figure 5.6: Trees with four leaves along with their symmetry factors

- Tree (b)

$$3s\{[(1-f)s(o^{\text{dr}})^2]^{\ast\text{dr}}\}^2 = 3s\{[(1-f)s(o^{\text{dr}})^2]^{\text{dr}}\}^2 \\ + 3s(1-f)^2(o^{\text{dr}})^4 - 6(1-f)(o^{\text{dr}})^2[(1-f)s(o^{\text{dr}})^2]^{\text{dr}}$$

- Tree (c)

$$12sq^{\text{dr}}\{(1-f)sq^{\text{dr}}[(1-f)s(q^{\text{dr}})^2]^{\ast\text{dr}}\}^{\ast\text{dr}} = 12sq^{\text{dr}}\{(1-f)sq^{\text{dr}}[(1-f)s(q^{\text{dr}})^2]^{\text{dr}}\}^{\text{dr}} \\ - 12(1-f)(q^{\text{dr}})^2[(1-f)s(q^{\text{dr}})^2]^{\text{dr}} - 12sq^{\text{dr}}[(1-f)^2(q^{\text{dr}})^3]^{\text{dr}} + 12(1-f)^2s(q^{\text{dr}})^4$$

- Tree (d)

$$6(1-2f)(q^{\text{dr}})^2[(1-f)s(q^{\text{dr}})^2]^{\ast\text{dr}} = 6(f-2)(q^{\text{dr}})^2[(1-f)s(q^{\text{dr}})^2]^{\text{dr}} \\ - 6s(f-2)(1-f)(q^{\text{dr}})^4 + 18(1-f)(q^{\text{dr}})^2[(1-f)s(q^{\text{dr}})^2]^{\text{dr}} - 18s(1-f)^2(q^{\text{dr}})^4$$

- Tree (e)

$$4sq^{\text{dr}}[(1-f)(1-2f)(q^{\text{dr}})^3]^{\ast\text{dr}} = 4sq^{\text{dr}}[(1-f)(f-2)(q^{\text{dr}})^3]^{\text{dr}} \\ - 4s(q^{\text{dr}})^4(1-f)(f-2) - 12s(q^{\text{dr}})^4(1-f)^2 + 12sq^{\text{dr}}[(1-f)^2(q^{\text{dr}})^3]^{\text{dr}}$$

The discrepancies indeed cancel each other.

5.2.3 Comments on the conjecture

There are two plausible ways to prove our conjecture.

First, one can try to derive the matrix elements of the product of total currents. One can then repeat the same steps of section 2 to perform their summation. The correct matrix elements must guarantee that the resulting diagrams have energy derivative at their root and sign of the effective velocity at their odd internal vertices. Concerning these two properties, the former is expected while the latter is more puzzling. Let us elaborate on this point.

In our proof of the current average, it was understood that the form factor of a current is very similar to that of the corresponding charge: both are given by trees, the only difference

being the operator at the root. It is then natural that any average involving currents, if admits combinatorial structure of trees, would have the energy derivative at the roots.

As for the sign of the effective velocity, a naive guess would be to assign such sign for each bare propagator and for each external vertex. Most of them will cancel each other except for internal vertices of odd degrees. The flaw in this argument is that the weights of graph components should involve only bare quantities, like the ones in (2.15). Only after the graphs are summed over do we have renormalized (dressed) quantities, see (2.30). The effective velocity is a dressed quantity and as such cannot be included in the weight of bare propagators. In most cases however, the sign of the effective velocity coincides with that of the rapidity and the above modification could in principle be implemented.

Second, one can regard the combinatorial structure of the charge cumulants as a result of successive derivatives on the free energy (1.129). Simply speaking these derivatives generate branches and joints (internal vertices) of the trees. If one can prove the existence of a similar "free energy" whose derivatives lead to cumulants of the total transport, it is natural that the same combinatorial structure would arise. Such free energy should not be confused with the generating function (5.28): what we seek for is the derivative with respect to the GGE chemical potentials, not the auxiliary variable λ .

This approach seems possible in view of the following identity, proven in [69]

$$\int_0^t ds \langle J_i(0, s) \mathcal{O}(0, 0) \rangle^c = - \sum_j \text{sign}(A)_{ij} \frac{\partial}{\partial \beta_j} \langle \mathcal{O}(0, 0) \rangle \quad (5.36)$$

for any local observable \mathcal{O} . Here A is the flux Jacobian matrix, and the sign is defined as the sign matrix of its eigenvalues. If one can show that this identity is still valid when the local operator \mathcal{O} is replaced by the product of the total currents then one would be able to obtain their cumulants from successive derivatives of the current average.

5.2.4 Summary and outlook

Our systematic treatment not only reduces the computational complexity but also improves the conceptual understanding of these cumulants. First, the simple combinatorial structure of the cumulants of total currents potentially translates into an analytic property of the full counting statistics. It is interesting to find a new relation in addition to the one established in [68]. Second, such structure provides hints about what the corresponding matrix elements would look like. For the current average, this line of idea has been exploited in recent work [67]. Explicit expressions of these matrix elements would have significant impact on the understanding of related quantities, for instance the Drude weight. Last but not least, the observed similarity between the two families of cumulants suggests that one could think of a "free energy" that generates the time integrated currents in the same fashion that the usual TBA free energy generates the conserved charges.

In future work, we would like to see the extend of this combinatorial structure in dynamical correlation functions and related quantities. The study of large scale correlation functions in GHD has been addressed in [219]. For the charge-charge and charge-current correlation functions, the same combinatorial structure continues to hold, with the inclusion of a space-time propagator. The situation is more subtle for the current-current correlator and the Drude

weight. These quantities involve the inverse of a dressed quantity and it is currently not clear how such inversion could be represented in our formalism.

Conclusion

In this thesis we propose a new method to compute thermodynamic observables in integrable systems. The main idea is to use the matrix-tree theorem to express the Gaudin determinants as a sum over graphs. We have found two types of applications of this graph expansion.

First, it can be used to directly evaluate the cluster expansion of thermodynamic quantities. In this context, the Gaudin determinant appears as the Jacobian of the change of variables from mode numbers to rapidities. This change of variables is the only approximation in our formalism and it is exact to all orders of powers in inverse volume. The new method is thus more powerful than the standard TBA, which is insensitive to all corrections of order 1 and lower. We have applied it for a wide class of observable in theories with a diagonal S-matrix, confirming its versatility. There are however situations where it cannot be implemented. First, when a complete set of states is not known or is complicated. This happens for theories with a non-diagonal S-matrix and the standard TBA is more adapted to this situation as it only requires information about states that contribute to the thermodynamic limit. Nevertheless it is possible to interpret known TBA equations with strings in terms of diagrams. We have used this interpretation to study the boundary entropy of the corresponding theory and although we have not obtained a complete answer we have made several important observations. Second, when the action of the observable on unphysical states can not be determined. These unphysical states are inserted into the cluster expansion to compensate the strict order between mode numbers. For the observables that we have considered, the action on these states is a natural generalization of the action on physical states. For more involved examples however, this task might not be straightforward or even impossible. Last but not least, there could be exotic Gaudin determinants for which a graph expansion is not known.

The second type of applications is to use the diagrammatic representation to replace the algebraic manipulations of the Gaudin determinants. We have used this idea to derive the equations of state in GHD however we cannot make a general conclusion of when the diagrammatic representation is more useful than normal calculations.

There are several directions to explore with the new method

- Looking for situations where corrections of order $1/L$ or lower are needed. If the new method can be implemented in this case, its advantage over the standard TBA would be truly confirmed.
- Computing finite size corrections in the hexagon form factor approach. There might be simple setups where the form factors can be organized in a nice way and the exact summation can be carried out.
- Interpreting known quantities in terms of diagrams and finding the connection between quantities with similar diagrammatic structure.
- Obtaining finite-particle matrix elements and form factors from the thermodynamic expression by applying the steps in reverse.

- Explaining the origin of Gaudin determinants in spin chain scalar products [157]. One could for instance investigate the formation of trees in the algebra between the elements of the transfer matrix in the algebraic Bethe ansatz approach.
- Computing two point functions or one point function in open systems where the cluster expansion is sufficiently simple to be evaluated.
- Using the matrix elements of the current to derive other transport properties in GHD. These matrix elements can be obtained from the corresponding form factors and they also have a diagrammatic representation [67].
- Studying the graph expansion of other types of Gaudin determinant. It would be interesting to find an unconventional Gaudin determinant for which the graph expansion is not yet known in the mathematical literature.

Appendices

Appendix A

TBA and Y system

A.1 Chiral SU(2) Gross-Neveu model

The Bethe equations for a state of N physical rapidities $\theta_1, \dots, \theta_N$ and M magnonic rapidities u_1, \dots, u_M read

$$1 = e^{ip(\theta_j)L} \prod_{k \neq j}^N S_0(\theta_j - \theta_k) \prod_{m=1}^M \frac{\theta_j - u_m + i\pi/2}{\theta_j - u_m - i\pi/2}$$

$$1 = \prod_{j=1}^N \frac{u_k - \theta_j - i\pi/2}{u_k - \theta_j + i\pi/2} \prod_{l \neq k}^M \frac{u_k - u_l + i\pi}{u_k - u_l - i\pi}$$

String solutions are formed of magnon rapidities equally spaced in distance of i . Let $u_{k,n}$ be the real center of a string of length n then the ensemble of string rapidities are given by

$$u_{k,n}^a = u_{k,n} - i\pi \frac{n+1}{2} + i\pi a, \quad a = 1, \dots, n$$

The scattering phase between strings (and physical node) is the product between the scattering phases of their constituents

$$S_{0n}(\theta, u_{k,n}) = \frac{\theta - u_{k,n} + i\pi n/2}{\theta - u_{k,n} - i\pi n/2},$$

$$S_{nm}(u_{k,n}, u_{l,m}) = \frac{u_{k,n} - u_{l,m} + i\pi \frac{|n-m|}{2}}{u_{k,n} - u_{l,m} - i\pi \frac{|n-m|}{2}} \frac{u_{k,n} - u_{l,m} + i\pi \frac{n+m}{2}}{u_{k,n} - u_{l,m} - i\pi \frac{n+m}{2}} \prod_{s=\frac{|n-m|}{2}+1}^{\frac{n+m}{2}-1} \left[\frac{u_{k,n} - u_{l,m} + i\pi s}{u_{k,n} - u_{l,m} - i\pi s} \right]^2.$$

The corresponding scattering kernels are

$$K_{0n}(\theta - u) = -K_{n,0}(\theta - u) = -\frac{4\pi n}{4(\theta - u)^2 + \pi^2 n^2}, \quad (\text{A.1})$$

$$K_{nm}(u) = K_{m,n}(u) = (1 - \delta_{nm})K_{0,|n-m|}(u) + K_{0,n+m}(u) + 2 \sum_{s=\frac{|n-m|}{2}+1}^{\frac{n+m}{2}-1} K_{0,2s}(u). \quad (\text{A.2})$$

Their Fourier transforms are simple

$$\hat{K}_{0n}(w) = -\hat{K}_{n0}(w) = -e^{-\pi n|w|/2} \quad (\text{A.3})$$

$$\hat{K}_{nm}(w) = \delta_{nm} + (e^{\pi|w|} + 1) \frac{e^{-(n+m)\pi|w|/2} - e^{-|n-m|\pi|w|/2}}{e^{\pi|w|} - 1} \quad (\text{A.4})$$

Here we normalize the Fourier transformation as

$$\hat{f}(w) = \frac{1}{2\pi} \int_{-\infty}^{+\infty} f(t) e^{iwt} dt.$$

For the physical-physical scattering

$$K_{00}(\theta) = \frac{1}{\pi} \sum_{l=0}^{\infty} -\frac{l+1}{(l+1)^2 + \theta^2/4\pi^2} + \frac{l+1/2}{(l+1/2)^2 + \theta^2/4\pi^2} \Rightarrow \hat{K}_{00}(w) = \frac{e^{-\pi|w|/2}}{2 \cosh(\pi w/2)} \quad (\text{A.5})$$

The above kernels control the TBA equations

$$Y_n(u) = e^{-\delta_{0n} RE(\theta)} \exp \left[\sum_{m \geq 0} K_{m,n} \star \log(1 + Y_m)(u) \right]. \quad (\text{A.6})$$

By defining $\mathcal{Y}_n = Y_n^{-1}$ for $n \geq 1$ and $\mathcal{Y}_0 = Y_0$ we can transform this to the Y-system

$$\log \mathcal{Y}_n + \delta_{n0} RE = \sum_{m=0}^{\infty} I_{mn} s \star \log(1 + \mathcal{Y}_m). \quad (\text{A.7})$$

where the kernel s has the following Fourier transform

$$\hat{s}(w) = \frac{1}{2 \cosh(\pi w/2)}. \quad (\text{A.8})$$

To prove that (A.6) leads to (A.7) we first act by $-s$ to the TBA equation of Y_1

$$\log Y_1 = K_{01} \star \log(1 + Y_0) + K_{11} \star \log(1 + Y_1) + \sum_{n \geq 2} K_{n1} \star \log(1 + Y_n). \quad (\text{A.9})$$

With help of the following identities

$$-s \star K_{01} = K_{00}, \quad -s \star K_{11} = K_{1,0} - s, \quad s \star K_{n1} = K_{0n}, \quad n \geq 2.$$

We can write (A.9) as

$$\log Y_0 + RE = s \star \log(1 + \frac{1}{Y_1})$$

which is the first equation of Y system. Next, we act s to the TBA equation of Y_2

$$\log Y_2 = K_{02} \star \log(1 + Y_0) + K_{12} \star \log(1 + Y_1) + K_{22} \star \log(1 + Y_2) + \sum_{n \geq 3} K_{n2} \star \log(1 + Y_n).$$

this time we need the following identities

$$s \star K_{02} = K_{01} + s, \quad s \star K_{12} = K_{11}, \quad s \star K_{22} = K_{21} + s, \quad s \star K_{n2} = K_{n1}, \quad n \geq 3.$$

From which we have

$$\log \mathcal{Y}_1 = s \star \log(1 + Y_0) + s \star \log(1 + \mathcal{Y}_2).$$

For $n \geq 2$ we can show from the average property $s \star (K_{0,n-1} + K_{0,n+1}) = K_{0n}$ that

$$s \star \log Y_{n+1} + s \star \log Y_{n-1} = \log Y_n + s \star \log(1 + Y_{n+1}) + s \star \log(1 + Y_{n-1}).$$

A.2 Higher levels

A.2.1 The scattering and the kernels

The scalar factors and their exponential form [200]

$$S_0^{SU(2)}(\theta) = -\frac{\Gamma(1 - \theta/2\pi i) \Gamma(1/2 + \theta/2\pi i)}{\Gamma(1 + \theta/2\pi i) \Gamma(1/2 - \theta/2\pi i)},$$

$$S_0^{[k]}(\theta) = \exp \left[\int_{-\infty}^{+\infty} \frac{dx}{x} e^{2i\theta x/\pi} \frac{\sinh[(k+1)x] \sinh x}{\sinh[(k+2)x] \sinh(2x)} \right].$$

The Bethe equations involving N physical rapidities θ , M $SU(2)$ magnon rapidities u and P kink magnon rapidities v

$$e^{-ip(\theta_j)L} = -\epsilon_j \prod_{i=1}^N S_0^{SU(2)}(\theta_j, \theta_i) S_0^{[k]}(\theta_j, \theta_i) \prod_{k=1}^M \frac{\theta_j - u_k + i\pi/2}{\theta_j - u_k - i\pi/2} \prod_{q=1}^P \frac{\sinh \frac{\theta_j - v_q + i\pi/2}{k+2}}{\sinh \frac{\theta_j - v_q - i\pi/2}{k+2}},$$

$$\prod_{j=1}^N \frac{u_k - \theta_j + i\pi/2}{u_k - \theta_j - i\pi/2} = \Omega_k \prod_{l=1}^M \frac{u_k - u_l + i\pi}{u_k - u_l - i\pi},$$

$$\prod_{j=1}^N \frac{\sinh \frac{v_q - \theta_j + i\pi/2}{k+2}}{\sinh \frac{v_q - \theta_j - i\pi/2}{k+2}} = \Omega_q \prod_{p=1}^P \frac{\sinh \frac{v_q - v_p + i\pi}{k+2}}{\sinh \frac{v_q - v_p - i\pi}{k+2}}.$$

with some constants $\epsilon_j, \Omega_k, \Omega_q$. String solutions

$$\begin{aligned} \text{u strings of length } n = \overline{1, \infty}: \quad u_{k,n}^a &= u_{k,n} - i\pi \frac{n+1}{2} + i\pi a, \quad a = 1, \dots, n \\ \text{v strings of length } m = \overline{1, k}: \quad v_{q,m}^b &= v_{q,m} - i\pi \frac{m+1}{2} + i\pi b, \quad b = 1, \dots, m \end{aligned}$$

The scatterings between $SU(2)$ strings with themselves and between them and the physical rapidity are the same as before. For kink magnon strings

$$S_{0n}^{[k]}(\theta, v_{q,n}) = \frac{\{\theta - v_{q,n} + i\pi m/2\}_k}{\{\theta - v_{q,n} - i\pi m/2\}_k}$$

$$S_{nm}^{[k]}(v_{q,n}, v_{p,m}) = \frac{\{v_{q,n} - v_{p,m} + i\pi \frac{|n-m|}{2}\}_k \{v_{q,n} - v_{p,m} + i\pi \frac{n+m}{2}\}_k}{\{v_{q,n} - v_{p,m} - i\pi \frac{|n-m|}{2}\}_k \{v_{q,n} - v_{p,m} - i\pi \frac{n+m}{2}\}_k} \prod_{s=\frac{|n-m|}{2}+1}^{\frac{n+m}{2}-1} \left[\frac{\{v_{q,n} - v_{p,m} + i\pi s\}_k}{\{v_{q,n} - v_{p,m} - i\pi s\}_k} \right]^2$$

where we have noted for convenience

$$\{u\}_k = \sinh \frac{u}{k+2}.$$

The Fourier transforms of the kink magnon strings scattering kernel

$$\hat{K}_{0n}^{[k]}(w) = -\frac{\sinh[(k+2-n)\frac{\pi w}{2}]}{\sinh(k+2)\frac{\pi w}{2}},$$

$$\hat{K}_{nm}^{[k]}(w) = \delta_{nm} - 2\frac{\sinh[\min(n,m)\frac{\pi w}{2}]\sinh[(k+2-\max(n,m))\frac{\pi w}{2}]\cosh\frac{\pi w}{2}}{\sinh[(k+2)\frac{\pi w}{2}]\sinh\frac{\pi w}{2}}.$$

A.2.2 Maximal string reduction and reduced TBA

At this point we have the raw TBA equations

$$\log Y_{\tilde{n}} = \sum_{m=0}^k K_{mn}^{[k]} \star \log(1 + Y_{\tilde{m}}), \quad n = \overline{1, k},$$

$$\log Y_0 + RE = \sum_{n=0}^k K_{n0}^{[k]} \log(1 + Y_{\tilde{n}}) + \sum_{n=1}^{\infty} K_{n0}^{\text{SU}(2)} \log(1 + Y_n),$$

$$\log(1 + Y_n) = \sum_{m=0}^{\infty} K_{mn} \star \log(1 + Y_m), \quad n = \overline{1, \infty}.$$

where we have used the tilde indices to denote kink rapidities, also $\tilde{0} = 0$.



Maximal string reduction [200]: u string of length k doesn't contribute in the thermodynamic limit. The \tilde{k} string is frozen in the sense that $Y_{\tilde{k}} = \infty$. We look at the TBA equation for this string

$$\log Y_{\tilde{k}} = \sum_{m=0}^k K_{mk}^{[k]} \star \log(1 + Y_{\tilde{m}}).$$

Upon replacing $\log Y_{\tilde{k}}$ by $\log(1 + Y_{\tilde{k}})$, we can effectively remove the \tilde{k} node from our TBA system

$$\log(1 + Y_{\tilde{k}}) = \sum_{m=0}^{k-1} (1 - K_{kk}^{[k]})^{-1} \star K_{mk}^{[k]} \star \log(1 + Y_{\tilde{m}}).$$

The reduced system (only the kink magnon related part) read

$$\log Y_{\tilde{n}} = \sum_{m=0}^{k-1} \left[K_{kn}^{[k]} \star (1 - K_{kk}^{[k]})^{-1} \star K_{mk}^{[k]} + K_{mn}^{[k]} \right] \star \log(1 + Y_{\tilde{m}}), \quad n = \overline{1, k-1}$$

$$\log Y_0 + RE = \sum_{n=0}^{k-1} \left[K_{k0}^{[k]} \star (1 - K_{kk}^{[k]})^{-1} \star K_{nk}^{[k]} + K_{n,0}^{[k]} \right] \star \log(1 + Y_{\tilde{n}}) + \dots$$

The following identity drastically simplifies this system

$$K_{kn}^{[k]} \star (1 - K_{kk}^{[k]})^{-1} \star K_{mk}^{[k]} + K_{mn}^{[k]} = K_{mn}^{[k-2]}, \quad m, n = \overline{0, k-1}. \quad (\text{A.10})$$

To summarize, the reduced TBA system for integrable perturbed $SU(2)_k$ is

$$\log Y_n + \delta_{n,k} RE = \sum_{m,n} K_{mn} \star \log(1 + Y_m), \quad n = \overline{1, \infty}$$

where

$$\begin{aligned} \hat{K}_{kn}(w) &= -\hat{K}_{nk}(w) = -\frac{\sinh n \frac{\pi w}{2}}{\sinh k \frac{\pi w}{2}}, \quad n = \overline{1, k-1} \\ \hat{K}_{nm}(w) &= \delta_{nm} - 2 \frac{\sinh \left[\min(n, m) \frac{\pi w}{2} \right] \sinh \left[(k - \max(n, m)) \frac{\pi w}{2} \right] \cosh \frac{\pi w}{2}}{\sinh \left[k \frac{\pi w}{2} \right] \sinh \frac{\pi w}{2}}, \quad n, m = \overline{1, k-1} \\ \hat{K}_{kk}(w) &= \frac{\sinh \frac{\pi w}{2}}{\sinh \pi w} \left(1 + \frac{\sinh \left[(k-1) \frac{\pi w}{2} \right]}{\sinh \left[k \frac{\pi w}{2} \right]} \right) \\ \hat{K}_{kn} &= -\hat{K}_{n,k} = -e^{-(n-k)\pi|w|/2}, \quad n = \overline{k+1, \infty} \\ \hat{K}_{nm}(w) &= \delta_{nm} + (e^{\pi|w|} + 1) \frac{e^{-(n+m-2k)\pi|w|/2} - e^{|n-m|\pi|w|/2}}{e^{\pi|w|} - 1}, \quad n, m = \overline{k+1, \infty} \end{aligned}$$



Figure A.1: Maximum string removed and indices rearranged

A.2.3 Y system

To transform this into the Y system, we notice that the universal kernel s still satisfies the average property for the newly introduced hyperbolic kernels

$$\hat{s}(\hat{K}_{k,n-1} + \hat{K}_{k,n+1}) = \hat{K}_{kn}, \quad n = \overline{1, k-1}.$$

As a result, deep in the left or right wing, there would be no problem. We just need to check for the three nodes $k-1, k, k+1$. We act with $-s$ on the TBA equations of $k \pm 1$

$$\begin{aligned} \log Y_{k-1} &= \sum_{n=1}^{k-2} K_{n,k-1} \star \log(1 + Y_n) + K_{k-1,k-1} \star \log(1 + Y_{k-1}) + K_{k,k-1} \star \log(1 + Y_k), \\ \log Y_{k+1} &= \sum_{n=k+2}^{\infty} K_{n,k+1} \star \log(1 + Y_n) + K_{k+1,k+1} \star \log(1 + Y_{k+1}) + K_{k,k+1} \star \log(1 + Y_k). \end{aligned}$$

We need the following identities

$$\begin{aligned} -s \star K_{n,k-1} &= K_{nk}, \quad n \in \overline{1, k-2}, \quad -s \star K_{n,k+1} = K_{nk}, \quad n \in \overline{k+2, \infty}, \\ -s \star K_{k-1,k-1} &= K_{k-1,k} - s, \quad -s \star K_{k+1,k+1} = K_{k+1,k} - s, \quad -s \star K_{k,k-1} - s \star K_{k,k+1} = K_{kk}. \end{aligned}$$

Then it follows that

$$\begin{aligned} -s \star \log Y_{k-1} - s \star \log Y_{k+1} &= \log Y_k - s \star \log(1 + Y_{k-1}) - s \star \log(1 + Y_{k+1}), \\ \Leftrightarrow \log Y_k &= s \star \log(1 + \mathcal{Y}_{k-1}) + s \star (1 + \mathcal{Y}_{k+1}). \end{aligned}$$

The right wing is coupled to the physical node in the same way as Gross-Neveu. For the left wing, we act with s to the TBA equation of Y_{k-2}

$$\begin{aligned} \log Y_{k-2} &= K_{k,k-2} \star \log(1 + Y_k) + K_{k-1,k-2} \star \log(1 + Y_{k-1}) + K_{k-2,k-2} \star \log(1 + Y_{k-2}) \\ &\quad + \sum_{n=1}^{k-3} K_{n,k-2} \star \log(1 + Y_n). \end{aligned}$$

With help of the following identities

$$\begin{aligned} s \star K_{n,k-2} &= K_{n,k-1}, \quad n = \overline{1, k-3}, \quad s \star K_{k,k-2} = s + K_{k,k-1}, \\ s \star K_{k-1,k-2} &= K_{k-1,k-1}, \quad s \star K_{k-2,k-2} = s + K_{k-2,k-1}. \end{aligned}$$

We obtain

$$\begin{aligned} s \star \log Y_{k-2} &= s \star \log(1 + Y_k) + s \star \log(1 + Y_{k-2}) + \log Y_{k-1} \\ \Leftrightarrow \log \mathcal{Y}_{k-1} &= s \star \log(1 + Y_k) + s \star \log(1 + \mathcal{Y}_{k-2}). \end{aligned}$$

Appendix B

Determinants

We compute the determinants that appear in the main text. We have found these results by Mathematica. For simplicity we introduce the following notation $K_{ab} \equiv \int_{-\infty}^{+\infty} d\theta K_{ab}(\theta)/(2\pi)$.

B.0.1 The IR determinant

We compute $\det(1 - \hat{K})$ where

$$\hat{K}_{ab} = K_{ab} \sqrt{\frac{Y_a^{\text{IR}}(\kappa)}{1 + Y_a^{\text{IR}}(\kappa)} \frac{Y_b^{\text{IR}}(\kappa)}{1 + Y_b^{\text{IR}}(\kappa)}} = [\delta_{ab} - 2 \min(a, b)] \frac{(1 - \kappa)^2 \sqrt{\kappa^a \kappa^b}}{(1 - \kappa^{a+1})(1 - \kappa^{b+1})}, \quad a, b \geq 1.$$

This matrix can be implemented directly in Mathematica and we get five digit precision for twist parameters smaller than 1/2 using the first 30 magnon strings.

$\kappa = 0.5$	$\kappa = 0.6$	$\kappa = 0.7$	$\kappa = 0.8$	$\kappa = 0.9$
0.5	0.400001	0.30008	0.202126	0.121998

Table B.1: Approximation of $[\det(1 - \hat{K})]^{-1}$ for some values of the twist parameter

As the twist parameter tends to 1, more strings are needed to keep the precision. We can read from this numerical data that

$$\det(1 - \hat{K}) = (1 - \kappa)^{-1}. \quad (\text{B.1})$$

This gives the loop part of IR g-function (4.35). There is a more elegant way to obtain this result. We remark that the matrix \hat{K} can be written in a slightly different way without changing the determinant of $1 - \hat{K}$

$$\hat{K}_{ab} = [\delta_{ab} - 2 \min(a, b)] \frac{Y_b^{\text{IR}}(\kappa)}{1 + Y_b^{\text{IR}}(\kappa)}, \quad a, b \geq 1.$$

By factorizing the second factor we can show that (B.1) is equivalent to

$$\frac{\det[2Y^{\text{IR}}(\kappa) + \text{Cartan}_{\infty}^{\text{A}}]}{\det(\text{Cartan}_{\infty}^{\text{A}})} = \frac{1 + \kappa}{1 - \kappa}. \quad (\text{B.2})$$

From the usual method of computing the determinant of Cartan matrix of A type, we can reformulate the problem as follows. Let G_a be a sequence of numbers defined by the iterative relation

$$G_{a+1} + G_{a-1} = [2 + 2Y_a^{\text{IR}}(\kappa)]G_a, \quad G_0 = 0, G_1 = 1,$$

then

$$\lim_{a \rightarrow \infty} \frac{G_a}{a+1} = \frac{1+\kappa}{1-\kappa}. \quad (\text{B.3})$$

We owe this derivation to Romuald Janik. Unfortunately we can only verify numerically the asymptotic (B.3).

B.0.2 The UV determinant

We compute $\det(1 - \hat{K})$ where

$$\hat{K}_{ab} = K_{ab} \sqrt{\frac{Y_a^{\text{UV}}(\kappa) Y_b^{\text{UV}}(\kappa)}{[1 + Y_a^{\text{UV}}(\kappa)][1 + Y_b^{\text{UV}}(\kappa)]}},$$

with

$$K_{ab} = \delta_{ab} - 2 \frac{\min(a, b)[k - \max(a, b)]}{k}, \quad a, b \in \overline{1, k-1}, \quad K_{ab} = \delta_{ab} - 2 \min(a - k, b - k), \quad a, b \geq k+1$$

$$K_{ka} = -K_{ak} = -\frac{a}{k}, \quad 1 \leq a < k, \quad K_{kk} = 1 - \frac{1}{2k}, \quad K_{ka} = -K_{ak} = -1, \quad a \geq k+1$$

and

$$\frac{Y_a^{\text{UV}}(\kappa)}{1 + Y_a^{\text{UV}}(\kappa)} = \frac{a}{k} \frac{(1 - \kappa)^2}{(1 - \kappa^{a+1})^2} \quad a \in \overline{1, k-1} \cup \overline{k+1, \infty}, \quad \frac{Y_k^{\text{UV}}(\kappa)}{1 + Y_k^{\text{UV}}(\kappa)} = \frac{(1 - \kappa^k)(1 - \kappa^{k+2})}{(1 - \kappa^{k+1})^2}.$$

Again we choose a cut-off on $SU(2)$ magnon string length of 30. This gives five digit precision for values of the twist parameter smaller than 1/2.

	$\kappa = 0.5$	$\kappa = 0.6$	$\kappa = 0.7$	$\kappa = 0.8$	$\kappa = 0.9$
$k = 2$	2	1.6	1.20032	0.80851	0.487993
$k = 3$	3	2.40001	1.80048	1.21276	0.731989
$k = 4$	4	3.20001	2.40064	1.61701	0.975986
$k = 5$	5	4.00001	3.0008	2.02126	1.21998
$k = 6$	6	4.80001	3.60096	2.42552	1.46398
$k = 7$	7	5.60002	4.20112	2.82977	1.70797
$k = 8$	8	6.40002	4.80128	3.23402	1.95197
$k = 9$	9	7.20002	5.40144	3.63828	2.19597

Table B.2: Approximation of $[\det(1 - \hat{K})]^{-1}$ for some twist parameters and levels

We predict from this data that $\det(1 - \hat{K}) = [2k(1 - \kappa)]^{-1}$. This leads to the loop part of UV g-function (4.45).

Appendix C

Normal modes of hydrodynamics

In this appendix we derive the normal modes of Euler hydrodynamic equations. For the ease of following we repeat here the expressions we found for the hydrodynamic matrices

$$\sum_k A_i^j q_j^{\text{dr}}(\theta) = v^{\text{eff}}(\theta) q_i^{\text{dr}}(\theta), \quad (\text{C.1})$$

$$B_{ij} = \int d\theta v^{\text{eff}}(\theta) \rho_{\text{p}}(\theta) [1 - f(\theta)] q_i^{\text{dr}}(\theta) q_j^{\text{dr}}(\theta), \quad (\text{C.2})$$

$$C_{ij} = \int d\theta \rho_{\text{p}}(\theta) [1 - f(\theta)] q_i^{\text{dr}}(\theta) q_j^{\text{dr}}(\theta). \quad (\text{C.3})$$

The computation of the normal modes is simpler if we work with integral operators representing these matrices. These operators act on the space of functions of rapidity and are defined as follows

$$\sum_j A_i^j q_j(\theta) = (\mathcal{A}^t q_i)(\theta), \quad B_{ij} = q_i \cdot \mathcal{B} q_j, \quad C_{ij} = q_i \cdot \mathcal{C} q_j. \quad (\text{C.4})$$

The dressing operation (1.114) can also be expressed via an integral operator

$$\psi^{\text{dr}} = (1 - \mathcal{T} f)^{-1} \psi \quad \text{where} \quad (\mathcal{T} \psi)(\theta) \equiv \int \frac{d\eta}{2\pi} K(\theta - \eta) \psi(\eta). \quad (\text{C.5})$$

The transpose in the definition of \mathcal{A} allows the relation $B = AC$ among hydrodynamic matrices to transcend into the same relation among the corresponding integral operators

$$q_i \cdot \mathcal{B} q_j \equiv B_{ij} = A_i^k C_{kj} \equiv \mathcal{A}^t q_i \cdot \mathcal{C} q_j = q_i \cdot \mathcal{A} \mathcal{C} q_j.$$

Applying the dressing operation on the definition of \mathcal{A} we obtain $(\mathcal{A}^t q_i)^{\text{dr}}(\theta) = v^{\text{eff}}(\theta) q_i^{\text{dr}}(\theta)$, which means

$$\mathcal{A} = (1 - f \mathcal{T})^{-1} v^{\text{eff}} (1 - f \mathcal{T}) \quad (\text{C.6})$$

Other operators can be directly read off the expressions (C.2) and (C.3)

$$\mathcal{B} = (1 - f \mathcal{T})^{-1} v^{\text{eff}} \rho_{\text{p}} (1 - f) (1 - \mathcal{T} f)^{-1}, \quad \mathcal{C} = (1 - f \mathcal{T})^{-1} \rho_{\text{p}} (1 - f) (1 - \mathcal{T} f)^{-1}. \quad (\text{C.7})$$

To remind, the normal modes are defined in such a way that their Jacobian matrix with respect to average charge densities is given by the matrix that diagonalizes A

$$\partial n_i / \partial \mathcal{Q}_j = R_i^j \quad R A R^{-1} = v^{\text{eff}}.$$

It follows from the integral representation (C.6) that the the integral operator \mathcal{R} corresponding to the matrix R is given by $\mathcal{R} = 1 - f \mathcal{T}$. The equation that defines the normal modes, can be written as $-\partial n_i / \partial \beta^j = R_i^k C_{kj}$. In terms of integral operators, the right-hand side is

$$R_i^k C_{kj} = \int d\theta q_i(\theta) R C q_j(\theta) = \int d\theta q_i(\theta) \rho_{\text{p}}(\theta) f(\theta) q_j^{\text{dr}}(\theta) = q_i \cdot \rho_{\text{p}} (1 - f) q_j^{\text{dr}}.$$

We can take $n_i = q_i \cdot n$ for some normal-mode function $n(\theta)$ that satisfies

$$\partial n / \partial \beta^j = -\rho_p (1 - f) q_j^{\text{dr}}. \quad (\text{C.8})$$

We conclude from this equation that n is given by the TBA filling factor f . \square

Bibliography

- [1] M. Takahashi. Thermodynamics of the heisenberg-ising model for $|\delta| < 1$ in one dimension. *Physics Letters A*, 36(4):325 – 326, 1971.
- [2] M. Gaudin. Thermodynamics of the heisenberg-ising ring for $\delta \geq 1$. *Phys. Rev. Lett.*, 26:1301–1304, May 1971.
- [3] M. Steiner, J. Villain, and C.G. Windsor. Theoretical and experimental studies on one-dimensional magnetic systems. *Advances in Physics*, 25(2):87–209, 1976.
- [4] D. Alan Tennant, Roger A. Cowley, Stephen E. Nagler, and Alexei M. Tsvelik. Measurement of the spin-excitation continuum in one-dimensional KCuF_3 using neutron scattering. *Phys. Rev. B*, 52:13368–13380, Nov 1995.
- [5] Jean-Michel Maillet. Heisenberg Spin Chains: From Quantum Groups to Neutron Scattering Experiments. *Prog. Math. Phys.*, 53:161–201, 2007.
- [6] Elliott H. Lieb and Werner Liniger. Exact analysis of an interacting Bose gas. 1. The General solution and the ground state. *Phys. Rev.*, 130:1605–1616, 1963.
- [7] Chen-Ning Yang and C. P. Yang. Thermodynamics of one-dimensional system of bosons with repulsive delta function interaction. *J. Math. Phys.*, 10:1115–1122, 1969.
- [8] Toshiya Kinoshita, Trevor Wenger, and David S. Weiss. Local pair correlations in one-dimensional bose gases. *Phys. Rev. Lett.*, 95:190406, Nov 2005.
- [9] D. M. Gangardt and G. V. Shlyapnikov. Stability and phase coherence of trapped 1d bose gases. *Phys. Rev. Lett.*, 90:010401, Jan 2003.
- [10] Toshiya Kinoshita, Trevor Wenger, and David Weiss. A quantum newton’s cradle. *Nature*, 440:900–3, 05 2006.
- [11] Hans Albrecht Bethe. Zur Theorie der Metalle; 1, Eigenwerte und Eigenfunktionen der linearen Atomkette. *Z. Phys.*, 71:205–226, 1931.
- [12] R. Orbach. Linear antiferromagnetic chain with anisotropic coupling. *Phys. Rev.*, 112:309–316, Oct 1958.
- [13] L. R. Walker. Antiferromagnetic linear chain. *Phys. Rev.*, 116:1089–1090, Dec 1959.
- [14] C. N. Yang and C. P. Yang. One-dimensional chain of anisotropic spin-spin interactions. i. proof of bethe’s hypothesis for ground state in a finite system. *Phys. Rev.*, 150:321–327, Oct 1966.
- [15] L.D. Faddeev, E.K. Sklyanin, and L.A. Takhtajan. The Quantum Inverse Problem Method. 1. *Theor. Math. Phys.*, 40:688–706, 1980.

- [16] L.A. Takhtajan and L.D. Faddeev. The Quantum method of the inverse problem and the Heisenberg XYZ model. *Russ. Math. Surveys*, 34(5):11–68, 1979.
- [17] R.J. Baxter. *Exactly solved models in statistical mechanics*. 1982.
- [18] Peter P. Kulish. Classical and quantum inverse problem method and generalized bethe ansatz. *Physica D: Nonlinear Phenomena*, 3(1):246 – 257, 1981.
- [19] P P Kulish and N Yu Reshetikhin. Diagonalisation of $GL(n)$ invariant transfer matrices and quantum n-wave system (lee model). *Journal of Physics A: Mathematical and General*, 16(16):L591–L596, nov 1983.
- [20] A. H. van Amerongen, J. J. P. van Es, P. Wicke, K. V. Kheruntsyan, and N. J. van Druten. Yang-yang thermodynamics on an atom chip. *Phys. Rev. Lett.*, 100:090402, Mar 2008.
- [21] Minoru Takahashi. One-dimensional heisenberg model at finite temperature. *Progress of Theoretical Physics - PROG THEOR PHYS KYOTO*, 46:401–415, 08 1971.
- [22] Miki Yamada and Minoru Takahashi. Critical behavior of spin-1/2 one-dimensional heisenberg ferromagnet at low temperatures. *Journal of the Physical Society of Japan*, 55(6):2024–2036, 1986.
- [23] P. Schlottmann. Critical behavior of the isotropic ferromagnetic quantum heisenberg chain. *Phys. Rev. Lett.*, 54:2131–2134, May 1985.
- [24] Minoru Takahashi. One-dimensional hubbard model at finite temperature. *Progress of Theoretical Physics - PROG THEOR PHYS KYOTO*, 47:69–82, 01 1972.
- [25] A. B. Zamolodchikov. Integrals of Motion in Scaling Three State Potts Model Field Theory. *Int. J. Mod. Phys.*, A3:743–750, 1988.
- [26] Alexander B. Zamolodchikov and Alexei B. Zamolodchikov. Factorized s Matrices in Two-Dimensions as the Exact Solutions of Certain Relativistic Quantum Field Models. *Annals Phys.*, 120:253–291, 1979.
- [27] Jan Ambjorn, Romuald A. Janik, and Charlotte Kristjansen. Wrapping interactions and a new source of corrections to the spin-chain/string duality. *Nucl. Phys. B*, 736:288–301, 2006.
- [28] Gleb Arutyunov and Sergey Frolov. On String S-matrix, Bound States and TBA. *JHEP*, 12:024, 2007.
- [29] Gleb Arutyunov and Sergey Frolov. String hypothesis for the $AdS(5) \times S^{*5}$ mirror. *JHEP*, 03:152, 2009.
- [30] Gleb Arutyunov and Sergey Frolov. Thermodynamic Bethe Ansatz for the $AdS(5) \times S(5)$ Mirror Model. *JHEP*, 05:068, 2009.

- [31] Diego Bombardelli, Davide Fioravanti, and Roberto Tateo. Thermodynamic Bethe Ansatz for planar AdS/CFT: A Proposal. *J. Phys. A*, 42:375401, 2009.
- [32] Nikolay Gromov, Vladimir Kazakov, Andrii Kozak, and Pedro Vieira. Exact Spectrum of Anomalous Dimensions of Planar $N = 4$ Supersymmetric Yang-Mills Theory: TBA and excited states. *Lett. Math. Phys.*, 91:265–287, 2010.
- [33] Nikolay Gromov, Vladimir Kazakov, and Pedro Vieira. Exact Spectrum of Anomalous Dimensions of Planar $N=4$ Supersymmetric Yang-Mills Theory. *Phys. Rev. Lett.*, 103:131601, 2009.
- [34] Andrea Cavaglia, Davide Fioravanti, and Roberto Tateo. Extended Y-system for the AdS_5/CFT_4 correspondence. *Nucl. Phys. B*, 843:302–343, 2011.
- [35] Andrea Cavaglia, Davide Fioravanti, Massimo Mattelliano, and Roberto Tateo. On the AdS_5/CFT_4 TBA and its analytic properties. In *Infinite Analysis 10: Developments in Quantum Integrable Systems (IA 10)*, 3 2011.
- [36] Janos Balog and Arpad Hegedus. $AdS_5 \times S^5$ mirror TBA equations from Y-system and discontinuity relations. *JHEP*, 08:095, 2011.
- [37] Nikolay Gromov, Vladimir Kazakov, Sebastien Leurent, and Dmytro Volin. Quantum Spectral Curve for Planar $\mathcal{N} = 4$ Super-Yang-Mills Theory. *Phys. Rev. Lett.*, 112(1):011602, 2014.
- [38] Benjamin Basso, Shota Komatsu, and Pedro Vieira. Structure Constants and Integrable Bootstrap in Planar $N=4$ SYM Theory. 2015.
- [39] A. Leclair and G. Mussardo. Finite temperature correlation functions in integrable QFT. *Nucl. Phys.*, B552:624–642, 1999.
- [40] H. Saleur. A Comment on finite temperature correlations in integrable QFT. *Nucl. Phys.*, B567:602–610, 2000.
- [41] Balazs Pozsgay. Mean values of local operators in highly excited Bethe states. *J. Stat. Mech.*, 1101:P01011, 2011.
- [42] Zoltan Bajnok and Chao Wu. Diagonal form factors from non-diagonal ones. 7 2017.
- [43] Zoltan Bajnok and Istvan Vona. Exact finite volume expectation values of conserved currents. 11 2019.
- [44] Patrick Dorey and Roberto Tateo. Excited states by analytic continuation of TBA equations. *Nucl. Phys.*, B482:639–659, 1996.
- [45] A. LeClair, G. Mussardo, H. Saleur, and S. Skorik. Boundary energy and boundary states in integrable quantum field theories. *Nucl. Phys.*, B453:581–618, 1995.
- [46] F. Woynarovich. $O(1)$ contribution of saddle point fluctuations to the free energy of Bethe Ansatz systems. *Nucl. Phys.*, B700:331–360, 2004.

- [47] Patrick Dorey, Davide Fioravanti, Chaiho Rim, and Roberto Tateo. Integrable quantum field theory with boundaries: The Exact g function. *Nucl. Phys.*, B696:445–467, 2004.
- [48] Seth Chaiken. A combinatorial proof of the all minors matrix tree theorem, 1982.
- [49] Immanuel Bloch, Jean Dalibard, and Sylvain Nascimbène. Quantum simulations with ultracold quantum gases. *Nature Physics*, 8(4):267–276, April 2012.
- [50] M. Gring, M. Kuhnert, T. Langen, T. Kitagawa, B. Rauer, M. Schreitl, I. Mazets, D. Adu Smith, E. Demler, and J. Schmiedmayer. Relaxation and prethermalization in an isolated quantum system. *Science*, 337(6100):1318–1322, 2012.
- [51] Abhishek Dhar. Heat transport in low-dimensional systems. *Advances in Physics*, 57(5):457–537, 2008.
- [52] Henk van Beijeren. Exact results for anomalous transport in one-dimensional hamiltonian systems. *Phys. Rev. Lett.*, 108:180601, Apr 2012.
- [53] Lorenzo Bertini, Alberto De Sole, Davide Gabrielli, Giovanni Jona-Lasinio, and Claudio Landim. Macroscopic fluctuation theory. *Rev. Mod. Phys.*, 87:593–636, Jun 2015.
- [54] X. Zotos. Finite temperature drude weight of the one-dimensional spin- 1/2 heisenberg model. *Phys. Rev. Lett.*, 82:1764–1767, Feb 1999.
- [55] X. Zotos, F. Naef, and P. Prelovsek. Transport and conservation laws. *Phys. Rev. B*, 55:11029–11032, May 1997.
- [56] Tomaž Prosen. Open xxz spin chain: Nonequilibrium steady state and a strict bound on ballistic transport. *Phys. Rev. Lett.*, 106:217206, May 2011.
- [57] J. Sirker, R. G. Pereira, and I. Affleck. Diffusion and ballistic transport in one-dimensional quantum systems. *Phys. Rev. Lett.*, 103:216602, Nov 2009.
- [58] Marko Ljubotina, Marko Znidaric, and Tomaž Prosen. Spin diffusion from an inhomogeneous quench in an integrable system. *Nature Communications*, 8, 02 2017.
- [59] Marko Medenjak, Christoph Karrasch, and Tomaž Prosen. Lower bounding diffusion constant by the curvature of drude weight. *Phys. Rev. Lett.*, 119:080602, Aug 2017.
- [60] Enej Ilievski, Jacopo De Nardis, Marko Medenjak, and Tomaž Prosen. Superdiffusion in one-dimensional quantum lattice models. *Phys. Rev. Lett.*, 121:230602, Dec 2018.
- [61] Olalla A. Castro-Alvaredo, Benjamin Doyon, and Takato Yoshimura. Emergent hydrodynamics in integrable quantum systems out of equilibrium. *Phys. Rev.*, X6(4):041065, 2016.
- [62] Bruno Bertini, Mario Collura, Jacopo De Nardis, and Maurizio Fagotti. Transport in out-of-equilibrium xxz chains: Exact profiles of charges and currents. *Phys. Rev. Lett.*, 117:207201, Nov 2016.

- [63] Jacopo De Nardis, Denis Bernard, and Benjamin Doyon. Hydrodynamic diffusion in integrable systems. *Phys. Rev. Lett.*, 121:160603, Oct 2018.
- [64] Benjamin Doyon and Takato Yoshimura. A note on generalized hydrodynamics: inhomogeneous fields and other concepts. *SciPost Phys.*, 2:014, 2017.
- [65] M. Schemmer, Isabelle Bouchoule, Benjamin Doyon, and J’erome Dubail. Generalized hydrodynamics on an atom chip. *Physical review letters*, 122 9:090601, 2019.
- [66] Jorn Mossel and Jean-Sebastien Caux. Generalized TBA and generalized Gibbs. *J. Phys.*, A45:255001, 2012.
- [67] Márton Borsi, Balázs Pozsgay, and Levente Pristvýák. Current operators in bethe ansatz and generalized hydrodynamics: An exact quantum-classical correspondence. *Phys. Rev. X*, 10:011054, Mar 2020.
- [68] Jason Myers, M. J. Bhaseen, Rosemary J. Harris, and Benjamin Doyon. Transport fluctuations in integrable models out of equilibrium. *SciPost Phys.*, 8:7, 2020.
- [69] Benjamin Doyon and Jason Myers. Fluctuations in ballistic transport from Euler hydrodynamics. *Annales Henri Poincare*, 21(1):255–302, 2019.
- [70] Go Kato and Miki Wadati. Graphical representation of the partition function of a one-dimensional delta-function bose gas. *Journal of Mathematical Physics*, 42(10):4883–4893, 2001.
- [71] Go Kato and Miki Wadati. Direct calculation of thermodynamic quantities for the heisenberg model. *Journal of Mathematical Physics*, 43(10):5060–5078, 2002.
- [72] Go Kato and Miki Wadati. Bethe ansatz cluster expansion method for quantum integrable particle systems. *Journal of the Physical Society of Japan*, 73(5):1171–1179, 2004.
- [73] L. D. Faddeev and L. A. Takhtajan. ESSENTIALLY NONLINEAR ONE-DIMENSIONAL MODEL OF THE CLASSICAL FIELD THEORY. *Theor. Math. Phys.*, 21:1046, 1975. [Teor. Mat. Fiz.21,160(1974)].
- [74] Mark J. Ablowitz, David J. Kaup, Alan C. Newell, and Harvey Segur. Nonlinear-evolution equations of physical significance. *Phys. Rev. Lett.*, 31:125–127, Jul 1973.
- [75] D. W. McLaughlin. Four examples of the inverse method as a canonical transformation. *Journal of Mathematical Physics*, 16(1):96–99, 1975.
- [76] P. P Kulish and E. R. Nissimov. Anomalies of Quantum Currents in Exactly Solvable Models. *Theor. Math. Phys.*, 29:992–998, 1976. [Teor. Mat. Fiz.29,161(1976)].
- [77] Roger F. Dashen, Brosl Hasslacher, and André Neveu. Particle spectrum in model field theories from semiclassical functional integral techniques. *Phys. Rev. D*, 11:3424–3450, Jun 1975.

- [78] V. E. Korepin and L. D. Faddeev. Quantization of Solitons. *Theor. Math. Phys.*, 25:1039–1049, 1975. [Teor. Mat. Fiz.25,147(1975)].
- [79] Sidney Coleman. Quantum sine-gordon equation as the massive thirring model. *Phys. Rev. D*, 11:2088–2097, Apr 1975.
- [80] A. Neveu and N. Papanicolaou. Integrability of the classical $[\bar{\psi}_i\psi_i]_2^2$ and $[\bar{\psi}_i\psi_i]_2^2 - [\bar{\psi}_i\gamma_5\psi_i]_2^2$ interactions. *Comm. Math. Phys.*, 58(1):31–64, 1978.
- [81] N. Andrei and J.H. Lowenstein. Derivation of the chiral gross-neveu spectrum for arbitrary $su(n)$ symmetry. *Physics Letters B*, 90(1):106 – 110, 1980.
- [82] D. Zanon. *Quantum Integrability and Exact S-Matrices for Affine Toda Theories*, pages 141–156. Springer US, Boston, MA, 1993.
- [83] J.-L. Gervais and A. Neveu. New quantum treatment of liouville field theory. *Nuclear Physics B*, 224(2):329 – 348, 1983.
- [84] Paul Mansfield. Light-cone quantisation of the liouville and toda field theories. *Nuclear Physics B*, 222(3):419 – 445, 1983.
- [85] E. Braaten, T. Curtright, G. Ghandour, and C. Thorn. A class of conformally invariant quantum field theories. *Physics Letters B*, 125(4):301 – 304, 1983.
- [86] D. Olive and Neil Turok. The symmetries of dynkin diagrams and the reduction of toda field equations. *Nuclear Physics B*, 215(4):470 – 494, 1983.
- [87] George Wilson. The modified lax and two-dimensional toda lattice equations associated with simple lie algebras. *Ergodic Theory and Dynamical Systems*, 1(3):361–380, 1981.
- [88] A. V. Mikhailov, M. A. Olshanetsky, and A. M. Perelomov. Two-dimensional generalized toda lattice. *Comm. Math. Phys.*, 79(4):473–488, 1981.
- [89] G.W. Delius, M.T. Grisaru, and D. Zanon. Quantum conserved currents in affine toda theories. *Nuclear Physics B*, 385(1):307 – 328, 1992.
- [90] A. B. Zamolodchikov. Higher Order Integrals of Motion in Two-Dimensional Models of the Field Theory with a Broken Conformal Symmetry. *JETP Lett.*, 46:160–164, 1987. [Pisma Zh. Eksp. Teor. Fiz.46,129(1987)].
- [91] V. A. Fateev. Integrable deformations in $Z(N)$ symmetrical models of conformal quantum field theory. *Int. J. Mod. Phys.*, A6:2109–2132, 1991.
- [92] V. A. Fateev and A. B. Zamolodchikov. Integrable perturbations of $Z(N)$ parafermion models and $O(3)$ sigma model. *Phys. Lett.*, B271:91–100, 1991.
- [93] P.G.O. Freund, T.R. Klassen, and E. Melzer. S-matrices for perturbations of certain conformal field theories. *Physics Letters B*, 229(3):243 – 247, 1989.

- [94] F.A. Smirnov. Reductions of the sine-gordon model as a perturbation of minimal models of conformal field theory. *Nuclear Physics B*, 337(1):156 – 180, 1990.
- [95] A. B. Zamolodchikov. Integrable field theory from conformal field theory. *Adv. Stud. Pure Math.*, 19:641–674, 1989.
- [96] Edward Witten. Nonabelian Bosonization in Two-Dimensions. *Commun. Math. Phys.*, 92:455–472, 1984. [,201(1983)].
- [97] P. Di Vecchia and P. Rossi. On the Equivalence Between the Wess-Zumino Action and the Free Fermi Theory in Two-dimensions. *Phys. Lett.*, B140:344, 1984. [,219(1984)].
- [98] V. G. Knizhnik and A. B. Zamolodchikov. Current Algebra and Wess-Zumino Model in Two-Dimensions. *Nucl. Phys.*, B247:83–103, 1984. [,690(1984)].
- [99] H. Eichenherr and M. Forger. On the dual symmetry of the non-linear sigma models. *Nuclear Physics B*, 155(2):381 – 393, 1979.
- [100] L. D. Faddeev and N. Yu. Reshetikhin. Integrability of the Principal Chiral Field Model in (1+1)-dimension. *Annals Phys.*, 167:227, 1986.
- [101] E. Brezin and Jean Zinn-Justin. Spontaneous Breakdown of Continuous Symmetries Near Two-Dimensions. *Phys. Rev. B*, 14:3110, 1976.
- [102] William A. Bardeen, Benjamin W. Lee, and Robert E. Shrock. Phase Transition in the Nonlinear σ Model in $2 + \epsilon$ Dimensional Continuum. *Phys. Rev. D*, 14:985, 1976.
- [103] A.M. Polyakov. Hidden symmetry of the two-dimensional chiral fields. *Physics Letters B*, 72(2):224 – 226, 1977.
- [104] R. Shankar and E. Witten. s matrix of the supersymmetric nonlinear σ model. *Phys. Rev. D*, 17:2134–2143, Apr 1978.
- [105] Stephen Parke. Absence of particle production and factorization of the s -matrix in $1 + 1$ dimensional models. *Nuclear Physics B*, 174(1):166 – 182, 1980.
- [106] Richard John Eden, Peter V. Landshoff, David I. Olive, and John Charlton Polkinghorne. *The analytic S-matrix*. Cambridge Univ. Press, Cambridge, 1966.
- [107] P. Dorey. Exact S matrices. In *Conformal field theories and integrable models. Proceedings, Eotvos Graduate Course, Budapest, Hungary, August 13-18, 1996*, pages 85–125, 1996.
- [108] M. Karowski. On the bound state problem in $1+1$ dimensional field theories. *Nuclear Physics B*, 153:244 – 252, 1979.
- [109] M. Karowski and H.J. Thun. Complete s -matrix of the $o(2n)$ gross-neveu model. *Nuclear Physics B*, 190(1):61 – 92, 1981. Volume B190 [FS3] No.2 To Follow in Approximately Two Months.

- [110] E. Ogievetsky, P. Wiegmann, and N. Reshetikhin. The Principal Chiral Field in Two-Dimensions on Classical Lie Algebras: The Bethe Ansatz Solution and Factorized Theory of Scattering. *Nucl. Phys.*, B280:45–96, 1987.
- [111] A. B. Zamolodchikov. Integrals of Motion and S Matrix of the (Scaled) $T=T(c)$ Ising Model with Magnetic Field. *Int. J. Mod. Phys.*, A4:4235, 1989.
- [112] H.W. Braden, E. Corrigan, P.E. Dorey, and R. Sasaki. Affine toda field theory and exact s-matrices. *Nuclear Physics B*, 338(3):689 – 746, 1990.
- [113] G.W. Delius, M.T. Grisaru, and D. Zanon. Exact s-matrices for nonsimply-laced affine toda theories. *Nuclear Physics B*, 382(2):365 – 406, 1992.
- [114] Giuseppe Mussardo. Off-critical statistical models: Factorized scattering theories and bootstrap program. *Physics Reports*, 218(5):215 – 379, 1992.
- [115] G.W. Delius. Exact s-matrices with affine quantum group symmetry. *Nuclear Physics B*, 451(1):445 – 465, 1995.
- [116] B. Berg, M. Karowski, P. Weisz, and V. Kurak. Factorized $u(n)$ symmetric s-matrices in two dimensions. *Nuclear Physics B*, 134(1):125 – 132, 1978.
- [117] B. Berg and P. Weisz. Exact s-matrix of the chiral invariant $su(n)$ thirring model. *Nuclear Physics B*, 146(1):205 – 214, 1978.
- [118] R. Köberle, V. Kurak, and J. A. Swieca. Scattering theory and $\frac{1}{N}$ expansion in the chiral gross-neveu model. *Phys. Rev. D*, 20:897–902, Aug 1979.
- [119] L. D. Faddeev. How algebraic Bethe ansatz works for integrable model. In *Relativistic gravitation and gravitational radiation. Proceedings, School of Physics, Les Houches, France, September 26-October 6, 1995*, pages pp. 149–219, 1996.
- [120] I.V. Cherednik. Factorizing Particles on a Half Line and Root Systems. *Theor. Math. Phys.*, 61:977–983, 1984.
- [121] Subir Ghoshal and Alexander B. Zamolodchikov. Boundary S matrix and boundary state in two-dimensional integrable quantum field theory. *Int. J. Mod. Phys.*, A9:3841–3886, 1994. [Erratum: *Int. J. Mod. Phys.*A9,4353(1994)].
- [122] Andreas Fring and Roland Koberle. Factorized scattering in the presence of reflecting boundaries. *Nucl. Phys. B*, 421:159–172, 1994.
- [123] V. A. Fateev and A. B. Zamolodchikov. Conformal Field Theory and Purely Elastic S-Matrices. *International Journal of Modern Physics A*, 5(6):1025–1048, Jan 1990.
- [124] Edward Corrigan, P. E. Dorey, R. H. Rietdijk, and R. Sasaki. Affine Toda field theory on a half line. *Phys. Lett.*, B333:83–91, 1994.

- [125] M. Takahashi and M. Suzuki. A reply to the comments of Johnson et al. on the thermodynamics of the Heisenberg-Ising ring for $|\delta| < 1$. *Physics Letters A*, 41(1):81 – 82, 1972.
- [126] H. W. J. Blöte, John L. Cardy, and M. P. Nightingale. Conformal invariance, the central charge, and universal finite-size amplitudes at criticality. *Phys. Rev. Lett.*, 56:742–745, Feb 1986.
- [127] G. E. Andrews, R. J. Baxter, and P. J. Forrester. Eight vertex SOS model and generalized Rogers-Ramanujan type identities. *J. Statist. Phys.*, 35:193–266, 1984.
- [128] V. V. Bazhanov and N. Yu. Reshetikhin. Critical RSOS Models and Conformal Field Theory. *Int. J. Mod. Phys.*, A4:115–142, 1989.
- [129] Timothy R. Klassen and Ezer Melzer. Purely Elastic Scattering Theories and their Ultraviolet Limits. *Nucl. Phys.*, B338:485–528, 1990.
- [130] Anatol N. Kirillov. Dilogarithm identities and spectra in conformal field theory. In *Preprint - Kirillov, A.N. (rec.Dec.92) 10 p.B e: LANL hep-th/9211137*, 1992.
- [131] Anatol N. Kirillov. Dilogarithm identities, partitions and spectra in conformal field theory. 1. 1993.
- [132] A. Kuniba and T. Nakanishi. Spectra in conformal field theories from the Rogers dilogarithm. *Mod. Phys. Lett.*, A7:3487–3494, 1992.
- [133] Minoru Takahashi. *Thermodynamics of One-Dimensional Solvable Models*. Cambridge University Press, 1999.
- [134] H. Saleur and B. Wehefritz-Kaufmann. Thermodynamics of the complex SU(3) Toda theory. *Phys. Lett.*, B481:419–426, 2000.
- [135] Gleb Arutyunov, Marius de Leeuw, and Stijn J. van Tongeren. The Quantum Deformed Mirror TBA I. *JHEP*, 10:090, 2012.
- [136] F. Woynarovich. On the $S(Z)=0$ Excited States of an Anisotropic Heisenberg Chain. *J. Phys.*, A15:2985, 1982.
- [137] F. Woynarovich. On the eigenstates of a Heisenberg chain with complex wavenumbers not forming strings. *Journal of Physics C: Solid State Physics*, 15(31):6397–6401, Nov 1982.
- [138] O. Babelon, H. J. de Vega, and C. M. Viallet. Analysis of the Bethe Ansatz Equations of the XXZ Model. *Nucl. Phys.*, B220:13–34, 1983.
- [139] A.M. Tsvelick and P.B. Wiegmann. Exact results in the theory of magnetic alloys. *Advances in Physics*, 32(4):453–713, 1983.
- [140] Vladimir E. Korepin and Fabian H. L. Essler. *THE ONE-DIMENSIONAL HUBBARD MODEL*, pages 2–8.

- [141] Atsuo Kuniba, Tomoki Nakanishi, and Junji Suzuki. T-systems and Y-systems in integrable systems. *J. Phys.*, A44:103001, 2011.
- [142] Changrim Ahn, Zoltan Bajnok, Diego Bombardelli, and Rafael I. Nepomechie. TBA, NLO Luscher correction, and double wrapping in twisted AdS/CFT. *JHEP*, 12:059, 2011.
- [143] Timothy R. Klassen and Ezer Melzer. The Thermodynamics of purely elastic scattering theories and conformal perturbation theory. *Nucl. Phys.*, B350:635–689, 1991.
- [144] Carl M. Bender and Tai Tsun Wu. Anharmonic oscillator. *Phys. Rev.*, 184:1231–1260, Aug 1969.
- [145] F. A. Smirnov. Form-factors in completely integrable models of quantum field theory. *Adv. Ser. Math. Phys.*, 14:1–208, 1992.
- [146] Zoltan Bajnok and Romuald A. Janik. String field theory vertex from integrability. *JHEP*, 04:042, 2015.
- [147] Axel Cortés Cubero and Miłosz Panfil. Thermodynamic bootstrap program for integrable QFT’s: form factors and correlation functions at finite energy density. *JHEP*, 01:104, 2019.
- [148] J. De Nardis and M. Panfil. Particle-hole pairs and density-density correlations in the Lieb-Liniger model. *Journal of Statistical Mechanics: Theory and Experiment*, 3(3):033102, Mar 2018.
- [149] Tai Tsun Wu, Barry M. McCoy, Craig A. Tracy, and Eytan Barouch. Spin spin correlation functions for the two-dimensional Ising model: Exact theory in the scaling region. *Phys. Rev.*, B13:316–374, 1976.
- [150] Olivier Babelon and Denis Bernard. From form-factors to correlation functions: The Ising model. *Phys. Lett.*, B288:113–120, 1992.
- [151] O. A. Castro-Alvaredo and A. Fring. Identifying the operator content, the homogeneous sine-Gordon models. *Nucl. Phys.*, B604:367–390, 2001.
- [152] Peter Orland. Seeing asymptotic freedom in an exact correlator of a large- N matrix field theory. *Phys. Rev.*, D90(12):125038, 2014.
- [153] Axel Cortés Cubero. *Yang-Mills Theories as Deformations of Massive Integrable Models*. PhD thesis, CUNY, Graduate School - U. Ctr., 2014.
- [154] Hratchya M. Babujian, A. Fring, M. Karowski, and A. Zapletal. Exact form-factors in integrable quantum field theories: The Sine-Gordon model. *Nucl. Phys.*, B538:535–586, 1999.
- [155] G. Delfino, G. Mussardo, and P. Simonetti. Nonintegrable quantum field theories as perturbations of certain integrable models. *Nucl. Phys. B*, 473:469–508, 1996.

- [156] B. Pozsgay and G. Takacs. Form factors in finite volume. II. Disconnected terms and finite temperature correlators. *Nucl. Phys.*, B788:209–251, 2008.
- [157] V. E. Korepin. CALCULATION OF NORMS OF BETHE WAVE FUNCTIONS. *Commun. Math. Phys.*, 86:391–418, 1982.
- [158] B. Pozsgay and G. Takacs. Form-factors in finite volume I: Form-factor bootstrap and truncated conformal space. *Nucl. Phys.*, B788:167–208, 2008.
- [159] A. Leclair, F. Lesage, S. Sachdev, and H. Saleur. Finite temperature correlations in the one-dimensional quantum Ising model. *Nucl. Phys.*, B482:579–612, 1996.
- [160] O.A. Castro-Alvaredo and A. Fring. Finite temperature correlation functions from form-factors. *Nucl. Phys. B*, 636:611–631, 2002.
- [161] Benjamin Doyon. Finite-temperature form-factors in the free Majorana theory. *J. Stat. Mech.*, 0511:P11006, 2005.
- [162] Benjamin Doyon. Finite-temperature form-factors: A Review. *SIGMA*, 3:011, 2007.
- [163] Yixiong Chen and Benjamin Doyon. Form factors in equilibrium and non-equilibrium mixed states of the ising model. *Journal of Statistical Mechanics: Theory and Experiment*, 2014(9):P09021, sep 2014.
- [164] Robert M. Konik. Haldane-gapped spin chains: Exact low-temperature expansions of correlation functions. *Phys. Rev. B*, 68:104435, Sep 2003.
- [165] Fabian H.L. Essler and Robert M. Konik. Finite-temperature lineshapes in gapped quantum spin chains. *Phys. Rev. B*, 78:100403, 2008.
- [166] A. J. A. James, F. H. L. Essler, and R. M. Konik. Finite-temperature dynamical structure factor of alternating heisenberg chains. *Phys. Rev. B*, 78:094411, Sep 2008.
- [167] B. Pozsgay and G. Takacs. Form factor expansion for thermal correlators. *J. Stat. Mech.*, 1011:P11012, 2010.
- [168] I.M. Szecsenyi and G. Takacs. Spectral expansion for finite temperature two-point functions and clustering. *J. Stat. Mech.*, 1212:P12002, 2012.
- [169] B. Pozsgay and I. M. Szécsényi. LeClair-Mussardo series for two-point functions in Integrable QFT. *JHEP*, 05:170, 2018.
- [170] Jacopo De Nardis, Denis Bernard, and Benjamin Doyon. Diffusion in generalized hydrodynamics and quasiparticle scattering. *SciPost Phys.*, 6:49, 2019.
- [171] Benjamin Doyon and Herbert Spohn. Dynamics of hard rods with initial domain wall state. *Journal of Statistical Mechanics: Theory and Experiment*, 2017(7):073210, jul 2017.
- [172] Denis Bernard and Benjamin Doyon. Energy flow in non-equilibrium conformal field theory. *Journal of Physics A: Mathematical and Theoretical*, 45(36):362001, aug 2012.

- [173] F. Woynarovich. On the normalization of the partition function of Bethe Ansatz systems. *Nucl. Phys.*, B852:269–286, 2011.
- [174] Balázs Pozsgay. Form factor approach to diagonal finite volume matrix elements in Integrable QFT. *JHEP*, 07:157, 2013.
- [175] Zoltan Bajnok and Romuald A. Janik. From the octagon to the SFT vertex — gluing and multiple wrapping. *JHEP*, 06:058, 2017.
- [176] Z. Bajnok and Zs. Simon. Solving topological defects via fusion. *Nucl. Phys. B*, 802:307–329, 2008.
- [177] Benjamin Basso, Vasco Goncalves, and Shota Komatsu. Structure constants at wrapping order. *JHEP*, 05:124, 2017.
- [178] Balazs Pozsgay. On $O(1)$ contributions to the free energy in Bethe Ansatz systems: The Exact g-function. *JHEP*, 08:090, 2010.
- [179] Balázs Pozsgay. Overlaps between eigenstates of the xxz spin-1/2 chain and a class of simple product states. *Journal of Statistical Mechanics: Theory and Experiment*, 2014(6):P06011, 2014.
- [180] M Brockmann, J De Nardis, B Wouters, and J-S Caux. Néel-xxz state overlaps: odd particle numbers and lieb-liniger scaling limit. *Journal of Physics A: Mathematical and Theoretical*, 47(34):345003, 2014.
- [181] M Brockmann, J De Nardis, B Wouters, and J-S Caux. A gaudin-like determinant for overlaps of néel and xxz bethe states. *Journal of Physics A: Mathematical and Theoretical*, 47(14):145003, 2014.
- [182] M Brockmann. Overlaps of q-raised néel states with xxz bethe states and their relation to the lieb-liniger bose gas. *Journal of Statistical Mechanics: Theory and Experiment*, 2014(5):P05006, 2014.
- [183] B Pozsgay. Overlaps with arbitrary two-site states in the xxz spin chain. *Journal of Statistical Mechanics: Theory and Experiment*, 2018(5):053103, 2018.
- [184] Marius de Leeuw, Charlotte Kristjansen, and Konstantin Zarembo. One-point Functions in Defect CFT and Integrability. *JHEP*, 08:098, 2015.
- [185] Isak Buhl-Mortensen, Marius de Leeuw, Charlotte Kristjansen, and Konstantin Zarembo. One-point Functions in AdS/dCFT from Matrix Product States. *JHEP*, 02:052, 2016.
- [186] Marius de Leeuw, Charlotte Kristjansen, and Stefano Mori. AdS/dCFT one-point functions of the $SU(3)$ sector. *Phys. Lett.*, B763:197–202, 2016.
- [187] Marius De Leeuw, Charlotte Kristjansen, and Georgios Linardopoulos. Scalar one-point functions and matrix product states of AdS/dCFT. *Phys. Lett.*, B781:238–243, 2018.

- [188] Tamas Gombor and Zoltan Bajnok. Boundary states, overlaps, nesting and bootstrapping AdS/dCFT. 4 2020.
- [189] Y. Jiang, S. Komatsu, and Edoardo Vescovi. Structure Constants in $\mathcal{N} = 4$ SYM at Finite Coupling as Worldsheet g -Function. 6 2019.
- [190] Patrick Dorey, Roberto Tateo, and Ruth Wilbourne. Exact g -function flows from the staircase model. *Nucl. Phys.*, B843:724–752, 2011.
- [191] Alexei B. Zamolodchikov. Resonance factorized scattering and roaming trajectories. *J. Phys.*, A39:12847–12862, 2006.
- [192] B. Pozsgay and O. Rákos. Exact boundary free energy of the open XXZ chain with arbitrary boundary conditions. *ArXiv e-prints*, April 2018.
- [193] Nobuyuki Ishibashi. The Boundary and Crosscap States in Conformal Field Theories. *Mod. Phys. Lett.*, A4:251, 1989.
- [194] John L. Cardy. Boundary Conditions, Fusion Rules and the Verlinde Formula. *Nucl. Phys.*, B324:581–596, 1989.
- [195] M. R. Gaberdiel, A. Recknagel, and G. M. T. Watts. The Conformal boundary states for $SU(2)$ at level 1. *Nucl. Phys.*, B626:344–362, 2002.
- [196] Patrick Dorey, Ingo Runkel, Roberto Tateo, and Gerard Watts. g function flow in perturbed boundary conformal field theories. *Nucl. Phys.*, B578:85–122, 2000.
- [197] Patrick Dorey, Anna Lishman, Chaiho Rim, and Roberto Tateo. Reflection factors and exact g -functions for purely elastic scattering theories. *Nucl. Phys.*, B744:239–276, 2006.
- [198] C. Ahn, D. Bernard, and A. Leclair. Fractional supersymmetries in perturbed coset cfts and integrable soliton theory. *Nuclear Physics B*, 346(2):409 – 439, 1990.
- [199] A. B. Zamolodchikov. TBA equations for integrable perturbed $SU(2)$ - $k \times SU(2)$ - $l / SU(2)$ - $k+l$ coset models. *Nucl. Phys.*, B366:122–132, 1991.
- [200] Timothy J. Hollowood. From am-1 trigonometric s-matrices to the thermodynamic bethe ansatz. *Physics Letters B*, 320(1):43 – 51, 1994.
- [201] A. Babichenko. From S matrices to the thermodynamic Bethe ansatz. *Nucl. Phys.*, B697:481–512, 2004.
- [202] V. Bazhanov and N. Reshetikhin. Restricted Solid on Solid Models Connected With Simply Based Algebras and Conformal Field Theory. *J. Phys.*, A23:1477, 1990.
- [203] Ines Aniceto, Zoltan Bajnok, Tamas Gombor, Minkyoo Kim, and Laszlo Palla. On integrable boundaries in the 2 dimensional $O(N)$ σ -models. *J. Phys.*, A50(36):364002, 2017.

- [204] Tamás Gombor. Nonstandard Bethe Ansatz equations for open $O(N)$ spin chains. *Nucl. Phys.*, B935:310–343, 2018.
- [205] Dinh-Long Vu and Takato Yoshimura. Equations of state in generalized hydrodynamics. *SciPost Phys.*, 6:23, 2019.
- [206] Dinh-Long Vu. Cumulants of conserved charges in GGE and cumulants of total transport in GHD: exact summation of matrix elements? *J. Stat. Mech.*, 2002(2):023103, 2020.
- [207] Andrea De Luca, Mario Collura, and Jacopo De Nardis. Nonequilibrium spin transport in integrable spin chains: Persistent currents and emergence of magnetic domains. *Phys. Rev. B*, 96:020403, Jul 2017.
- [208] Enej Ilievski and Jacopo De Nardis. Microscopic origin of ideal conductivity in integrable quantum models. *Phys. Rev. Lett.*, 119:020602, Jul 2017.
- [209] Vir B. Bulchandani, Romain Vasseur, Christoph Karrasch, and Joel E. Moore. Bethe-boltzmann hydrodynamics and spin transport in the xxz chain. *Phys. Rev. B*, 97:045407, Jan 2018.
- [210] Vir B. Bulchandani, Romain Vasseur, Christoph Karrasch, and Joel E. Moore. Solvable hydrodynamics of quantum integrable systems. *Phys. Rev. Lett.*, 119:220604, Nov 2017.
- [211] Lorenzo Piroli, Jacopo De Nardis, Mario Collura, Bruno Bertini, and Maurizio Fagotti. Transport in out-of-equilibrium xxz chains: Nonballistic behavior and correlation functions. *Phys. Rev. B*, 96:115124, Sep 2017.
- [212] Mario Collura, Andrea De Luca, and Jacopo Viti. Analytic solution of the domain-wall nonequilibrium stationary state. *Phys. Rev. B*, 97:081111, Feb 2018.
- [213] Enej Ilievski and Jacopo De Nardis. Ballistic transport in the one-dimensional hubbard model: The hydrodynamic approach. *Phys. Rev. B*, 96:081118, Aug 2017.
- [214] Takato Yoshimura and Herbert Spohn. Collision rate ansatz for quantum integrable systems. 4 2020.
- [215] M. Kormos, G. Mussardo, and A. Trombettoni. Expectation values in the lieb-liniger bose gas. *Phys. Rev. Lett.*, 103:210404, Nov 2009.
- [216] Hugo Touchette. The large deviation approach to statistical mechanics. *Physics Reports*, 478(1):1 – 69, 2009.
- [217] Benjamin Doyon and Herbert Spohn. Drude Weight for the Lieb-Liniger Bose Gas. *SciPost Phys.*, 3:039, 2017.
- [218] Christian B Mendl and Herbert Spohn. Current fluctuations for anharmonic chains in thermal equilibrium. *Journal of Statistical Mechanics: Theory and Experiment*, 2015(3):P03007, mar 2015.

- [219] Benjamin Doyon. Exact large-scale correlations in integrable systems out of equilibrium. *SciPost Phys.*, 5(5):054, 2018.